FUNCTIONAL ANALYSIS OF TRANSCRIPTIONAL PROMOTERS OF MACAQUE LYMPH NODE CHEMOKINES

by

Lauren Ann Sciullo

B.S., Molecular Biology, Grove City College, 2010

Submitted to the Graduate Faculty of

Graduate School of Public Health in partial fulfillment

of the requirements for the degree of

Master of Science

University of Pittsburgh

2012

UNIVERSITY OF PITTSBURGH

GRADUATE SCHOOL OF PUBLIC HEALTH

This thesis was presented

by

Lauren Ann Sciullo

It was defended on

June 21, 2012

and approved by

Jeremy Martinson, DPhil
Assistant Professor
Departments of Infectious Diseases and Microbiology and Human Genetics
Graduate School of Public Health, University of Pittsburgh

Tianyi Wang, PhD
Associate Professor
Department of Infectious Diseases and Microbiology
Graduate School of Public Health, University of Pittsburgh

Michael Murphey-Corb, PhD
Professor
Department of Microbiology and Molecular Genetics, School of Medicine
Department of Infectious Diseases and Microbiology
Graduate School of Public Health, University of Pittsburgh

Thesis Advisor: Todd Reinhart, ScD
Professor
Department of Infectious Diseases and Microbiology
Graduate School of Public Health, University of Pittsburgh

Todd Reinhart, ScD

FUNCTIONAL ANALYSIS OF TRANSCRIPTIONAL PROMOTERS OF MACAQUE LYMPH NODE CHEMOKINES

Lauren Ann Sciullo, M.S.

University of Pittsburgh, 2012

Inflammation has been shown to play a part in the disease processes of human immunodeficiency virus type-1 (HIV-1) and simian immunodeficiency virus (SIV) infections. The chemokines CCL20, CCL21, and CXCL13 all play important roles in the immune response and have each been, in some manner, linked to HIV-1 and SIV infection. Expression of these chemokine genes has been shown to affect disease state and it is, therefore, important to study the transcriptional regulation of these genes as a possible mechanism of controlling their expression. Transcriptional regulation occurs primarily via the promoter region of a gene. This promoter is the target for binding by transcription factors that can either activate or repress the expression of that specific gene. In this study, the promoter regions of the macaque chemokines CCL20, CCL21, and CXCL13 were analyzed. These promoter regions were characterized via sequence alignments and analyses, as well as by mapping putative transcription factor binding sites. Not only were differences between multiple clones of each chemokine promoter identified, but the homology between the rhesus macaque, cynomolgus macaque, and human promoter regions were explored. By cloning the three promoters into the pGL2-Basic vector, a promoterless luciferase expression plasmid, transcriptional control was measured from each promoter via levels of luciferase expression. A dual-luciferase reporter assay was designed and optimized as a method of quantitating transcriptional control from macaque chemokine promoters. After stimulation, an increase in CCL20 transcriptional levels, but no change in

CCL21 and CXCL13 transcriptional levels, was observed. Possible methods of inhibiting transcription from the CCL20 promoter were explored by testing the effects of glycerol monolaurate (GML), (-)-epigallocatechin gallate (EGCG), and ethyl gallate (EG) on transcriptional levels. In summary, we have amplified three macaque chemokine promoters, characterized their basal and induced transcriptional control of the luciferase gene, and have identified potential inhibitors of their upregulation. The public health relevance of this study is its ability to potentially pave the way for additional approaches to modulating chemokine expression as a method of combating the inflammation associated with HIV-1-driven disease.

TABLE OF CONTENTS

LIST OF TABLES

LIST OF FIGURES

PREFACE

First and foremost, I would like to sincerely thank my thesis advisor and mentor, Dr. Todd Reinhart, for his continued help and support throughout this process. Without his constant involvement and genuine interest in my project I would not have grown into the enthusiastic and inquisitive scientist I am today. I must attribute my strong desire to consistently perform to the best of my ability, as well as my constant striving to learn more and to better, not only myself, but also my project, to him. For this, I am truly grateful and extend my sincere gratitude.

I would also like to thank my committee members, Dr. Jeremy Martinson, Dr. Tianyi Wang, and Dr. Michael Murphey-Corb, for their input in my project. Their suggestions, ideas, and help were greatly appreciated and allowed me to improve my project so as to have the best thesis possible. I would like to further thank Dr. Martinson and Blair Gleeson, for providing me with the rhesus genomic DNA used throughout this project and for their assistance with my genomic analyses, and Dr. Wang, for providing me with the pGL4.74 vector and for the use of his plate reader.

I must also extend my sincere gratitude to the entire Reinhart lab: Dr. Shulin Qin, Beth Junecko, Cynthia Klamar, Carissa Lucero, Stella Berendam, and Todd Looney, as well as past lab member, Chris Bowen. Without their help and willingness to pause whatever they were doing to help and teach me, this thesis would not have been possible. I also thank them for all the conversations had, both scientific and otherwise, always making time in lab more enjoyable.

To my fellow students and friends, I always have a great time with you and you have all made my days here at GSPH much more enjoyable. Thanks, not only for the scientific conversations, but for all the laughs and memories.

Finally, I'd like to express my sincere thanks to my family for their love and support. My parents, Anthony and Sheila Sciullo, and my grandmother, Ann Sikorski, have been a constant source of help and encouragement. Without them fully supporting my career path, believing in me, and encouraging me to follow my dreams and never give up, I would not be where I am today. Thank you and I love you.

1.0 INTRODUCTION

1.1 CHEMOKINES AND THE IMMUNE SYSTEM

Chemokines are small, secreted proteins that promote cellular migration and chemotactic response through the binding of appropriate receptors on the surfaces of cells.[1] The intracellular domains of these seven transmembrane-spanning G-protein coupled receptors (GPCRs) activate intracellular messengers that initiate cellular signaling pathways.[2] Chemokines play important roles in development, organogensis, normal physiology, and immune response.[3, 4]

Currently, approximately 50 chemokine ligands and 20 chemokine receptors have been identified.[4, 5] The differences in the numbers of ligands and receptors imply there is a redundancy in the binding of ligands to receptors. This redundancy is unlikely to be random because chemokines with similar spatial and temporal properties tend to form the same receptor interactions.[3] Whereas chemokine receptors are able to bind more than one chemokine, CC and CXC receptors only signal via CC- and CXC-chemokines, respectively, as a result of the receptor's quaternary structure.[6] When a chemokine binds its receptor, it triggers downstream events that allow for the internalization of the receptor and eventual signal transduction that causes integrin activation and polarization of the actin cytoskeleton, ultimately allowing for cell migration via actomyosin contraction and tail retraction.[3] Chemokine expression is often induced by pro-inflammatory cytokines, such as IL-1, IL-6, and TNF-α, as well as by some

bacterial products, and can conversely be suppressed by anti-inflammatory molecules, such as IL-10 and glucocorticoid hormones.[7]

Chemokines are grouped into four families based on the arrangement of NH_2-terminal cysteine residues that link the N-terminus with the C-terminus via two disulfide bridges.[8, 9] The chemokine families include CXC, CC, CX_3C, and C. The CXC family of chemokines is referred to as the α-chemokines, whereas the CC family of chemokines is referred to as the β-chemokines.[10] The α-chemokines mostly recruit neutrophils and lymphocytes, whereas the β-chemokines mainly bind lymphocytes, monocytes, mast cells, and eosinophils.[7] Chemokines play important roles in development and homeostasis and can further be categorized as either homeostatic or inflammatory. Homeostatic chemokines are involved in immune system genesis and organization, whereas inflammatory chemokines are activated during acute inflammation, chronic inflammation, and the adaptive immune response.[3]

Chemokines have been shown to play important roles in numerous inflammatory diseases. For example, CXCL9 is upregulated in rhesus macaque spleen upon SIV infection.[11, 12] CXCL10 has been linked to the pathogenesis of psoriasis, as it is upregulated in the epidermis of infected patients.[13] Increased CXCL10 has also been associated with Dengue virus infection, as have CCL2, CCL3, CCL5, and CCL17.[14, 15] Numerous chemokines, including CXCL10, CCL5, CCL2, and CCL3, play a role in influenza virus infection.[16, 17] Furthermore, CXCL1 and CXCL2 have been associated with CNS-based autoimmune disorders, such as multiple sclerosis (MS) and experimental autoimmune encephalomyelitis (EAE), in mice.[18, 19, 20]

While there are 50 chemokines that could potentially be studied, I have focused on three: CCL20, CCL21, and CXCL13. These chemokines are central to the body's immune responses and have been studied in conjunction with HIV/SIV infection. These three chemokines are all

found in lymph nodes (LNs), but each in a different compartment. CCL20 can be found in the subcapsular sinus, whereas CCL21 and CXCL13 are found more internally in the cortex. More specifically, CCL21 is expressed in the paracortex and CXCL13 is expressed in the germinal centers of the B-cell follicles.[21] Transcriptional control of the expression of these chemokines could inform the design of future HIV-1 vaccines. A number of studies have examined the human CCL20 promoter (huCCL20p), but no studies have been performed on macaque chemokine promoters. Further, very few studies have been conducted looking at the CCL21 and CXCL13 promoters in any model system.

1.1.1 Chemokine CCL20

CC-chemokine ligand 20 (CCL20), also known as macrophage inflammatory protein-3α (MIP-3α), liver activation regulated chemokine (LARC), and SCYA20, is a chemokine that attracts immature dendritic cells (DCs), effector and memory T-cells, and B-cells.[22] The *ccl20* gene is located on chromosome 2 in humans and chromosome 12 in rhesus macaques. It serves as the only known chemokine ligand for CC-chemokine receptor 6 (CCR6) and is highly expressed in lung, liver, and inflamed tissue.[22, 23] CCL20 plays a central role in managing both innate and acquired immunity via the chemoattraction of immune cells to a site of infection.[23] It draws immature DCs to the skin and mucosa under both homeostatic and inflammatory conditions and has also been shown to possess antimicrobial activity.[24] Increased CCL20 levels have been suggested to contribute to the transmission of SIV via the female reproductive tract.[25] Pro-inflammatory cytokines, such as tumor necrosis factor-α (TNF-α), interleukin-1 (IL-1), IL-17, and interferon-γ (IFN-γ), as well as lipopolysaccharide (LPS) and viral infection, can

stimulate cells to produce CCL20.[22] This upregulation of CCL20 has been shown to occur via the NFκB pathway as deletion of the NFκB binding site decreases huCCL20p activity.[23, 26]

1.1.2 Chemokine CCL21

CC-chemokine ligand 21 (CCL21), also known as secondary lymphoid tissue chemokine (SLC), 6Ckine, and exodus, regulates the homing of naïve T cells, natural killer (NK) cells, DCs, and central memory T cells to lymphoid tissues by binding CC-chemokine receptor 7 (CCR7).[1] The gene for CCL21 is located on human chromosome 9 and rhesus chromosome 15. CCL21, produced by stromal cells, is constitutively expressed in the LNs, spleen, and Peyer's patches, in addition to being expressed in high endothelial vessels (HEVs) in LNs and lymphatic vessels in peripheral tissues.[27]

CCL21 is necessary for migration, via afferent lymphatic vessels, of antigen-presenting DCs and tumor cells from peripheral tissues to draining LNs.[28] When expression and secretion of CCL21 is disrupted, lymphocyte circulation and recruitment of cells to LNs is affected.[1] As shown by CCR7-deficient mice, CCL21 and CCR7 are needed for normal migration, entry, and retention of T cells and DCs in lymphatic vessels and secondary lymphoid organs.[29, 30]

1.1.3 Chemokine CXCL13

CXC-chemokine ligand 13 (CXCL13) is the most prominent B cell chemoattractant.[31] It is also known as B-lymphocyte chemoattractant (BLC) and B cell-attracting chemokine 1 (BCA-1), with its gene located on human chromosome 4 and rhesus chromosome 5. Expression of its receptor, CXC-chemokine receptor 5 (CXCR5), also known as Burkitt's lymphoma receptor 1

(BLR-1), is present on B cells, follicular B helper T (TFH) cells, osteoblasts, podocytes, and a subset of skin-derived dendritic cells.[32] CXCL13 is largely produced by follicular dendritic cells (FDCs) and is important for the recruitment of B cells and T cells to sites of infection and inflammation during the inflammatory process.[31, 33, 34] This chemokine further plays a critical role in the formation of germinal centers.[31] B cell follicles of secondary lymphoid organs, in addition to pleural and peritoneal cavities and ectopic lymphoid follicles within the synovial membrane of rheumatoid arthritis patients, constitutively express CXCL13.[31, 32] Our lab has previously demonstrated its expression within Paneth cells of the intestinal tract (C. Lucero, unpublished observation) making it the first chemokine shown to be expressed by cells specialized in the production of antimicrobial peptides. This discovery implies multiple transcriptional regulators of the gene, as CXCL13's expression in Paneth cells and lymphoid tissue germinal centers is likely controlled by different sets of transcription factors.

1.2 TRANSCRIPTIONAL CONTROL AND TRANSCRIPTION FACTOR BINDING SITES

For any gene to be expressed, transcription is the first process that must occur. The transcription of genes is regulated by a promoter region of DNA containing regulatory elements, or transcription factor binding sites, where transcription factors bind to either activate or repress transcription of a specific gene.[35] In contrast to an enhancer region, which may or may not be necessary for the transcription of a particular gene, a promoter is always needed. In order for transcription to occur, an RNA polymerase complex must sit down on the DNA at the TATA box generally located approximately 25 to 35 bp upstream of the transcription start site. The

initiation of transcription, as well as much transcriptional control, relies on the promoter region. A number of transcription factors studied in relation to chemokine expression are highlighted here.

1.2.1 Transcriptional Process

During the process of transcription, an RNA polymerase duplicates the information found on a strand of DNA into RNA.[36] The act of transcription is comprised of three main steps: initiation, elongation, and termination. It is during initiation that an RNA polymerase finds the promoter region of a gene and begins the process of copying DNA into RNA.[37] Three RNA polymerases are found in eukaryotes. Here, I focus on genes that are transcribed into mRNA by RNA polymerase II, which is responsible for the transcription of protein encoding genes. Alternatively, RNA polymerase I transcribes rRNA and RNA polymerase III transcribes tRNA.[36] The copying of DNA into RNA continues during elongation of the RNA transcript and ends when both the RNA polymerase and the newly synthesized RNA transcript disconnect from the DNA template during the termination step.[37] Here, the focus falls mainly on the initiation step and the role of the promoter region.

The promoter region is located upstream of the coding region of a gene and functions to aid the RNA polymerase in determining where and in what direction to begin transcription.[36] The core promoter is necessary for the accurate initiation of this process.[38] Different from promoters are enhancers that aid in increasing transcription of a certain gene, but are not necessary for the gene to be transcribed.

RNA polymerase II cannot recognize the core promoter and, therefore, a pre-initiation complex must first form in order for the polymerase to bind and for transcription to begin.[38] This

complex is comprised of general transcription factors that recognize the core promoter and allow the RNA polymerase to bind. Site-specific transcription factors govern the rate of complex formation.[39] This complex often encounters abortive initiation, where short transcripts are released when the polymerase is unable to dissociate from the core promoter.[37]

Gene expression is often induced via environmental, mechanical, chemical, or microbiological stimuli.[40] Here, I use various pro-inflammatory cytokines to induce transcription from macaque chemokine promoters. Cytokines used in the following studies include tumor necrosis factor-α (TNF-α) and interleukin-1β (IL-1β). In addition, interferon-γ (IFN-γ) served as a negative control as 293T cells lack its receptor. Oncostatin M (OSM) was also used in an attempt to stimulate the CCL21 promoter. In addition to cytokines, sodium butyrate was utilized in an effort to stimulate the macaque chemokine promoters and LPS served as a second negative control.

1.2.2 Transcription Factor NFκB

NFκB, a transcription factor common in the control of immune-relevant genes, has been identified in numerous cell types and tissues and regulates more than 200 genes involved in inflammation, immunity, growth, and cell death.[41, 42, 43] Increased NFκB often contributes to inflammatory disease.[40, 44] In mammals, the NFκB family is comprised of five members: RelA/p65, RelB, c-Rel, p50, and p52.[40]

NFκB has three potential subunits, as it is usually expressed as a heterodimer of two DNA-binding proteins, p50, a 48-55 kDa protein, and p65, a 65-68 kDa protein. In its inactive form, a third subunit, the inhibitory IκB binds the p65 subunit.[42] When IκB is bound, NFκB is considered to be in a resting state, remaining inactive in the cytoplasm.[40]

Activation of NFκB can occur in response to free radicals, inflammatory stimuli, cytokines, carcinogens, tumor promoters, endotoxins, γ-radiation, UV light, or X-rays.[43] Soluble and membrane-bound extracellular ligands, including members of the TNFR, TLR, IL-1R, and antigen receptor superfamilies, can activate the pathway.[40] The activation of a protein tyrosine kinase phosphorylates the IκB subunit, activating NFκB.[45] Phosphorylation allows for the ubiquitination of IκB, and its subsequent degradation by a 26S proteasome, allowing the remaining heterodimer of NFκB to migrate from the cytoplasm to the nucleus, where it binds a κB site, a compatible DNA sequence in the promoter region of a gene.[40, 43, 46] NFκB is believed to recruit transcriptional coactivators, changing chromatin and allowing transcription to occur. [40]

With respect to chemokine transcriptional regulation, transcription factor binding sites, including those for NFκB, have been identified in chemokine promoter regions.[22, 23, 47, 48] NFκB binds DNA regulatory sequences of 5'-GGGRNNYYCC-3′, where R refers to a purine, Y refers to a pyrimidine, and N refers to any nucleotide.[49] NFκB has also been shown to be a potent regulatory factor of HIV replication.[50]

1.2.3 Other Common Immune-Related Transcription Factors

There are a large number of transcription factors controlling the transcription of immune-related genes, including chemokines. The following are some of those factors.

Activator protein 1 (AP-1) controls genes for modulators of invasion and metastasis, proliferation, differentiation, and survival, as well as hypoxia- and angiogenesis-associated genes.[51] AP-1 coactivated with NFκB is necessary for the expression of CCR7 mRNA.[52] Activator protein 4 (AP-4) is constitutively expressed and, while it can activate both viral and cellular genes, was first identified as a transcription factor binding Simian Virus (SV) 40,

activating viral late gene transcription.[53, 54] CCAAT/enhancer-binding protein α (c/EBPα) serves as an important regulator of granulocytic differentiation of common myeloid progenitor cells.[55] The GATA family of transcription factors contributes to embryogenesis, cell differentiation, regulation of tissue-specific genes, and carcinogenesis.[56] Upstream stimulating factor (USF) is a constitutively expressed, stress responsive transcription factor regulating a number of genes involved in humoral-antibody response mediated by B-cell production of immunoglobin and cell-mediated immune response involving cytotoxic and helper T lymphocytes.[57] Furthermore, activation by the USF transcription factor may require coactivators and other transcription factors and, in some situations, USF represses transcription.[58]

1.3 HIV/SIV

The HIV/AIDS pandemic has taken over 25 million lives since its discovery approximately 30 years ago.[108] On average, the disease takes as many lives as three World Trade Center attacks daily.[59] The virus was discovered in 1983 by Barre-Sinousi and others.[6] The first known positive human sample of HIV-1 was recorded in Kinshasa, Zaire in 1959, but the virus is estimated to have made the species jump from nonhuman primate to human around 1931, plus or minus twelve years.[59] The HIV virus eventually leads to acquired immunodeficiency syndrome (AIDS), weakening the immune systems of those affected, usually allowing opportunistic infections to take hold, eventually causing death. Tuberculosis is the most common of these secondary infections.[59] Approximately 75% of HIV infections occur via a mucosal route, with much of the other 25% stemming from blood infections via contaminated needles and transmission from mother to fetus.[60] Currently no cure exists, but the disease can be managed in

many patients via highly active anti-retroviral therapy (HAART), which uses a combination of reverse transcriptase and protease inhibitors; HAART cannot, however, eliminate virus.[6]

1.3.1 HIV Virus Structure and Life Cycle

The HIV virus is a member of the *Retroviridae* family and *Lentivirus* genus. The mature virion is an approximately 100 nm icosahedral sphere.[6] This enveloped retrovirus requires a human host for replication, as it does not itself possess all the necessary enzymes for replication. HIV infects macrophages, monocytes, and some $CCR5^+$ T cells.[7] However, the initial mucosal targets of HIV are $CD4^+$ T cells.[61] Its entry into cells occurs via interaction with CD4, but various co-receptors, most commonly the chemokine receptor CCR5, are also crucial for infection.[62] Viral entry is attributed to the gp120 protein of the virus, as mutant virus lacking gp120 is unable to bind CCR5.[63] After glycoprotein binding to CD4, conformational changes occur enhancing the virus' ability to bind CCR5, as well as other chemokine receptors, and, therefore, to enter into the host cell.[6, 62] Increases in affinity of gp120 for CCR5 of 100- to 1000-fold result after incubation with soluble CD4.[63] The ability of the virus to bind chemokine receptors results in competitive binding with chemokines. Soluble forms of gp120 inhibit binding of radiolabeled chemokines to their appropriate chemokine receptors.[62, 64, 65, 66]

Once gp120 binds to receptors on the cell it will infect, its viral envelope fuses with the target cell's membrane, allowing for release of the HIV capsid into the cell. HIV RNA is then reverse transcribed into DNA using virally encoded reverse transcriptase, which is transported to the nucleus where virally encoded integrase incorporates it into the host genome. Host encoded transcription factors are needed for production of virus, most commonly NFκB, which is upregulated upon activation of T cells.[49] Once the viral DNA is transcribed, the mRNA is

spliced and multiply spliced mRNAs are exported to the cytoplasm and translated into the regulatory proteins Tat and Rev. Rev is necessary for allowing unspliced mRNA to leave the nucleus. Once a sufficient amount of Rev has built up, full-length viral mRNA can leave the nucleus. The structural proteins Gag and Env can then be produced and new viral particles are formed, with the host cell membrane composing the viral envelope.[6, 59]

1.3.2 Use of SIV as an Experimental Model for HIV

Simian immunodeficiency virus (SIV) has proven very similar to HIV-1 infection and serves as a good model system for the virus. Similar to what is seen in HIV-1 infected patients, the severity and speed of progress of SIV directly correlates to viral load.[67] It has been shown in macaques that are not naturally infected with SIV, that SIV infection causes high levels of viral replication, progressive $CD4^+$ T-cell depletion, chronic immune activation, and a mucosal and systemic immunodeficiency very similar to human AIDS.[68] SIV also serves as a good model for HIV as the two viruses share a similar genome structure and replication mechanism, in addition to sharing a tropism for CD4 and requiring cofactors, commonly CCR5, for infection of cells.[67] Additionally, both HIV-1 and SIV are capable of using either human or macaque CD4 as a receptor.[69] SIV is further a good model system for HIV-1 due to the wide availability of multiple molecular clones that differ in cellular tropism and virulence.[70] Currently, the most successful vaccine against SIV uses live attenuated virus and provides broad protection.[71]

1.3.3 Role of Chemokines in HIV/SIV Infection

As previously mentioned, HIV-1 uses chemokine receptors as co-receptors for entry into host cells. The discovery that CD4 is necessary, but not sufficient, for HIV-1 entry into host cells was made in 1984.[6] A 32 bp deletion in the CCR5 chemokine receptor allele has shown the necessity of a co-receptor for HIV entry. Homozygotes for the mutation possess a strong resistance to infection, whereas heterozygotes, while not completely protected, exhibit a slower rate of progression to AIDS and a lower viral load associated with decreased CCR5 surface expression.[7]

Additionally, the ability of HIV-1 to switch from using CCR5 as a co-receptor to using CXCR4 is a hallmark of progression to AIDS. Most HIV-1s are M-tropic, or partial to entering macrophages via CCR5. As the disease progresses, the virus undergoes random mutations that alter its affinity for chemokine receptors. Often, in approximately 50% of patients progressing to AIDS, the virus becomes T-tropic, showing greater affinity for T cells via the receptor CXCR4, leading to increased virulence, T cell depletion, and eventual immune system collapse, heightened by opportunistic infections.[7]

Data show slower progression of HIV-1 results from higher levels of CC-chemokines, but also that HIV-1 infection, in vitro, is increased as a result of cell activation via these chemokines.[6] Upon HIV-1 infection, leukocytes gather in both lymphoid and non-lymphoid patients, correlating with increased chemokine expression.[70] In regard to SIV infection, both rhesus and cynomolgus macaques show increased inflammatory chemokine levels in the LNs and spleen upon infection.[72]

The three chemokines studied in this thesis, CCL20, CCL21, and CXCL13, have each been previously shown to share a connection to HIV-1 and/or SIV infection. Inflammatory

chemokine CCL20 facilitates nuclear migration and integration of HIV-1 and increased CCL20 levels contribute to the transmission of SIV via the female reproductive tract.[8, 25] CCL20 has also been shown to possess anti-viral activity against HIV-1.[73]

CCL21, as well as CCL17, CCL22, CCL25, and CXCL12, is among the chemokines downregulated upon SIV infection.[72] Increased permissiveness of resting $CD4^+$ T cells to HIV-1 infection has been demonstrated in response to increased CCL21 levels.[8] Perhaps most important is the link between DCs and CCL21 during HIV-1/SIV infection. It has been shown in lymphoid tissues that DCs increase during early HIV-1/SIV infection, but significantly decrease during AIDS, in correlation with chemokine expression changes.[72] Specifically, CCL21 expression decreases in LNs upon SIV infection. This is important because, upon antigen uptake, DCs mature and express increased levels of the CCL21 chemokine receptor CCR7. This allows the DCs to migrate toward CCL21 expressed in draining lymphatics and paracortical regions of LNs.[72] With decreased amounts of CCL21, many DCs are less likely to make their way to the site of immune induction.

Finally, CXCL13, a homeostatic chemokine expressed in germinal centers, undergoes upregulation after SIV infection. This could potentially alter trafficking of DCs, B cells, and follicular helper T cells to germinal centers and affect antibody responses to infectious agents.[72]

1.4 POTENTIALLY ANTI-INFLAMMATORY AND/OR ANTIVIRAL COMPOUNDS

There are a number of pharmaceutical and natural product anti-inflammatory compounds. For example, green tea has numerous health benefits and therapeutic properties, including antibacterial, antiviral, antifungal, and anti-toxin effects.[43, 50] In addition, glycerol monolaurate,

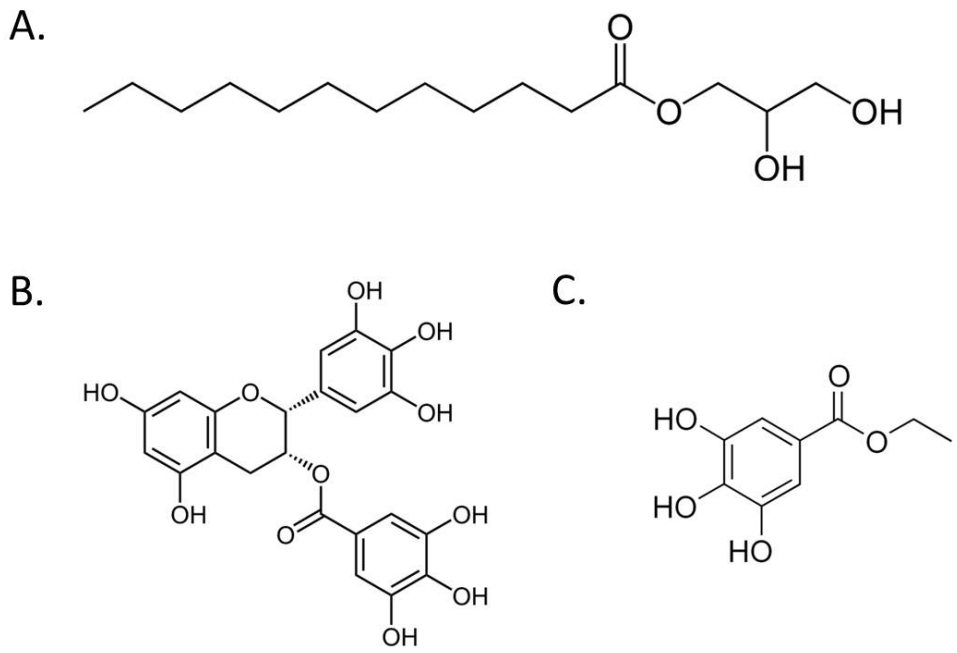

Figure 1. Structures of (A) GML, (B) EGCG, and (C) EG. Images from Wikipedia.com.[109, 110, 111]

added to foods and cosmetics, possesses antimicrobial properties.[74, 75, 76, 77] Further, ethyl gallate holds antioxidant, antiparasitic, and antimicrobial functions.[71, 78, 79, 80] In this thesis, the effects of some of these compounds on chemokine promoter transcriptional regulation have been explored.

1.4.1 Glycerol Monolaurate

Glycerol monolaurate (GML, 2,3-dihydroxypropyl dodecanoate) is a naturally occurring 12 carbon fatty acid monoester (Figure 1A).[74] It occurs naturally in humans, found especially in breast milk.[74, 75] The Food and Drug Administration (FDA) has declared GML safe for oral use and it is often used as an emulsifier and preservative in foods and cosmetics.[74, 75, 76] GML

possesses bactericidal properties against many Gram-positive bacteria, decreases the production of proinflammatory cytokines and chemokines, and blocks the activation of T cells.[74, 76, 77] It acts through an interference with membrane signal transduction, thus inhibiting transcription.[74, 75] At low concentrations, GML can inhibit numerous toxins, and, at high concentrations, can inhibit the replication of several viruses.[77]

A study by Li *et al*., explored the use of GML as a microbicide. It was discovered that GML decreases production of CCL20 among cells of the female reproductive tract, possibly inhibiting the recruitment of $CD4^+$ T cells to sites of infection.[81] These $CD4^+$ T cells, along with macrophages, are target cell populations of the HIV-1 and SIV viruses. In this model for inflammation-driven SIV transmission, CCL20 production allows for the recruitment of plasmacytoid dendritic cells (pDCs), which express the chemokines CCL3 and CCL4, as well as high levels of type I IFNs (Figure 2). These chemokines are ligands for the chemokine receptor CCR5, expressed on the surface of $CD4^+$ T cells. HIV-1 and SIV use CCR5 as a coreceptor to infect cells and replicate, resulting in competition for binding sites between HIV-1/SIV and CCL3/CCL4. Overall, the authors of the paper observed a decrease in SIV transmission upon mucosal treatment with GML.[81] In this thesis, the effects of GML and other compounds on chemokine transcriptional regulation are tested.

1.4.2 (-)-Epigallocatechin Gallate

Green tea, brewed from the leaves of the plant *Camellia sinensis*, possesses numerous health benefits, showing therapeutic benefits for diabetes, Parkinson's disease, Alzheimer's disease, stroke, and obesity.[43] Green tea possesses antibacterial, antiviral, antifungal, and anti-

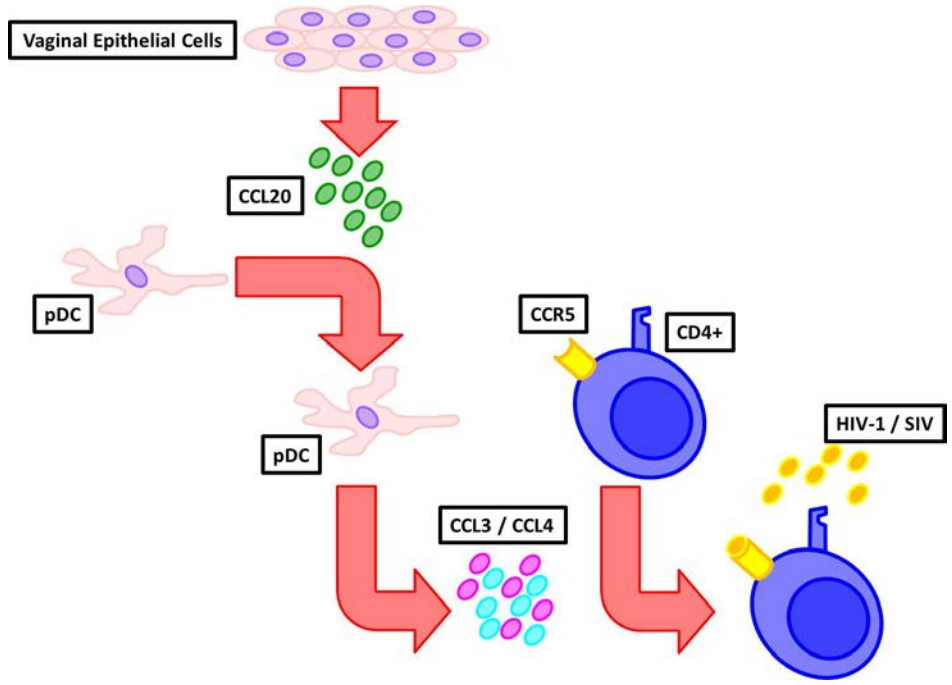

Figure 2. Schematic of a model proposed by Li *et al.*[81] for the role of CCL20 in HIV/SIV mucosal transmission. In response to viral encounter, vaginal epithelial cells (VECs) secrete CCL20. CCL20, in turn, recruits plasmacytoid dendritic cells (pDCs) to the site of infection. pDCs secrete the chemokines CCL3 and CCL4, both of which bind the receptor CCR5. CCR5 is found on $CD4^+$ T cells, which then migrate to the site of infection. HIV-1/SIV use CCR5 as a coreceptor for entry, causing competitive binding of the virus with CCL3 and CCL4.

toxin effects, in addition to having potential anti-tumor properties.[50] The polyphenols of green tea inhibit cell proliferation and exert strong antiradical activity.[43]

The polyphenols of green tea are comprised mostly of catechins, a type of flavonoid found in some plant-derived products, such as berries, fruits, chocolate, wine, and green tea.[41, 82] Numerous isomers of catechins exist as a result of the addition of pyrogallol or galloyl groups on the main flavan-3-ol structure.[50] Catechins compose roughly 10-15% of green tea, with (-)-epigallocatechin gallate (EGCG) comprising approximately 50-80% of the catechin isomers.[43] Furthermore, EGCG remains the most potent of these isomers, containing both pyrogallol and

galloyl moieties (Figure 1B).[50] Each brewed cup of green tea contains approximately 200-300 mg of EGCG.[43]

EGCG interferes with numerous signal transduction pathways, including inhibition of protein kinases, blocking of growth receptor mediated pathways, and suppression of the activation of transcription factors.[43] One pathway EGCG interferes with is that of NFκB, which is necessary for the activation of the transcriptional promoters of numerous genes.[50] EGCG has specifically been shown to interfere with the NFκB pathway in H891 head and neck cancer cells and MDA-MB-231 breast cancer cells, among other cell types.[43] EGCG also interferes with RNA and DNA polymerases.[50]

A study performed by Jacob *et al*., examined the ability of EGCG to affect the transcription of human Brf1 and Brf2 by RNA polymerase III.[41] The researchers observed a decrease in protein expression of both Brf1 and Brf2 after exposure to EGCG and further hypothesized three possible mechanisms of action. They believed the decrease resulted from an increased rate of Brf1 and Brf2 protein turnover, a decrease in the stability of Brf1 and Brf2 mRNA, or a decrease in the expression of Brf1 and Brf2 genes. They further showed a decrease in luciferase expression from under the control of the Brf2 promoter after exposure to EGCG. The decline could result from EGCG's mechanisms of action on the NFκB site of the Brf2 promoter, as EGCG affects this transcription factor.[41]

1.4.3 Ethyl Gallate

Ethyl gallate (EG), a derivative of gallic acid, is an antioxidant phenolic compound often used as a food additive (Figure 1C).[78] It is relatively nontoxic and is found in numerous food substances, including red wine and walnuts.[83] EG has been shown to possess numerous

biological activities, including antiparasitic and radical scavenger properties, as well as exhibiting a possible antioxidant mechanism.[79, 80, 84] Anticancer activities were shown as EG induces apoptotic cell death in various cancer cell lines.[85] In addition, EG has been shown to be an antimicrobial agent, as it increases β-lactam susceptibility in methicillin-resistant and methicillin-sensitive strains of *Staphylococcus aureus*.[71] The anti-inflammatory effects of EG have also been explored via the treatment of macrophages, which displays a significant inhibition of LPS-stimulated nitric oxide production.[78] It has also been shown to block the transcription factor AP-1, whereas it has not been shown to have an effect on NFκB.[86]

2.0 STATEMENT OF THE PROBLEM

HIV/AIDS has greatly impacted worldwide public health, taking over 25 million lives throughout the past 30 years. As a result, it remains one of the world's leading infectious killers.[108] Currently, no cure exists for HIV, only antiretroviral therapy (ART) that slows viral replication. The need for a cure and/or a vaccine, however, remains. Simian immunodeficiency virus (SIV) serves as a good model for studying HIV-1 infection and disease.

Inflammation is a component of the disease process of HIV-1 and SIV infection. Involved in cellular migration and inflammation are small, secreted proteins called chemokines. Their importance arises as they play a role in the immune system's recruitment of immune cells to areas of infection. For this reason, I set out to study the transcriptional regulation of a subset of macaque chemokines important for the body's immune response, particularly CCL20, CCL21, and CXCL13, and adapted methods to do so.

It has been shown that SIV transmission via the female reproductive tract is associated with higher levels of CCL20 expression. It would, therefore, seem rational to hypothesize that by decreasing CCL20 levels in the female reproductive tract, SIV transmission could be decreased. CCL20, CCL21, and CXCL13 have all been shown to be affected in some way by HIV-1/SIV infection and all have homeostatic inflammatory roles in LN immunobiology. It is, therefore, reasonable to study ways of blocking changes in the transcriptional levels of these genes. **The objective of this study was to develop a system for studying macaque chemokine**

transcriptional regulation by cloning and examining the promoter regions of multiple macaque chemokines.

2.1 SPECIFIC AIM 1: TO DEVELOP A LUCIFERASE-BASED REPORTER ASSAY FOR STUDYING THE TRANSCRIPTIONAL CONTROL ELEMENTS OF MACAQUE CHEMOKINES CCL20, CCL21, AND CXCL13

Cellular transcription controls gene expression, determining which cells will express which genes and at what times these genes will be expressed. It is, therefore, necessary to understand the controllers of chemokine gene expression and how expression might affect disease and immune response. Previous studies have looked at the role of the promoter regions of human chemokine genes.[22, 23, 26, 87] I, however, wished to look at these promoter regions in the macaque model system and, more specifically, study the transcriptional control of the macaque chemokines CCL20, CCL21, and CXCL13.

To study macaque chemokine transcriptional control, I began by isolating the promoter regions of the rhesus macaque chemokines CCL20, CCL21, and CXCL13, which I subsequently sequenced. Putative transcription factor binding sites were then mapped, allowing for an in depth window into possible transcriptional regulation. To measure transcriptional control via each of these promoters, each promoter region was subcloned into the promoterless pGL2-Basic reporter plasmid vector and a dual-luciferase reporter assay for measuring gene expression via chemokine promoters was developed.

By developing such an assay, factors, such as cytokine stimulation, reagent inhibition, viruses, and potential vaccine or therapeutic agents, that may upregulate or downregulate

chemokine expression can be further studied. These studies could aid understanding of the mechanisms controlling the expression of macaque chemokines in various cell types. Findings of this research could potentially pave the way for methods of further studying approaches to modulate chemokine expression of combating disease, as well as possible vaccination and/or treatment strategies.

2.2 SPECIFIC AIM 2: TO APPLY A LUCIFERASE-BASED REPORTER ASSAY TO EXAMINE POTENTIAL THERAPEUTIC REGULATORS OF CHEMOKINE TRANSCRIPTION

By identifying a method of controlling gene expression, we open the door to potential developments for vaccines and treatments of numerous diseases. Transcriptional control is one way to regulate gene expression. Chemokines play a part in immune responses and perform roles in numerous diseases. It is, therefore, important to study possible mechanisms of chemokine transcriptional control.

Glycerol monolaurate (GML), an emulsifier and preservative in the cosmetic and food industries, has been linked to reduced CCL20 levels in the female reproductive tract, inhibiting the recruitment of HIV-1/SIV target cells and reducing the spread of HIV-1/SIV.[81] However, whether this link is direct, or through some other mechanism, remains unknown. EGCG, the main catechin of green tea, boasts numerous potential health benefits, and recent research shows it blocks transcription of some chemokines via interference of the NFκB pathway.[43, 50, 88] EG also possesses numerous biological activities and health benefits and has been shown to block the transcription factor AP-1.[86]

Here I studied the effects GML, EGCG, and EG treatments have on macaque chemokine transcriptional control via the CCL20, CCL21, and CXCL13 promoters by using 293T cells and the luciferase-based assay I developed for macaque chemokine promoters. If luciferase expression decreased after treatment with a potentially anti-inflammatory and/or anti-viral compound, transcription from chemokine promoters was likely blocked. Both basal and stimulated levels of transcriptional control were measured and the effects of these treatments on those levels were observed. Stimulation induction was via treatment with pro-inflammatory cytokines, including TNF-α and IL-1β. Results of these stimulation and inhibition studies can help further the understanding of chemokine transcriptional regulation.

3.0 MATERIALS AND METHODS

3.1 SUBCLONING OF MACAQUE CHEMOKINE PROMOTERS INTO THE PGEMT VECTOR SYSTEM

The predicted promoter regions of three macaque chemokines, CCL20, CCL21, and CXCL13, were PCR amplified from rhesus genomic DNA (gDNA) (courtesy of Dr. Jeremy Martinson and Blair Gleeson). Primers were constructed (Integrated DNA Technologies) approximately 1,000 bp upstream and 200 bp downstream of the translation start site and are outlined in Table 1. PCR cocktails were prepared using these primer pairs (Table 2) and PCR reactions were performed using a PTC-200 Peltier thermal cycler (MJ Research). The PCR program used is outlined in Table 3. PCR products were visualized via gel electrophoresis in a 1% agarose gel using GelRed (Biotium).

Bands of sizes corresponding to expected amplicons were extracted and purified using a QIAquick gel extraction kit (Qiagen). Isolated and extracted DNA were ligated into the pGEMT vector system (Promega) via incubation for one hour at room temperature. Reaction conditions are outlined in Table 4. Ligation products were transformed into *E. coli* (strain DH5α) competent cells (subcloning efficiency, Invitrogen). After one hour incubation on ice, cells were subjected to heat shock by placement in a 42°C water bath for 90 seconds, followed by a two minute incubation on ice. Then 300 μL SOC media (Invitrogen) was added and the cells were

Table 1. Primers used to amplify putative chemokine promoter regions from rhesus genomic DNA

Target		Primer Name	Sequence (5' → 3')
CCL20	Forward	LS_rhCCL20p_F1	ATA GGC ATC ACC AAC TCC GGT TC
	Reverse	LS_rhCCL20p_R1	CAC TCC CTC TTG TGT ACT TTC
CCL21	Forward	LS_rhCCL21p_F2	GCC AGA CCC TGA GTC AA
	Reverse	LS_rhCCL21p_R1	GCA GGG TGG GAT TCA CAG GGA
CXCL13	Forward	LS_rhCXCL13p_F2	CCA GAC CAG CCA CTT TCT CC
	Reverse	LS_rhCXCL13p_R2	CCC CCT TTA GTC AGA CTT

incubated for 45 minutes at 37°C, 150 RPM. Transformation products were plated on LB (Luria Bertani) plates supplemented with ampicillin (stock 100 mg/mL, Sigma), IPTG (isopropyl β-D-1-thiogalactopyranoside, stock 100 mg/ml, Fisher), and Xgal (5-bromo-4-chloro-indolyl galactopyranoside, stock 20mg/ml, Roche), and grown overnight (approximately 18 hours) at 37°C.

Single colonies chosen via blue-white selection were grown in 3 mL LB media, supplemented with 3 μL ampicillin (stock 100 mg/mL), at 37°C, 150 RPM overnight (approximately 18 hours). DNA was purified using the Wizard Plus SV Miniprep DNA Purification System (Promega). Purified DNA was subjected to PCR reactions using sequence-specific primers (Table 1) utilizing the same reaction conditions outlined above. The resulting DNAs were visualized on a 1% agarose gel to determine the sizes of the amplified insert sequences.

3.2 SUBCLONING OF MACAQUE CHEMOKINE PROMOTERS INTO A LUCIFERASE REPORTER VECTOR

To subclone the rhesus CCL20, CCL21, and CXCL13 promoters into a promoterless luciferase-expression vector, primers were constructed (Integrated DNA Technologies) to amplify the promoter sequences off the pGEMT-promoter constructs previously generated. These primers, described in Table 5, were designed to shorten each promoter insert so as not to include the translation start site. In addition, each primer was designed to contain a GCC clamp at the 5' end to facilitate the double-strandedness, as well as an overhang restriction enzyme site corresponding to useful sites present in the pGL2-Basic vector (Promega, E1641). Forward primers contained a SacI site and reverse primers contained an XhoI site.

Table 2. PCR reaction conditions

Reagents	Cocktail for One Reaction (µL)	Final Concentration
5X GoTaq Gene Buffer (Promega)	5.0	1X
2 mM dNTPs (Invitrogen)	2.5	5.0 µmol
Forward Primer (25 µM) (IDT)	1.0	1.0 µmol
Reverse Primer (25 µM) (IDT)	1.0	1.0 µmol
GoTaq DNA Polymerase (5 u/µL) (Promega)	0.1	0.5 units
Nuclease-Free Water (Ambion)	14.4	--
Genomic DNA Template (5 ng/µL)	1.0	5.0 ng
Total Volume	**25.0**	

Table 3. PCR program

Step	
1	94°C for 3 minutes
2	94°C for 30 seconds
3	56°C for 30 seconds
4	72°C for 1 minute
5	GoTo 2, 29 times
6	72°C for 10 minutes
7	4°C forever

PCR cocktails were generated in accordance to the outline in Table 2, and PCR reactions were performed in a PTC-200 Peltier thermal cycler (MJ Research) under the conditions outlined in Table 3. DNA products were subjected to gel electrophoresis in a 1% Agarose gel and visualized with the use of GelRed (Biotium). Bands of the appropriate size were extracted and purified using a QIAquick gel extraction kit (Qiagen).

Isolated and extracted promoter inserts, as well as the empty pGL2-Basic vector were subjected to restriction enzyme digest to create cohesive ends for ligation. Cocktails were prepared as per Table 6 and digestion was carried out in a 37°C water bath for three hours. Restriction enzyme products were separated in a 1% agarose gel and bands of corresponding size to targets were gel extracted and purified using a QIAquick gel extraction kit (Qiagen). Digested inserts were ligated into the digested pGL2-Basic vector and subsequently transformed into *E. coli* (strain DH5α) competent cells (Table 7). Transformation products were plated on LB plates supplemented with ampicillin (stock 100 mg/mL) and grown overnight (approximately 18 hours) at 37°C.

Resulting colonies were chosen and grown overnight (approximately 18 hours) in 3 mL LB media supplemented with 3 μL ampicillin (stock 100 mg/mL) at 37°C, 150 RPM. DNA was

Table 4. Ligation reaction conditions for cloning into pGEMT.

Reagents	Cocktail for One Reaction (μL)	Final Concentration
2X Ligation Buffer (Promega)	5.0	1X
pGEMT Vector (50ng/μL)	1.0	50 ng
PCR Product	3.0	--
T4 DNA Ligase (3 u/μL) (Promega)	1.0	3 units
Total Volume	**10.0**	

purified using the Wizard Plus SV Miniprep DNA Purification System (Promega). Purified DNA was subjected to restriction enzyme digest using the conditions previously described, and the resulting products were visualized in a 1% agarose gel to determine if clones contained the correct inserts. Inserts were further confirmed via DNA sequencing carried out by the University of Pittsburgh core sequencing facility and comparison with known sequences available on the UCSC genome browser (genome.UCSC.edu). Clones containing the correct insert were grown overnight and purified using the PureLink HiPure Plasmid Midiprep Kit (Invitrogen).

Cynomolgus macaque chemokine promoters were amplified off gDNA using the same primers detailed above (Table 3) and subcloned directly into the pGL2-Basic vector after restriction digestion with SacI and XhoI using the methods described above. The exception was the CXCL13 promoter, as new primers had to be designed. The forward primer (LS_rhCXCL13pRE_F3) read 5'-GCC GAG CTC CCA GAC CAG CCA CTT TCT CC-3' and the reverse primer (LS_rhCXCL13pRE_R6) read 5'-GCC CTC GAG TCT GTC TGG AGG TAG AG-3'. The gDNA was extracted from cynomolgus macaque cells using the DNeasy

Blood and Tissue Kit (Qiagen). Animals used were M7102 (uninfected, spleen), M6202 (uninfected, hilar LN), M7802 (acute, axillary LN), and M5802 (AIDS, lung).

3.3 SEQUENCING AND MAPPING OF PREDICTED MACAQUE CHEMOKINE PROMOTER REGIONS

Miniprepped plasmid DNAs containing predicted macaque chemokine promoters were sequenced by the University of Pittsburgh core sequencing facility and confirmed by comparison with known sequences available on the University of California Santa Cruz (UCSC) Genome Browser (genome.UCSC.edu). All sequencing was performed using vector specific primers (T7 and SP6 for pGEMT clones and GL1-forward and GL1-reverse for pGL2-Basic clones). Internal primers were designed to sequence the entire length of both strands of DNA and subsequently create a contiguous sequence for each clone. All alignments and analyses were performed using Vector NTI software (Invitrogen).

The sequences obtained for the predicted macaque chemokine promoters were mapped for putative transcription factor binding sites using TRANSFAC software (BioBase). The algorithm was set to minimize false negative results. The output was sorted and binding sites mapped were chosen based on the percentage match of the core and matrix scores.

Table 5. Primers used to amplify putative chemokine promoter regions from pGEMT-promoter constructs for insertion into pGL2-Basic vector.

Target		Primer Name	Sequence (5' → 3')
CCL20	Forward	LS_rhCCL20pRE_F1	GCC GAG CTC ATA GGC ATC ACC AAC TCC GGT TC
	Reverse	LS_rhCCL20pRE_R4	GCC CTC GAG TTA GCT CAA AGA ACA
CCL21	Forward	LS_rhCCL21pRE_F2	GCC GAG CTC GCC AGA CCC TGC GTC AA
	Reverse	LS_rhCCL21pRE_R2	GCC CTC GAG CTG TGG TAA AGG GTG A
CXCL13	Forward	LS_rhCXCL13pRE_F3	GCC GAG CTC CCA GAC CAG CCA CTT TCT CC
	Reverse	LS_rhCXCL13pRE_R4	GCC CTC GAG GTA GAG TTC AGA TTT GAG

3.4 CELL CULTURE AND TRANSFECTION OF HEK293T CELLS

HEK293T cells (ATCC) were cultured in T75 flasks until confluent at 37°C, 5% CO_2. Maintenance flasks were kept and split 1:20 approximately every four days. To split cells, the culture media was discarded and the cells were washed with 5 mL PBS (phosphate buffered saline, BioWhittaker). To detach cells from the culture flask, 3 mL trypsin / 0.05% EDTA (Invitrogen) was added and the cells were incubated at 37°C, 5% CO_2 for two minutes. 3 mL complete DMEM (Dulbecco's modified eagle's medium), supplemented with 5% FBS (fetal bovine serum, Fisher), 1X penicillin/streptomycin (250 units penicillin, 250 μg streptomycin, Gibco), and 1X L-glutamine (1.46 mg, Life Technologies) was subsequently added to the

Table 6. Restriction digest reaction conditions.

Reagents	Cocktail for One Reaction (µL)	Final Concentration
10X NEB Buffer 4 (New England BioLabs)	5.0	1X
10X BSA (New England BioLabs)	5.0	1X (0.5µg)
DNA	15.0	5.0 µg
SacI (20,000 u/mL) (New England BioLabs)	2.5	50 units
XhoI (20,000 u/mL) (New England BioLabs)	2.5	50 units
Nuclease Free Water (Ambion)	20.0	--
Total Volume	**50.0**	

trypsinized cells and the mixture was pipetted up and down to break up cell clumps. The cells were then subjected to centrifugation at 1,200 RPM for five minutes and resuspended in 10 mL complete DMEM. An appropriate amount of resuspended cells were added to culture vessels with fresh complete DMEM.

293T cells and LECs were transfected by using the PolyJet in vitro DNA transfection reagent (SignaGen). Before plating 293T cells, tissue culture treated six-well plates (Corning, #3516) were coated with poly l-lysine diluted 1:5 with nuclease free water. Cells were plated at a cell density of $8x10^5$ cells per well 18-24 hours prior to transfection, and grown at 37°C, 5% CO_2. Medium was discarded and complete DMEM culture medium with serum and antibiotics was added to each well 30-60 minutes prior to transfection. For one well of a six-well plate, 1.0 µg total of DNA was diluted in 50 µL of serum-free DMEM. Empty pGL2-Basic vector was used as 'filler' DNA, when necessary, to bring DNA concentrations to 1.0 µg. 3 µL of PolyJet

reagent was diluted in 50 µL of serum-free DMEM for each transfection and subsequently added to each diluted DNA solution. The PolyJet and DNA mixtures were incubated for 15 minutes at room temperature to allow PolyJet/DNA complexes to form. The complexes were then added to the medium in each well in a drop-wise fashion and the mixture was homogenized by gentle swirling of the plate. Cells were incubated at 37°C and the medium discarded and replaced by 2 mL fresh complete DMEM 18 hours post-transfection. Cells were either left untreated or treated with cytokine stimulation and/or potentially anti-inflammatory agents 18 hours post-transfection.

Cell lysates were harvested 42 hours post-transfection using 500 µL 1X passive lysis buffer (Promega) per well and cell scrapers. To ensure complete lysis of the cells, lysates were subjected to two freeze-thaw cycles (5 minutes on dry ice followed by 20 minutes at room temperature). Lysates were then cleared via centrifugation in a refrigerated microcentrifuge at top speed and the supernatant transferred to fresh tubes. Lysates were stored at -80°C.

Table 7. Ligation reaction conditions for cloning into the pGL2-Basic vector.

Reagents	**Cocktail for One Reaction (µL)**	**Final Concentration**
2X Ligation Buffer (Promega)	10.0	1X
pGL2-Basic Vector	3.0	--
PCR Product	6.0	100 ng
T4 DNA Ligase (3 u/µL) (Promega)	1.0	3 units
Total Volume	**20.0**	

3.5 DUAL-LUCIFERASE REPORTER ASSAYS

Lysates from transfected and control cells were subjected to dual-luciferase reporter (DLR) assays (Promega), following the manufacturer's instructions. Lysates were thawed at room temperature and LARII reagent was thawed in a room temperature water bath. Stop & Glo reagent was mixed just prior to performing the assay (addition of substrate to buffer). Differences from the manufacturer's protocol include using only 30 μL of LARII and Stop & Glo reagents instead of the called for 100 μL.

The settings for the plate reader (FLUOstar Optima) were adjusted based on the manufacturer's suggestion and a program was created (LUM WELL MODE). The positioning delay was 0.2 seconds and the number of kinetic windows was one. The kinetic window was set from 0 seconds to 24 seconds, consisting of 48 0.5 second measurement intervals. Injection of LARII reagent was set to occur at 0 seconds and injection of Stop & Glo reagent was set to occur at 12 seconds. Luminescence readings were taken using the top optic. The gain was set to 2,500 with lens as the emission filter and the number of multichromatics was one. 20 μL of lysate were loaded into the wells of a white polystyrene 96-well plate (Costar, #3912) for measurement. Before assays could be conducted, the automatic reagent injectors were primed with 500 μL of the appropriate reagent.

Lysates were obtained from cells co-transfected with an experimental vector encoding firefly luciferase driven by the promoter under study and a normalization vector, pGL4.74 (courtesy of Dr. Tianyi Wang, Promega, E692A) containing the *Renilla* luciferase gene. The LARII reagent activated the reaction for expression of firefly luciferase, while the Stop & Glo reagent quenched this first reaction and started a second reaction for expression of *Renilla* luciferase. The experimental design was such that the firefly luciferase values could be divided

by the *Renilla* luciferase values for normalization purposes. These obtained values were then multiplied by a constant of 10,000 to obtain the final transformed relative luciferase levels or ratios.

Three experimental controls were always included. A positive control plasmid, pGL2-Control (Promega, E1611), with the expression of firefly luciferase under the control of an SV-40 promoter, co-transfected with pGL4.74, was expected to show positive results for both firefly and *Renilla* readings. A negative control, utilizing empty, promoterless pGL2-Basic vector (Promega) co-transfected with the *Renilla* luciferase plasmid, was expected to be negative for firefly luciferase but positive for *Renilla* luciferase. Finally, a mock transfected sample underwent all the same conditions as the other transfected samples, but was transfected with only PolyJet and no plasmid. These samples were expected to be completely negative and show no reading for either luciferase. Finally, one well transfected with pEGFP was consistently included as a transfection control. By using fluorescence microscopy, transfection efficiency of the experiment could be estimated.

Data analysis was performed using MARS data analysis software (BMG Labtech). Results were further analyzed using Prism software (GraphPad Software, Inc., San Diego, CA).

4.0 RESULTS

4.1 CLONING, SEQUENCING, AND ANALYSIS OF MACAQUE CHEMOKINE PROMOTERS

4.1.1 Rhesus Macaque Chemokine Promoters

Predicted macaque chemokine promoter regions for *ccl20*, *ccl21*, and *cxcl13* were PCR amplified using three different samples of rhesus genomic DNA (gDNA) as template. Using the macaque genome sequence viewed through the UCSC genome browser to design primers, the amplified target of DNA began approximately 1,000 bp upstream and ended approximately 200 bp downstream of the translation start site (Figure 3). Primers were placed in these positions based on previous literature where the promoter region of human *ccl20* had been studied.[23, 75] For the rhesus CCL20 promoter (rhCCL20p), a band sized at 1,265 bp was expected; for CCL21, a band sized at 1,408 bp; and for CXCL13, a band sized at 1,132 bp. The amplified region of the predicted rhesus CCL21 promoter (rhCCL21p) was approximately 200 bp longer than that of the other chemokine promoters because the online reference sequence was incomplete, with a stretch approximately 1,000 bp upstream of the translation start site that had not yet been sequenced.

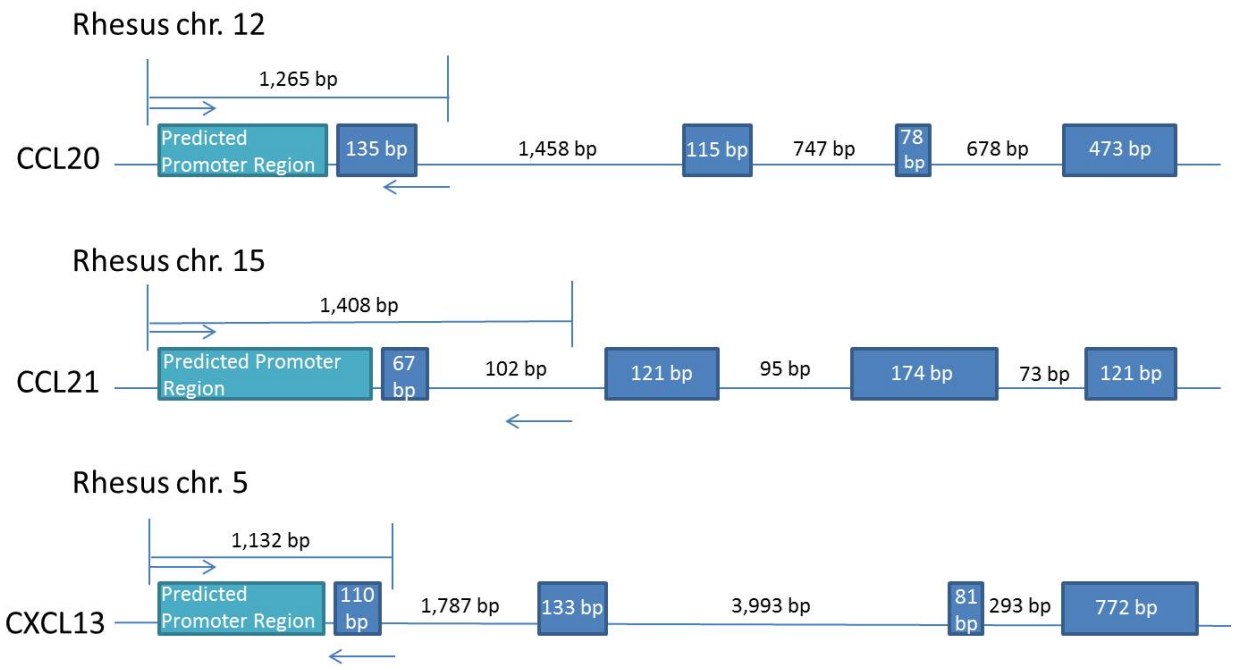

Figure 3. Schematic showing primer design for amplifying putative rhesus macaque transcriptional promoters for CCL20, CCL21, and CXCL13. To obtain what was anticipated to be the promoters of these chemokine genes, primers were designed 1,000 bp upstream and 200 bp downstream of the translation start site. Expected sizes were 1,265 bp, 1,408 bp, and 1,132 bp for the CCL20, CCL21, and CXCL13 promoters, respectively.

PCR products of correct size were obtained for each promoter using gDNA templates from monkeys 2 and 3. PCR using gDNA template from monkey 1 did not produce PCR product, indicating unsuccessful amplification. Because amplification using this template did not work for any of the chemokine promoters, it is likely the problem lied with the rhesus gDNA itself.

After insertion into the pGEMT vector system, one clone was sequenced for each chemokine promoter. An unexpected number of nucleotide differences were observed. To address if these were single nucleotide polymorphisms (SNPs) or errors from the Taq polymerase, additional clones were sequenced. Taq polymerase has been used historically by

our lab for diagnostic and preparative PCR reactions with no major history of Taq errors until recently. We have since moved to a higher fidelity polymerase. In addition, PCR reactions were repeated and a number of these clones sequenced as well.

The eight contiguous sequences for each chemokine promoter were compared to one another, as well as to reference sequences obtained from the UCSC genome browser. Each of these clones was sequenced with Taq polymerase and each revealed different variants. After analysis, it was apparent that, while many SNPs were present, numerous nucleotide changes appeared to be the result of Taq polymerase error (described in detail next for each promoter).

4.1.1.1 CCL20 Transcriptional Promoter

Eight clones of the predicted rhCCL20p were sequenced (Figure 4A). Alignment revealed nucleotide differences in fourteen positions (Figure 4B). Four differences were present in two or more clones, whereas the other 10 differences were each unique to a single clone. Because these 10 differences were unique to single clones, it was difficult to confidently consider them SNPs due to the low fidelity and proofreading error of Taq polymerase. For this analysis, I considered any differences present in a single clone to have arisen from Taq polymerase errors. Clones A and C, both amplified from monkey 2 gDNA, but each from a separate PCR reaction, appeared identical, possessing the same three SNPs at positions -583, -539, and -342. The other two clones amplified from monkey 2 gDNA, B and D, also appeared identical (excluding likely Taq polymerase errors), sharing a single nucleotide insertion at position -137. It is likely clones A and C were amplified from the same allele of monkey 2 gDNA, whereas clones B and D were amplified from the other allele.

Sequencing results from the clones amplified from monkey 3 gDNA were more complicated. Clones E and F, from the same PCR reaction, showed the same SNPs at positions

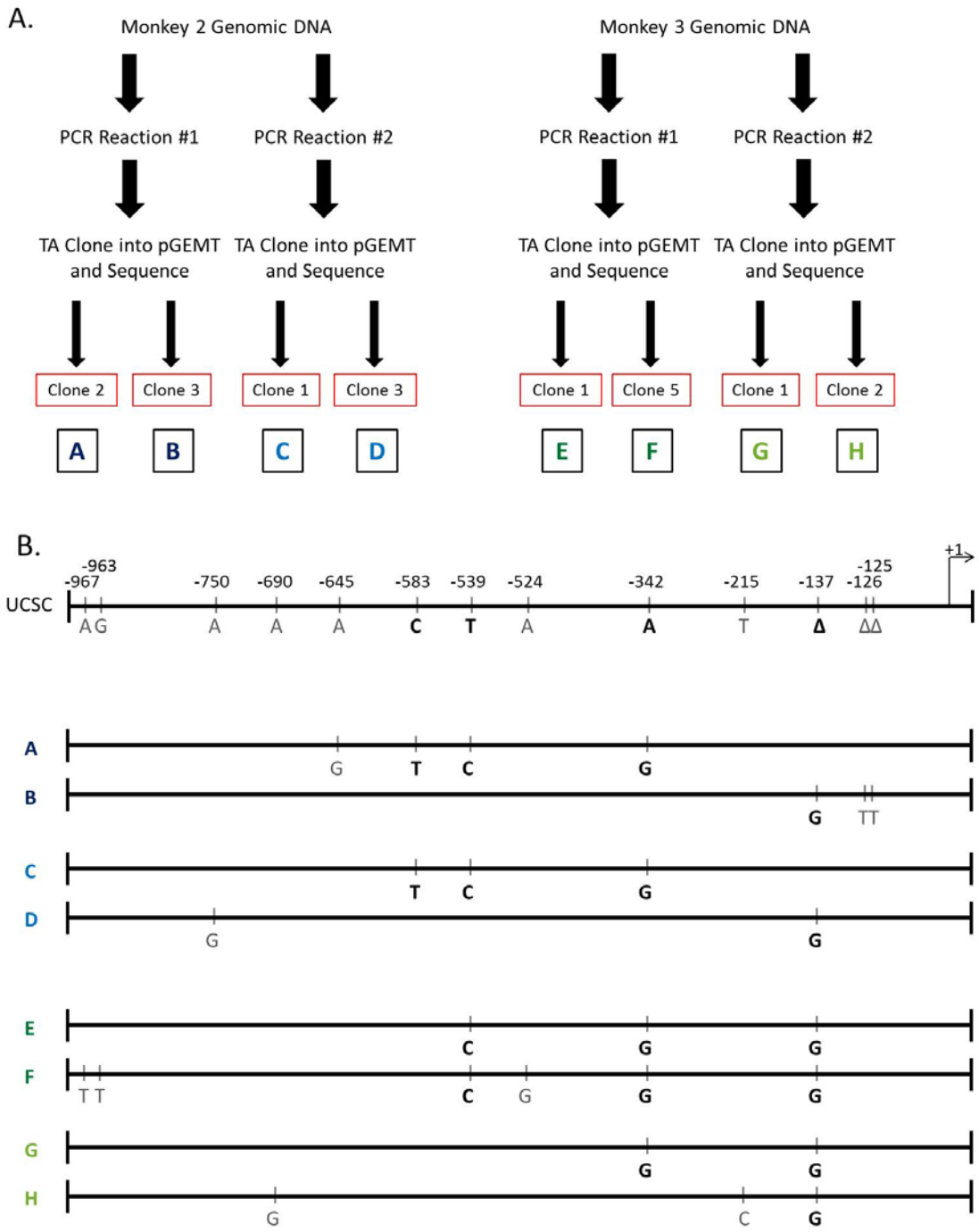

Figure 4. Strategy for sequencing and alignment of multiple rhesus CCL20 promoter clones. The putative CCL20 promoter was amplified from rhesus gDNA, cloned into the pGEMT vector system, and DNA sequenced. (A) Map showing origin of each clone. Two different genomic DNA templates were used in each of two PCR reactions, resulting in eight total clones. (B) Cartoon highlighting differences in sequence between the eight clones. Clones were aligned to a reference sequence (UCSC) downloaded from the UCSC genome browser (chromosome 12, positive strand, NT 91,698,138 - 91,699,355). Nucleotides shown in grey were present in a single clone and it is, therefore, uncertain if these changes are SNPs or errors of the Taq polymerase. Aside from differences unique to one clone, four SNPs were found in the rhesus CCL20 promoter. +1 designates the putative transcription start site. Δ denotes a base pair deletion.

-539 and -342, as well as the insertion of a G at position -137. Clone G also showed the SNP at position -342, and both clones G and H showed the insertion of a G at position -137. From these results, there were a total of three different sequences resulting from monkey 3 gDNA. This result is difficult to explain, but is likely the result of Taq polymerase error.

4.1.1.2 CCL21 Transcriptional Promoter

For the predicted rhCCL21p, eight clones were sequenced and demonstrated a total of thirteen differences (Figure 5). Six differences were unique to single sequences and five of these appeared likely due to Taq polymerase error. The sixth unique change was a thirteen bp deletion beginning at position -822 in clone E, amplified from monkey 3 gDNA. Another fifteen bp deletion beginning at position -973 was present in clones E, F, and G, all amplified from monkey 3 gDNA. All three of these clones also contained an A to C substitution at position -974, just upstream of the deletion. With the exception of the thirteen bp deletion in clone E, clones E and F, from the same PCR reaction, were identical in terms of SNPs. These three clones also contained five SNPs and a three bp deletion at position -1,108. At position -1,108, clone G showed only a one bp deletion. The G to A difference at position -892 and the T to C difference at position -822 were also present in clone G. The deletion of an A at position -388, the C to T substitution at position -276, and the A to G substitution at position -112, however, were present only in clones E and F. The deletion at position -338 was at the end of a long stretch of A's, signifying possible sequencing error.

Clones obtained using monkey 2 gDNA as template showed minimal changes from the UCSC reference sequence. Clones A, B, and C shared the three bp deletion at position -1,108 seen in clones E and F. Clone D showed only a two bp deletion at this position. Being this area

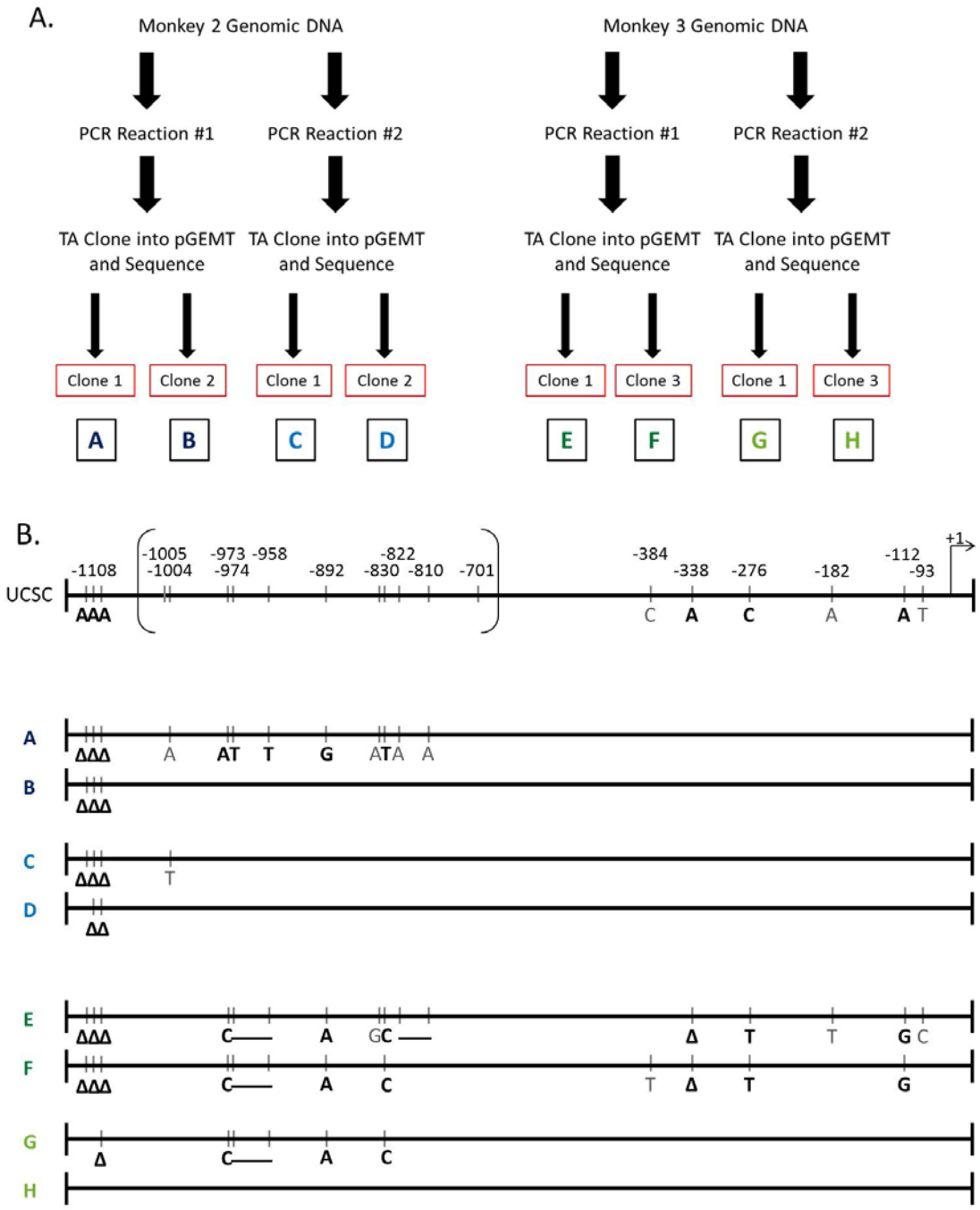

Figure 5. Strategy for sequencing and alignment of multiple rhesus CCL21 promoter clones. The putative CCL21 promoter was amplified from rhesus gDNA, cloned into the pGEMT vector system, and sequenced. (A) Map showing origin of each clone. Two different genomic DNA templates were used in each of two PCR reactions, resulting in eight total clones. (B) Cartoon highlighting differences in sequence between the eight clones. Clones were aligned to a reference sequence (UCSC) downloaded from the UCSC genome browser (chromosome 15, positive strand, NT 42,804,284 – 42,805,691). Nucleotides shown in grey were present in a single clone and it is, therefore, uncertain if these changes are SNPs or errors of the Taq polymerase. Aside from differences unique to one clone, eight SNPs were found in the rhesus CCL20 promoter. +1 designates the putative transcription start site. Δ denotes a base pair deletion.

consisted of a long stretch of As, the high number of differences between the clones could have resulted from sequencing read errors. Finally, it must be noted a reference sequence from positions -701 to -1,005 was unavailable, as this portion of the chromosome had yet to be sequenced.

4.1.1.3 CXCL13 Transcriptional Promoter

Eight clones of the predicted rhesus CXCL13 promoter (rhCXCL13p) were sequenced (Figure 6A). The sequences showed a total of 10 differences, with six unique to a single clone (Figure 6B). At positions -892 through -888, which fell in the middle of a long stretch of T's, numerous differences occurred between the clones. While clones A, B, and C appeared identical at position -892, each of the other clones presented a distinctive sequence. Because of the long stretch of T's, these differences may have been artifact of the sequencing reads. Clones E and F showed no differences in comparison to the reference sequence and all other clones appeared identical to one another, with a G to A substitution at position -641, C to G substitution at position -433, and G to A substitution at position -389. It could, therefore, be stated all clones amplified using monkey 3 gDNA template were identical, as well as showed complete similarity to two clones from monkey 2 gDNA template. Because the other two clones from monkey 3 gDNA remained identical to one another, the SNPs observed were likely present on a single chromosome.

4.1.2 Cynomolgus Macaque Chemokine Promoters

The predicted chemokine promoters of cynomolgus macaques were obtained in a similar fashion to the predicted chemokine promoters of rhesus macaques. Genomic DNA was extracted

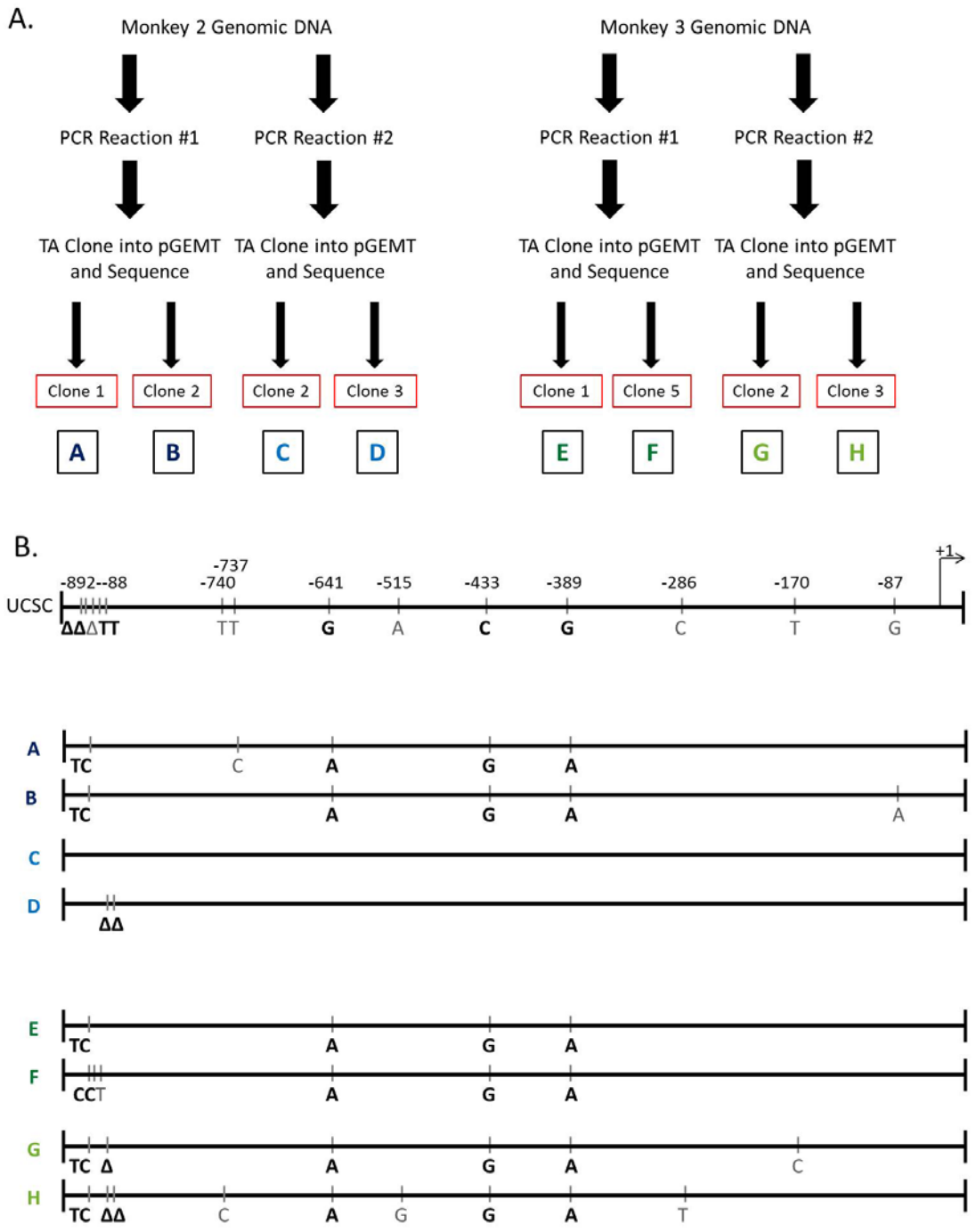

Figure 6. Strategy for sequencing and alignment of multiple rhesus CXCL13 promoter clones. The putative CXCL13 promoter was amplified from rhesus gDNA, cloned into the pGEMT vector system, and sequenced. (A) Map showing origin of each clone. Two different genomic DNA templates were used in each of two PCR reactions, resulting in eight total clones. (B) Cartoon highlighting differences in sequence between the eight clones. Clones were aligned to a reference sequence (UCSC) downloaded from the UCSC genome browser (chromosome 5, negative strand, NT 51,967,298 – 51,968,426). Nucleotides shown in grey were present in a single clone and it is, therefore, uncertain if these changes are SNPs or errors of the Taq polymerase. Aside from differences unique to one clone, seven SNPs were found in the rhesus CXCL13 promoter. +1 designates the putative transcription start site. Δ denotes a base pair deletion.

from cynomolgus macaque spleen, hilar lymph node (HLN), axillary lymph node (ALN), and lung cells and used as template in PCR reactions with the same primers as used for amplification of the rhesus chemokine promoters. These cynomolgus promoters were subcloned directly into the pGL2-Basic vector system without first running the promoters through the pGEMT plasmid vector.

Obtaining the cynomolgus CCL20 promoter (cyCCL20p) proved challenging, as much of the PCR reaction energy was devoted to amplifying primer dimers rather than amplifying the anticipated stretch of DNA. While the promoter was amplified, the amount of DNA obtained was too small to proceed with cloning. To address this, the amount of gDNA template used in the PCR reaction was increased from 12.5 ng to 100 ng. This proved to still not be enough DNA to continue, so the amount of gDNA template was further increased to 1 μg. After doing so, a strong band of the correct size for the cyCCL20p was obtained via gel electrophoresis. Cloning the promoter into the pGL2-Basic vector system could then be continued.

The cynomolgus macaque CXCL13 promoter (cyCXCL13p) region was also not easily obtained. Using the original rhesus primers resulted in the amplification of the *gli3* gene, a zinc finger protein. This gene amplified to be within 50 bp to the correct size of the predicted cyCXCL13p, and, therefore, it was not identified as the incorrect sequence until it had been sequenced. To address this, new primers were designed, checking the 3' ends did not result in potential hybridization to other sequences during a BLAST search.

For each promoter, one clone was sequenced using the vector-specific primers, GL1-forward and GL1-reverse. All sequenced clones were amplified from gDNA extracted from spleen cells of the uninfected cynomolgus macaque M7102. These sequences were compared to rhesus chemokine promoter sequences and exhibited high similarity, as expected.

Sequencing of the predicted CCL20, CCL21, and CXCL13 promoter regions of cynomolgus macaque gDNA revealed 99.7%, 98.8%, and 99.0% identity, respectively, to their corresponding rhesus sequences. For these analyses, the rhesus clones with the highest similarity to the cynomolgus sequence were used (clone E for CCL20, clone H for CCL21, and clone E for CXCL13).

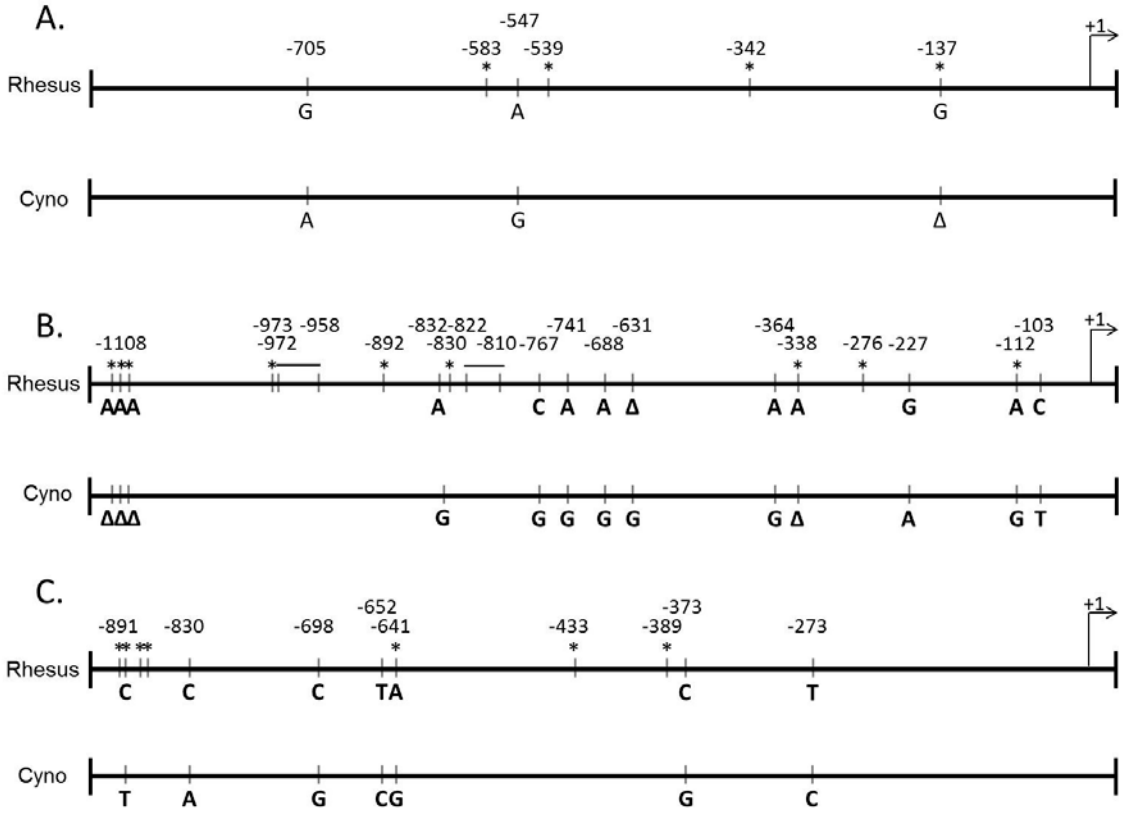

Figure 7. Alignment of chemokine promoters in rhesus and cynomolgus macaques. All three promoters show approximately 99% homology between macaque species. (A) The CCL20 promoter shows three differences between the species. One of these differences is the location of a SNP in the rhesus model. (B) The CCL21 promoter shows 10 differences between the species. Five of these differences represent locations of SNPs in the rhesus promoter. (C) The CXCL13 promoter shows seven differences between the species. Two of these differences represent locations of SNPs in the rhesus promoter. * denotes an identified SNP in the rhesus sequence.

Alignment of the predicted rhCCL20p sequence from clone E with the subcloned cynomolgus macaque sequence provided only three differences (Figure 7A). The difference at position -137 was a position of a SNP in the rhCCL20p clones. The other two changes, at positions -539 and -583, were unique to the cynomolgus macaque.

Alignment of the cynomolgus CCL21 promoter (cyCCL21p) region with the rhesus CCL21 clone H showed 10 differences (Figure 7B). Three of these nucleotide changes were identified as SNPs in the rhesus clones. The other seven were unique to the cynomolgus macaque sequence.

The rhCXCL13p sequence from clone E showed eight differences in comparison to the putative cyCXCL13p (Figure 7C). Two changes, at positions -641 and -891 were positions of SNPs in the rhesus clones. The other six changes were unique to the cynomolgus macaque. Therefore, multiple differences may exist between the predicted cynomolgus chemokine promoter regions as compared to their rhesus counterparts. It is possible some of these identified changes may have been due to Taq polymerase error and it is, therefore, difficult to make valid assumptions until additional clones are sequenced.

4.2 MAPPING OF PUTATIVE TRANSCRIPTION FACTOR BINDING SITES IN PREDICTED MACAQUE CHEMOKINE PROMOTER SEQUENCES

Using the computer algorithm TRANSFAC, putative transcription factor binding sites were mapped in the predicted promoter regions of rhesus CCL20, CCL21, and CXCL13. This knowledge base contains data on eukaryotic transcription factors, their experimentally-proven binding sites, and their regulated genes. All data have been previously published by other

research groups. The Match function of TRANSFAC can be used to search DNA sequences for predicted transcription factor binding sites through the utilization of positional weight matrices. A matrix is the short DNA sequence that describes a transcription factor binding site. The output provides both a core score and a matrix score. The core score describes the quality of a match between the core sequence of a matrix and a part of the input sequence. The matrix score describes the quality of a match between a matrix and a part of the input sequence.

When using TRANSFAC software, one can minimize either false positive or false negative results; for this analysis, false negatives were minimized. Consequently, the output of putative transcription factor binding sites was large and, as a result, only a select few binding sites were illustrated (Figure 8). Even when looking only at a limited set of target binding sites, each site produced multiple matches within the queried promoter regions. Therefore, for each, the match with the highest percentage identity to the expected sequence of the binding site was mapped.

Transcription factor binding sites chosen to be mapped included AP-1, AP-4, c/EBPα, GATA, NFκB, and USF. The corresponding transcription factors have all shown some importance in immunology and/or HIV-1/SIV infection. Each of these binding sites was observed in all three predicted chemokine promoter regions. Interestingly, most of the putative transcription factor binding sites were not in the same general area between chemokine promoters. For example, the USF binding site was located very close to the transcription start site in the rhCCL20p, whereas it was the furthest binding site upstream of the transcription start site in the rhCXCL13p, and lied somewhere in the middle of the rhCCL21p. The AP-1 binding site was located approximately 800 bp upstream of the transcription start site in both the rhCCL20p and rhCCL21p promoters, whereas it was located relatively close to the TATA box in

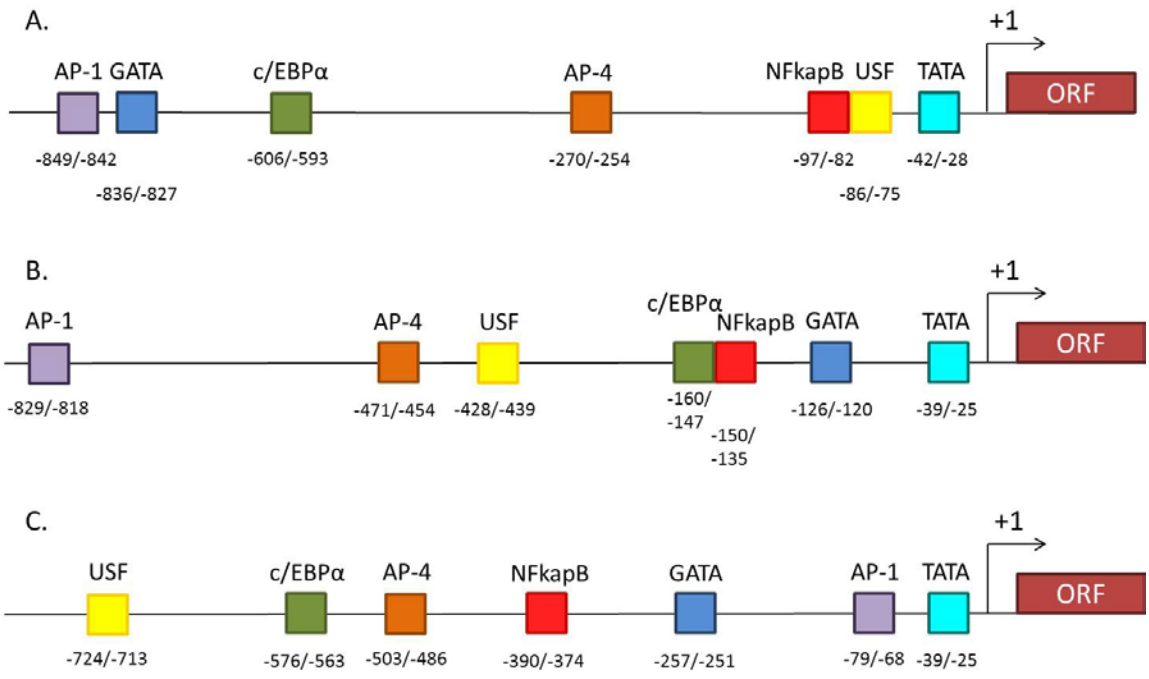

Figure 8. Schematic detailing mapped putative transcription factor binding sites in the predicted rhesus (A) CCL20, (B) CCL21, and (C) CXCL13 promoters. TRANSFAC software was used to determine potential transcription factor binding sites by the calculation of positional weight matrices. The option to minimize false negatives was used and the top scoring match for each transcription factor binding site was mapped. +1 represents the putative transcription start site and ORF designates the open reading frame.

the rhCXCL13p. In regard to NFκB binding sites, all predicted sites were placed relatively close to the open reading frame (ORF) in the rhCCL20p and the rhCCL21p, whereas all the putative Sites were further upstream in the rhCXCL13p. Furthermore, putative transcription start sites for the chemokine promoters were also able to be mapped downstream of the TATA box, approximately 25 nucleotides.

When compared to the cynomolgus macaque sequences, no nucleotide differences fell over putative transcription factor binding sites in any of the predicted chemokine promoters (Figure 7). In summary, transcription factor binding sites can be loosely predicted using online

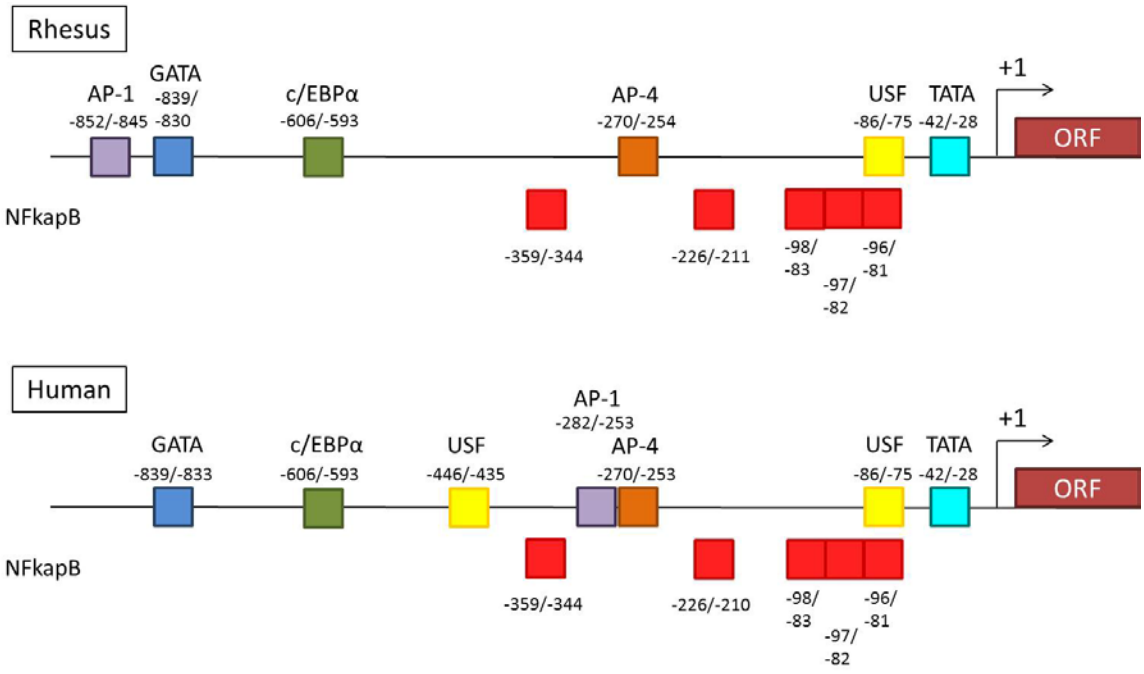

Figure 9. Alignment of the putative rhesus and human CCL20 promoters show 92% homology. Predicted rhesus macaque and human CCL20 promoter sequences were aligned and showed 92% homology. Putative transcription factor binding sites were mapped using TRANSFAC for both sequences and a comparison of the results are shown. Highest percentage matches for each promoter were mapped, as well as any corresponding matches in the opposing species. In addition, multiple NFκB sites were mapped in each putative promoter sequence. Many transcription factor binding sites were conserved between the species.

prediction software and these binding sites can be compared between species. Further analyses, however, are necessary to solidify a portion of DNA as a transcription factor binding site.

4.3 RHESUS MACAQUE CHEMOKINE PROMOTER REGIONS ARE HIGHLY HOMOLOGOUS TO THEIR HUMAN COUNTERPARTS

Humans possess a close genetic relationship to nonhuman primates. Many nonhuman primate species are, therefore, often used in preclinical and translational research. The research

presented in this thesis was performed largely in the rhesus macaque, an excellent model system for a number of human diseases. The putative rhesus macaque chemokine promoter sequences were aligned with the corresponding sequences in the human genome.

4.3.1 The Rhesus Macaque CCL20 Promoter is 92% Homologous to the Human CCL20 Promoter

The predicted rhCCL20p sequence was 92% similar to the corresponding human CCL20 promoter (huCCL20p) (Figure 9). Some differences fell over transcription factor binding sites and may have affected the ability of the site to be bound by that transcription factor. Shared sites between the species included a c/EBPα site at position -606, an AP-4 site at position -270, and a USF site at position -86. The USF site at position -86 exhibited a one nucleotide difference that fell outside the core matrix, but did not change the possibility of a binding site at that location. Also shared between the species, despite a one nucleotide substitution outside the core matrix, was the TATA box at position -42. The GATA site at position -839 was shared between the species; however, the site was three nucleotides shorter in the human genome despite there being no differences between the sequences. Unique to the rhesus macaque was an AP-1 site at position -852. A one nucleotide change between species in the core matrix likely reduced the likelihood of this being a binding site in human. Two binding sites were unique to the human sequence. These included a USF site at position -446 and an AP-1 site at position -282. The USF site contained a nucleotide substitution outside the core matrix, and the AP-1 site had a nucleotide change within the core matrix.

Because of the importance of NFκB in immune responses, multiple potential NFκB binding sites in both the rhesus macaque and human promoter sequences were mapped (Figure

9). All five potential binding sites were shared between the two species. The NFκB binding site at position -226 was present in both species, despite a one nucleotide deletion in the core matrix of the human and a one nucleotide difference between the species outside the core matrix. The deletion in the human sequence added an extra nucleotide to the end of the binding site compared to the rhesus macaque sequence. Three potential NFκB binding sites overlapped one another, beginning one nucleotide apart, starting at position -98. A one nucleotide difference had no effect on any of these three sites. The site beginning at position -96 had a lower probability (78%) of actually being a binding site than the other two sites with probabilities of 92% and 95%. Within these binding sites fell a previously defined human NFκB binding site from position -93 to position -103.[22, 23, 89] This NFκB site has been shown to have an impact on CCL20 transcription.[22, 23, 89]

4.3.2 The Rhesus Macaque CCL21 Promoter is 93% Homologous to the Human CCL21 Promoter

Based on nucleotide sequence similarity, the rhCCL21p demonstrated 93% similarity to the corresponding human CCL21 promoter (huCCL21p) (Figure 10). Some differences fell over putative transcription factor binding sites, sometimes exerting an effect on the probability of that site being a predicted binding site. The c/EBPα site at position -1,055, the AP-1 site at position -1,037, the USF site at position -447, the AP-4 site at position -157, and the GATA site at position -126 were present in both species and showed no dissimilarities. It appeared as long as differences in the nucleotide sequence did not affect the core sequence of the putative binding site, that site remained a predicted binding site between the two species. For example, the putative TATA box was present in both rhesus and human sequences at position -39. However,

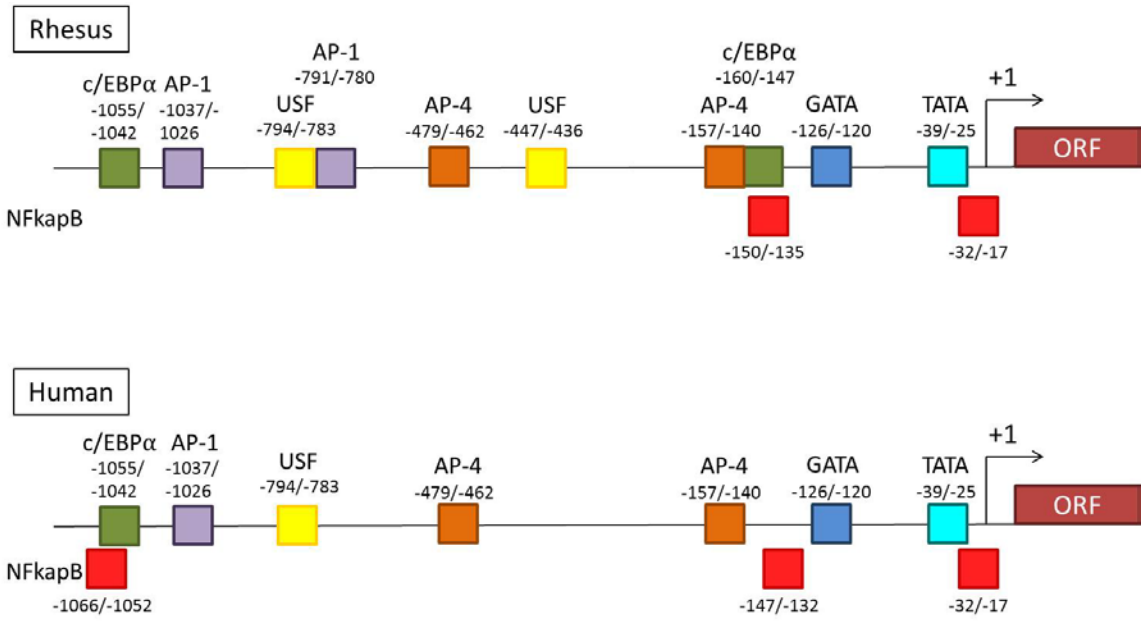

Figure 10. Alignment of the putative rhesus and human CCL21 promoters show 93% homology. Predicted rhesus macaque and human CCL21 promoter sequences were aligned and showed 93% homology. Putative transcription factor binding sites were mapped using TRANSFAC for both sequences and a comparison of the results are shown. Highest percentage matches for each promoter were mapped, as well as any corresponding matches in the opposing species. In addition, multiple NFκB sites were mapped in each putative promoter sequence. Many transcription factor binding sites were conserved between the species.

there was a one nucleotide substitution between the rhesus and human sequences outside the core sequence. In contrast, when the nucleotide change was present in the core sequence of the binding site, as for the rhesus macaque AP-1 site at position -791 and the rhesus c/EBPα site at position -160, the site had a higher probability of not being mapped in both species. Surprisingly, the predicted AP-4 site at position -157 in the human sequence was also present in the rhesus sequence despite a nucleotide substitution in the core sequence. This change, however, decreased the probability that this was a binding site from 91% in the human sequence to 79% in the rhesus sequence. This signified that the change in the core sequence, while not completely eliminating the binding site, did exert an impact.

Similar to the CCL20 promoter, multiple possible NFκB binding sites in both the rhesus and human sequences were mapped (Figure 10). Two predicted sites were present in the rhesus promoter, while three arose in the human promoter. Surprisingly, only one site was shared between the species and, not surprisingly, this was the most highly predicted site for both species with a probability of 84%. Also, interestingly, was the overlap of NFκB sites, on opposing strands of DNA, around nucleotide position -150. From rhesus to human, nucleotide changes at positions -150 and -32 resulted in an entirely different NFκB binding site in the opposite direction in the human sequence. The site at position -1,066 in human seemed unlikely, with a probability of 79%, as it was located much further downstream from the transcription start site than any other putative NFκB binding site observed in any of the three examined chemokine promoter sequences.

4.3.3 The Rhesus Macaque CXCL13 Promoter is 94% Homologous to the Human CXCL13 Promoter

The predicted rhCXCL13p exhibited 94% homology between the rhesus macaque and human sequences (Figure 11). Most transcription factor binding sites were unaffected by changes in sequence between the species. These sites included the USF binding site at position -725, the AP-4 site at position -504, the GATA site at position -258, the c/EBPα site at position -122, and the AP-1 site at position -79. In addition, the TATA box, located at position -39 also remained unchanged. The GATA site at position -855 had a nucleotide difference between the rhesus and human sequences within the core sequence of the binding site. This change, although in the core sequence, did not affect the prediction of this sequence being a binding site, apart from increasing the site's probability from 96% in the rhesus sequence to 98% in the human

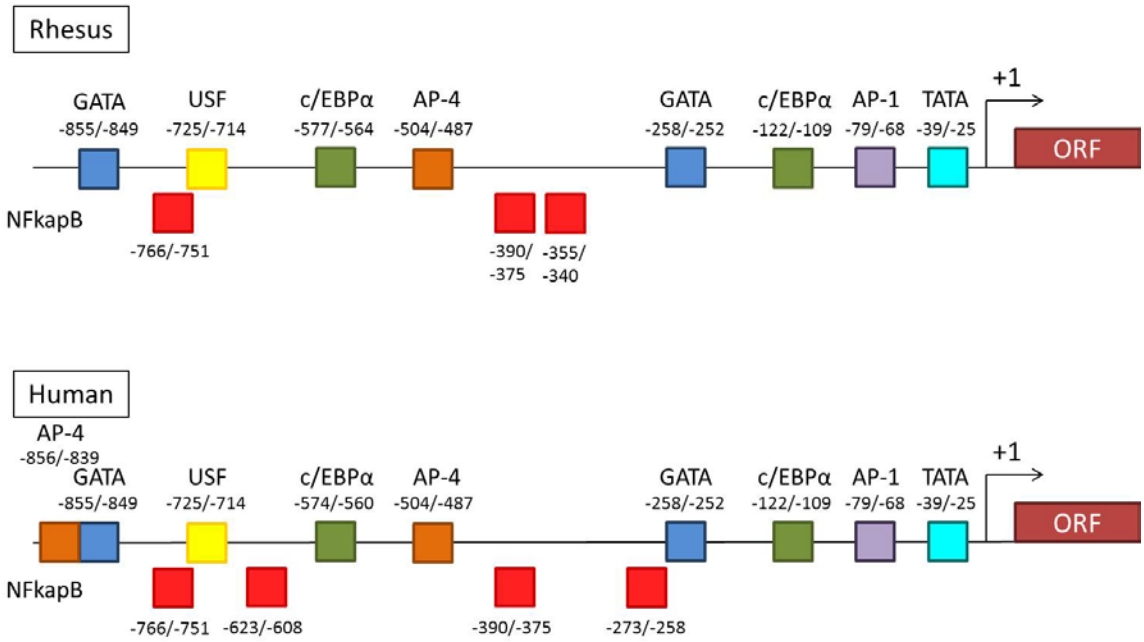

Figure 11. Alignment of the putative rhesus and human CXCL13 promoters show 94% homology. Predicted rhesus macaque and human CXCL13 promoter sequences were aligned and showed 94% homology. Putative transcription factor binding sites were mapped using TRANSFAC for both sequences and a comparison of the results are shown. Highest percentage matches for each promoter were mapped, as well as any corresponding matches in the opposing species. In addition, multiple NFκB sites were mapped in each putative promoter sequence. Many transcription factor binding sites were conserved between the species.

sequence. It did, however, in conjunction with an insertion, create an AP-4 binding site in the human sequence not present in the rhesus sequence at position -856. The c/EBPα site at rhesus position -577 was also affected by nucleotide differences outside of the core sequence. These changes shifted the human c/EBPα site downstream five nucleotides and to the opposite strand of DNA.

Again, due to its importance, multiple predicted NFκB binding sites in both the rhesus and human sequences were mapped (Figure 11). Two sites, at positions -766 and -390, were shared between the species, despite a nucleotide change in the latter. A predicted NFκB site unique to rhesus fell at position -355. In the human sequence, a three nucleotide substitution,

with one nucleotide falling over the core sequence, disrupted this binding site. Conversely, two NFκB binding sites were unique to the human sequence. The site at position -623 showed a nucleotide substitution outside of the core matrix. The other binding site fell at position -273, where a difference in comparison to the rhesus sequence was observed outside of the core matrix. None of the mapped NFκB sites had an overwhelmingly high probability of being a site, with most probabilities falling in the low eighties. In summary, comparison of putative rhesus and human chemokine promoter sequences showed high similarity. As a result, many predicted transcription factor binding sites were conserved between the species.

4.4 DEVELOPMENT AND OPTIMIZATION OF A DUAL-LUCIFERASE REPORTER ASSAY TO MEASURE TRANSCRIPTIONAL CONTROL OF MACAQUE CHEMOKINE PROMOTERS

To measure transcriptional control of each chemokine promoter, constructs were designed allowing the placement of the expression of the luciferase reporter gene (*luc*) under the control of each of these promoters. To do so, the chemokine promoter sequences were subcloned into the promoterless pGL2-Basic vector (Promega). This vector allowed the expression of firefly (*Photinus pyralis*) luciferase to be placed under the control of my isolated and inserted macaque chemokine promoters.

Unlike the pGEMT clone inserts, the pGL2-Basic clone inserts did not include the translation start site. The reverse primers were designed to include as much DNA up to, but not including, the translation start site as possible.

To measure transcriptional control from the predicted rhesus chemokine promoter regions, a dual-luciferase reporter (DLR) assay (Promega) specific for measuring luminescence resulting from transcriptional control by the rhesus chemokine promoters CCL20, CCL21, and CXCL13 was designed and developed. Luciferase assays allowed for the quantitation of control from each promoter via measured differences in the levels of luciferase enzymatic activity.

Once each promoter fragment was inserted into the pGL2-Basic reporter plasmid vector, constructs were transfected into the 293T cell line, in parallel with both positive and negative control plasmids. Rather than performing single transfections with each of my promoter constructs, a co-transfection design was utilized where each promoter construct was transfected alongside the sea pansy (*Renilla reniformis)* luciferase vector pGL4.74 (Promega; courtesy of Dr. Tianyi Wang). The levels of firefly luciferase expression resulting from each promoter construct could then be normalized to the level of *Renilla* luciferase expression from the same lysate. This vector placed expression of *Renilla* luciferase under the control of the Herpes Simplex Virus thymidine kinase (HSV-tk) promoter. The co-transfection design of this assay accounted for any differences in cell number, transfection efficiency, and lysis efficiency, allowing for greater accuracy and confidence in results.

The DLR assay was used to achieve luminescence readings. Addition of luciferase assay reagent (LARII) activated luminescence of the firefly luciferase. After 12 seconds, a second reagent, Stop & Glo, was added, quenching the reaction between the LARII and the firefly luciferase and beginning a second reaction for luminescence of *Renilla* luciferase. Throughout, readings were taken every 0.5 seconds, resulting in 24 readings each for both firefly and *Renilla* luciferase activity. Ranges for data analysis were from 2.5 seconds through 12 seconds for firefly luciferase activity and from 14.5 seconds through 24 seconds for *Renilla* luciferase

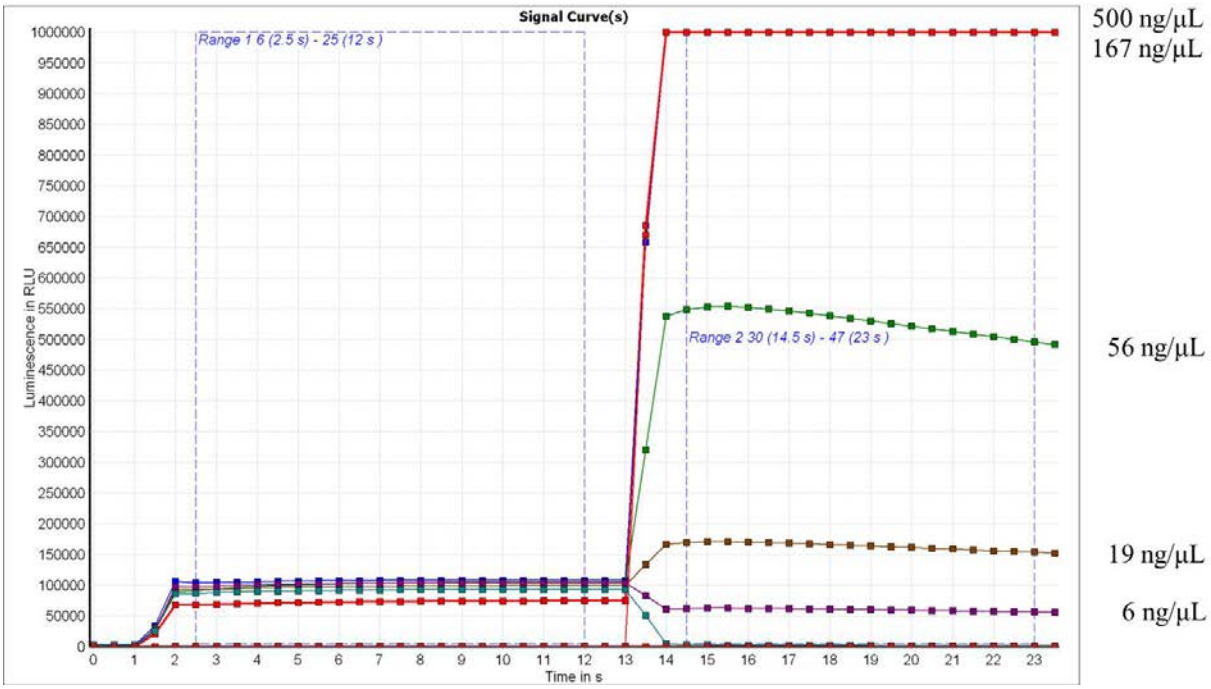

Figure 12. Titrations of pGL4.74 plasmid to determine optimal co-transfection concentration. *Renilla* luciferase was used as a normalization control for all DLR assays. A titration experiment was performed to determine an optimal transfection concentration of the *Renilla* vector, pGL4.74, via cotransfection of various dilutions with the pGL2-Control vector. The plate reader used could only read luciferase readings up to one million RLU and we aimed to have *Renilla* luciferase readings around 200,000 RLU. Range 1 represents firefly luciferase activity and range 2 represents *Renilla* luciferase activity. The optimal concentration for co-transfections was decided to be 6 ng/µL.

activity. The readings in the first 2.5 seconds for each enzyme were excluded as the reaction was not yet at full potential and equilibrating from the addition of reagent. The firefly luciferase readings were normalized to the *Renilla* luciferase readings by dividing the sum of range 1 (firefly luciferase readings) by the sum of range 2 (*Renilla* luciferase readings).

After performing the initial experiments with co-transfection of 500 ng pGL2-Basic vector constructs and 500 ng pGL4.74 vector, *Renilla* luciferase levels were reading at the highest possible value of one million RLU (relative luciferase units), rendering the normalization useless. To address this problem, a *Renilla* luciferase titration experiment was designed to

determine the optimal concentration of pGL4.74 vector to use for co-transfection, as well as to determine the optimal gain setting, or how much the strength of a signal is amplified, at which to run the assays. For the titration experiment, a dilution series of pGL4.74 was cotransfected with 500 ng of the pGL2-Control vector (SV-40 promoter). A three-fold dilution series of the pGL4.74 vector, starting with 500 ng/μL and ending with 6 ng/μL, was performed (Figure 12).

The first assay on these lysates was performed at the recommended gain value of 3,800. Both firefly and *Renilla* luciferase activity exceeded the plate reader's maximum readable value of one million RLU. In response, the gain was lowered and adjusted until a gain achieving *Renilla* readings of approximately 250,000 RLU was determined. An example of the *Renilla* titration curve at a gain of 1,900 is shown in Figure 12. After much optimization, it was decided the optimal conditions for the DLR assay when measuring promoter function of macaque chemokines was to transfect cells with 6 ng/μL of pGL4.74 and run the assay at a gain of 2,500.

4.5 THE MACAQUE CCL20 PROMOTER IS STIMULATED BY THE CYTOKINES TNF-ALPHA AND IL-1BETA

After intensely optimizing the DLR assay for studying macaque chemokine promoters, both basal and stimulated levels of luciferase production from the CCL20, CCL21, and CXCL13 promoters were measured. Co-transfection of 293T cells with the luciferase-promoter constructs and the *Renilla* luciferase vector pGL4.74 was performed. Initially, basal levels of activity from each promoter were measured (data not shown). The positive control vector read highest and the pGL2-Basic empty vector read lowest. The mock transfected samples read minimal levels for

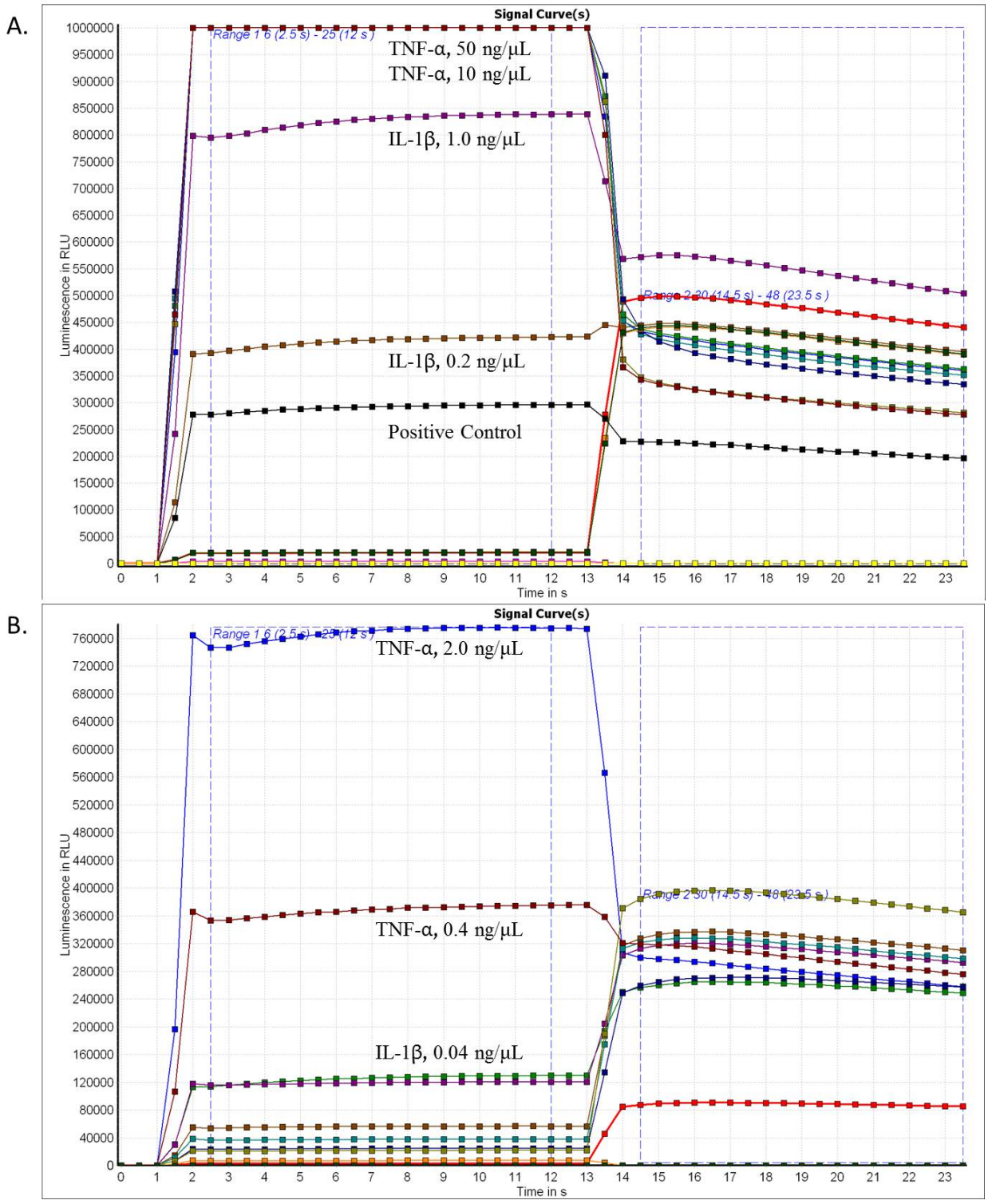

Figure 13. Cytokine titration to determine optimal amount of cytokine for stimulation. Stimulation of the CCL20 promoter with TNF-α and IL-1β resulted in high firefly luciferase readings. (A) Titration experiment using TNF-α concentrations 50 ng/μL and 10 ng/μL and IL-1β concentrations 1.0 ng/μL and 0.2 ng/μL. (B) Second titration experiment using TNF-α concentrations 2.0 ng/μL, 0.4 ng/μL, and 0.08 ng/μL and IL-1β concentrations 0.04 ng/μL and 0.01 ng/μL. Final concentrations chosen for further stimulation experiments were 0.8 ng/μL TNF-α and 0.08 ng/μL IL-1β.

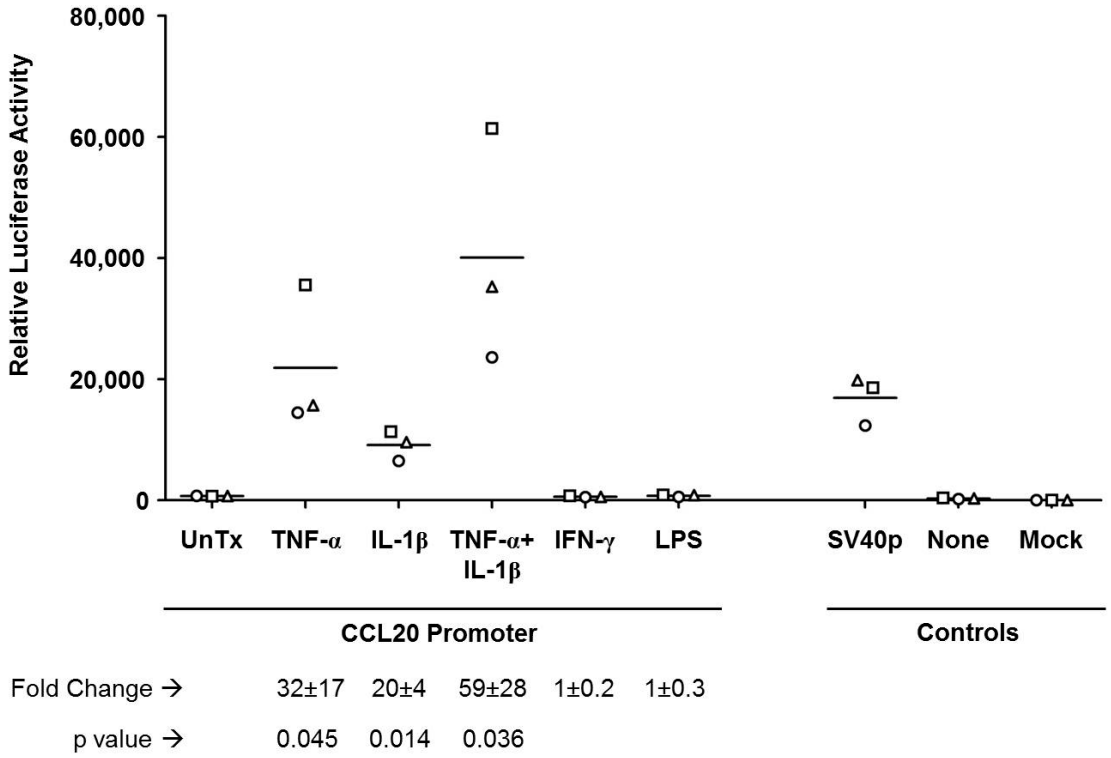

Figure 14. Cytokine stimulation of the rhesus CCL20 promoter. 293T cells were transfected with the pGL2-Basic vector containing the rhesus CCL20 promoter 20-24 hours after plating. Cells were stimulated with cytokines 18 hours post-transfection and lysates were harvested 24 hours later. Luminescence was measured using the optimized DLR assay. Three independent experiments were performed, represented by the different symbols. Each data point represents the average of two duplicate DLR readings of one experiment. Fold changes were calculated and are represented with standard deviation. Statistical significance was determined using a one-sided paired t-test.

both firefly and *Renilla* luciferase expression, as expected. The experimental vectors, containing the putative rhesus CCL20, CCL21, and CXCL13 promoters all expressed similar low levels of luciferase expression, suggesting a need for these promoters to be stimulated in order for transcription of the gene they regulate to occur.

Transfected 293T cells were stimulated with a subset of pro-inflammatory cytokines. Based on the literature, cells were stimulated with TNF-α and IL-1β. These cytokines were known to stimulate CCL20 production. Fujiie *et al*. showed stimulation of the mouse CCL20

promoter by these cytokines via a luciferase assay, and further showed the cytokines act synergistically by measuring CCL20 protein secretion in supernatants.[89] In addition to these cytokines, stimulation of cells with Interferon (IFN)-γ was performed as a negative control because the receptor for this cytokine is not present on 293T cells.[89] Lipopolysaccharide (LPS) was used as a second negative control stimulant.

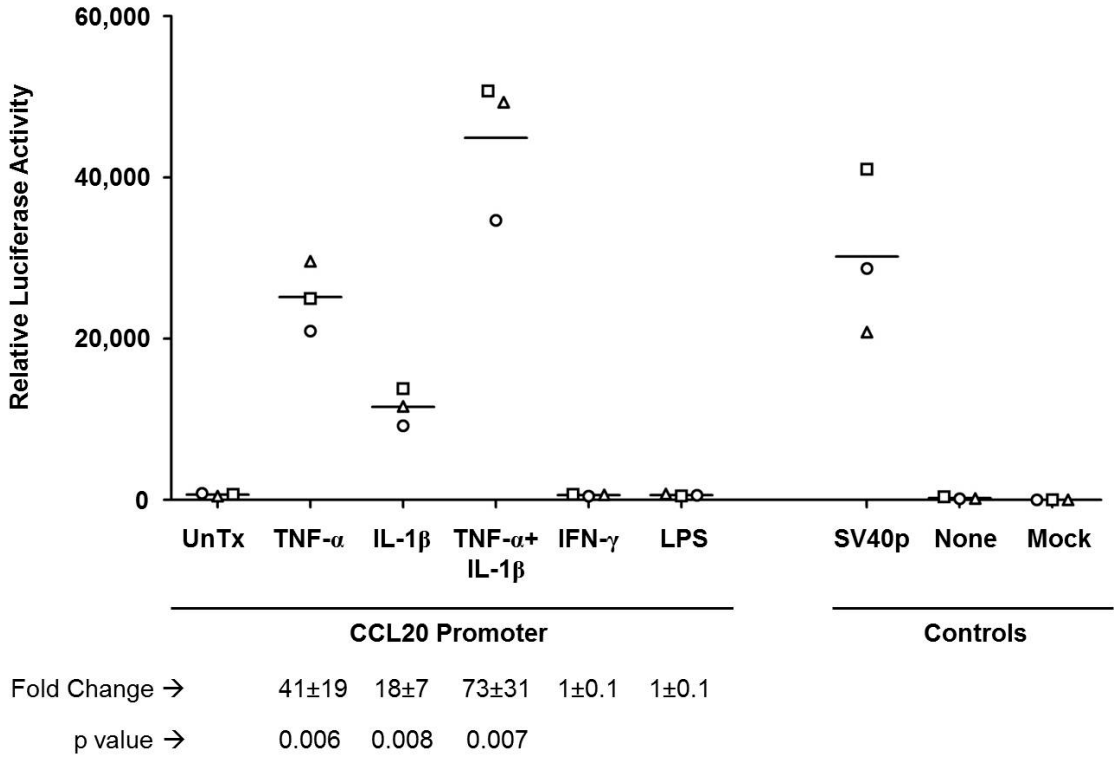

Figure 15. Cytokine stimulation of the cynomolgus CCL20 promoter. 293T cells were transfected with the pGL2-Basic vector containing the cynomolgus CCL20 promoter 20-24 hours after plating. Cells were stimulated with cytokines 18 hours post-transfection and lysates harvested 24 hours later. Luminescence was measured using the optimized DLR assay. Three independent experiments were performed, represented by the different symbols. Each data point represents the average of two duplicate DLR readings of one experiment. Fold changes were calculated and are represented with standard deviation. Statistical significance was determined using a one-sided paired t-test.

The initial experiments focused on the rhCCL20-luciferase construct since the most was known about this promoter from previous literature. For the first experiment, cells were treated with TNF-α at concentrations of 10 ng/mL and 50 ng/mL and IL-1β at concentrations of 0.2 ng/mL and 1 ng/mL. All samples treated with TNF-α produced readings above one million RLU. The IL-1β samples also read high, with the higher concentration reading above 800,000 RLU (Figure 13A). In response, a second titration experiment was performed to determine concentrations of TNF-α and IL-1β that lead to stimulation that was appreciable yet allowed for variability in both directions. The second experiment, performed with lower dilutions of each cytokine did not result in any readings surpassing one million RLU (Figure 13B). As a result, all subsequent stimulation assays used 0.8 ng/mL of TNF-α and 0.08 ng/mL of IL-1β.

Three independent stimulation experiments were performed with assays on each lysate read in duplicate. The rhCCL20p was induced approximately 30-fold when stimulated with TNF-α (Figure 14). Although the effect was not as great, the rhCCL20p was also stimulated by treatment of cells with IL-1β, approximately 20-fold. When transfected cells were treated with both TNF-α and IL-1β together, the resulting stimulation was additive with a fold increase of approximately 60-fold. The rhCCL20p was not stimulated by IFN-γ or LPS, as expected (Figure 14). Experiments performed using the putative cyCCL20p provided similar results (Figure 15).

4.6 MACAQUE CCL21 AND CXCL13 PROMOTERS ARE NOT EASILY STIMULATED

Stimulation of 293T cells with TNF-α and IL-1β did not lead to measurable induction of luciferase activity from the rhesus CCL21 (Figure 16) and CXCL13 (Figure 17) promoters as it

had for the rhCCL20p. The rhCCL21p and rhCXCL13p were not stimulated by either cytokine, alone or additively. Stimulation of the cyCCL21p (Figure 18) and cyCXCL13p (Figure 19) showed the same results.

Oncostatin M (OSM), an IL-6-like cytokine made by inflammatory cells, has also been shown to promote human dermal endothelial cell expression of CCL21 mRNA and protein.[28] Our lab then showed OSM, not TNF-α or IL-1β, to be the only cytokine, amongst those looked at, to induce CCL21 in LECs.[90] Stimulation the rhCCL21p with OSM was attempted. However,

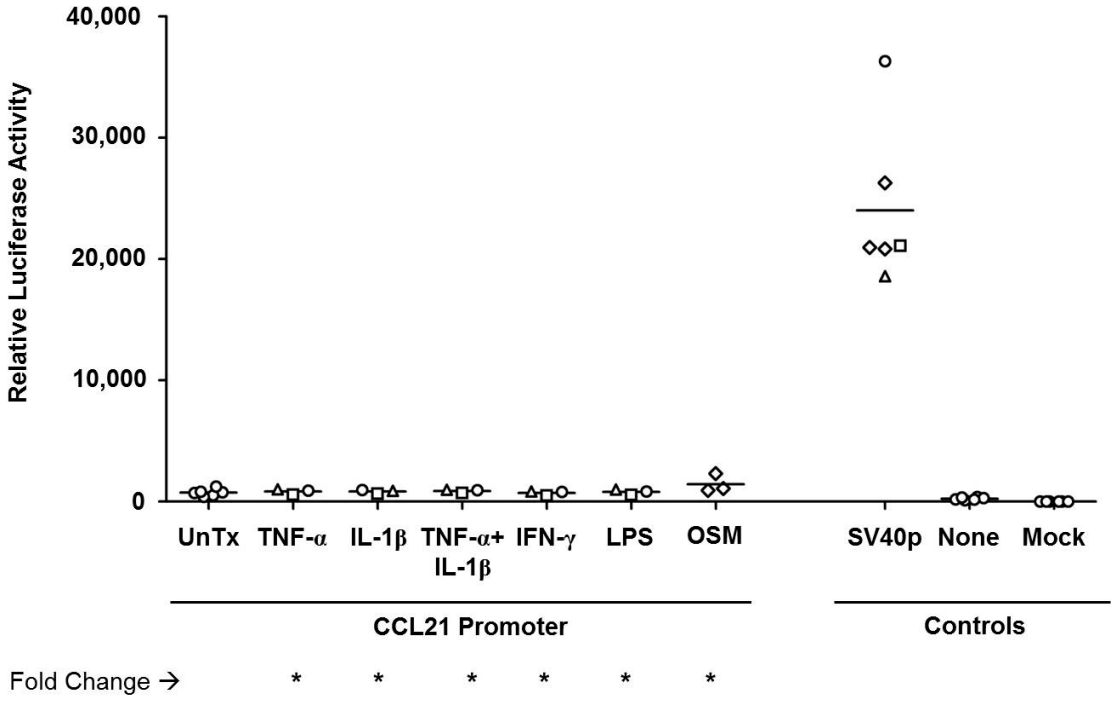

Figure 16. Cytokine stimulation of the rhesus CCL21 promoter. 293T cells were transfected with the pGL2-Basic vector containing the rhesus CCL21 promoter 20-24 hours after plating. Cells were stimulated with cytokines 18 hours post-transfection and lysates harvested 24 hours later. Luminescence was measured using the optimized DLR assay. Three independent experiments were performed, represented by different symbols. Each data point represents the average of two duplicate DLR readings of one experiment. Fold changes were calculated relative to an untreated control. * denotes fold change less than two.

OSM treatments lead to only a two-fold increase in luciferase activity relative to the unstimulated controls (Figure 16).

A possible reason the CCL21 and CXCL13 promoters were unable to be stimulated could be the cell type used for transfection, and, therefore, the set of transcription factors available to support transcription. In response, the experiment was repeated using lymphatic endothelial cells (LECs). LECs were examined given afferent LECs in peripheral tissues express CCL21.[90, 91] Primary cell lines are hard to transfect and LECs proved no different. Flow cytometry analysis

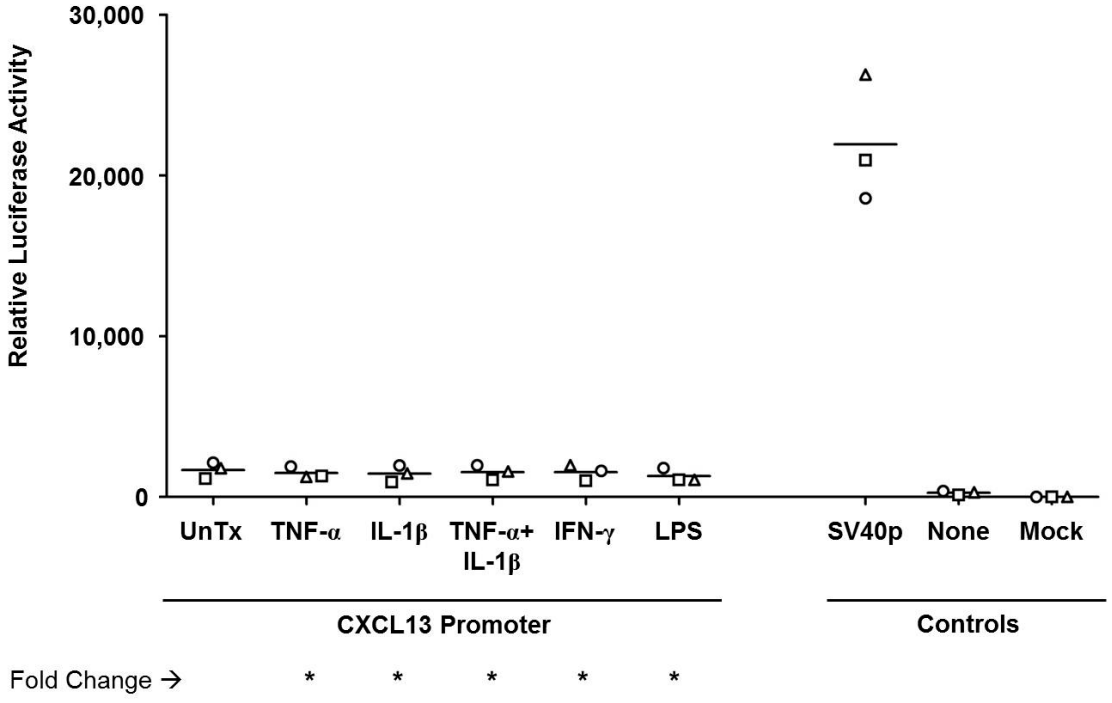

Figure 17. Cytokine stimulation of the rhesus CXCL13 promoter. 293T cells were transfected with the pGL2-Basic vector containing the rhesus CXCL13 promoter 20-24 hours after plating. Cells were stimulated with cytokines 18 hours post-transfection and lysates harvested 24 hours later. Luminescence was measured using the optimized DLR assay. Three independent experiments were performed, represented by different symbols. Each data point represents the average of two duplicate DLR readings of one experiment. Fold changes were calculated relative to an untreated control. * denotes fold change less than two.

of pEGFP transfected cells revealed a transfection efficiency of approximately 3% (Figure 20A and B). Luciferase activities, while low, were still measurable from transfected LECs. The relative patterns of these data resembled the pattern of results obtained with the transfected 293T cells (Figure 20C). However, one difference was observed. The rhCCL20p was stimulated by LPS, which served as a negative control in the studies using 293T cells. Whereas 293T cells do not possess a receptor for LPS, LECs do express this receptor.[92] Transfection of LECs did not result in increased transcription from the rhCCL21p. In addition, due to the lower transfection

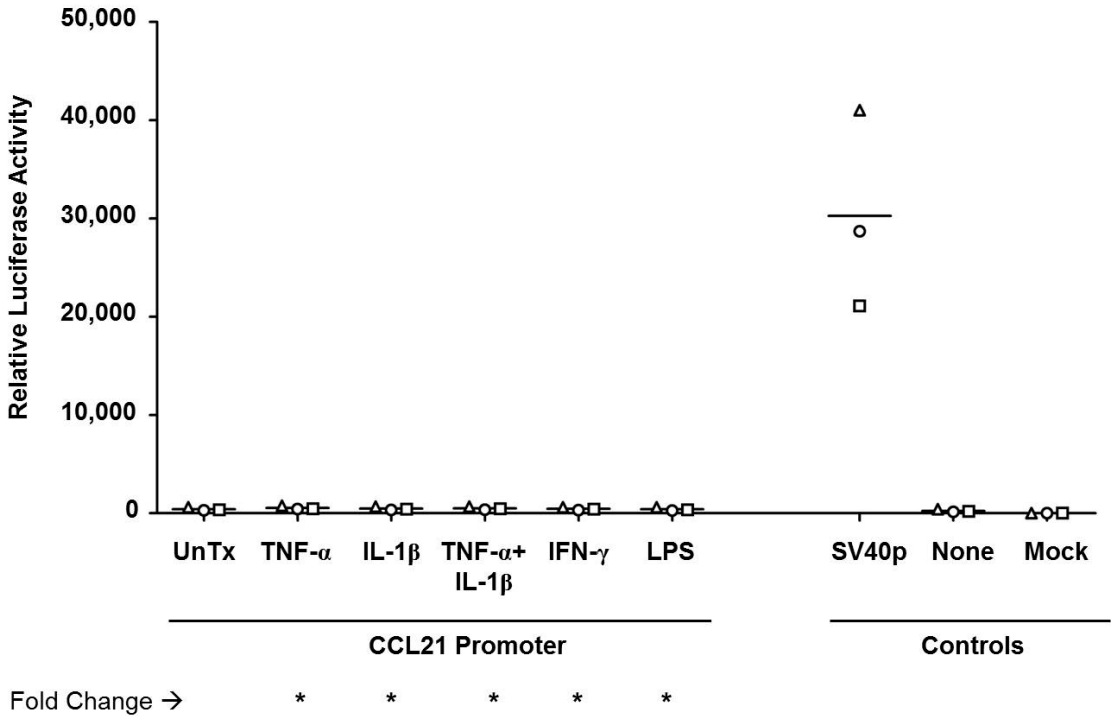

Figure 18. Cytokine stimulation of the cynomolgus CCL21 promoter. 293T cells were transfected with the pGL2-Basic vector containing the cynomolgus CCL21 promoter 20-24 hours after plating. Cells were stimulated with cytokines 18 hours post-transfection and lysates harvested 24 hours later. Luminescence was measured using the optimized DLR assay. Three independent experiments were performed, represented by different symbols. Each data point represents the average of two duplicate DLR readings of one experiment. Fold changes were calculated relative to an untreated control. * denotes fold change less than two.

efficiency, and hence the lower luciferase readings, small variations in the assay could lead to greater variation in the final data. Unlike experiments performed with 293T cells where the *Renilla* luciferase values showed limited variation, the *Renilla* luciferase values from the LEC experiments demonstrated higher levels of variation. It would be worth increasing the transfection efficiency and repeating the assay.

In addition to attempting to stimulate transcription from the rhCCL21p in LECs, co-transfecting 293T cells with either macaque or human prospero-related homeobox domain (Prox-

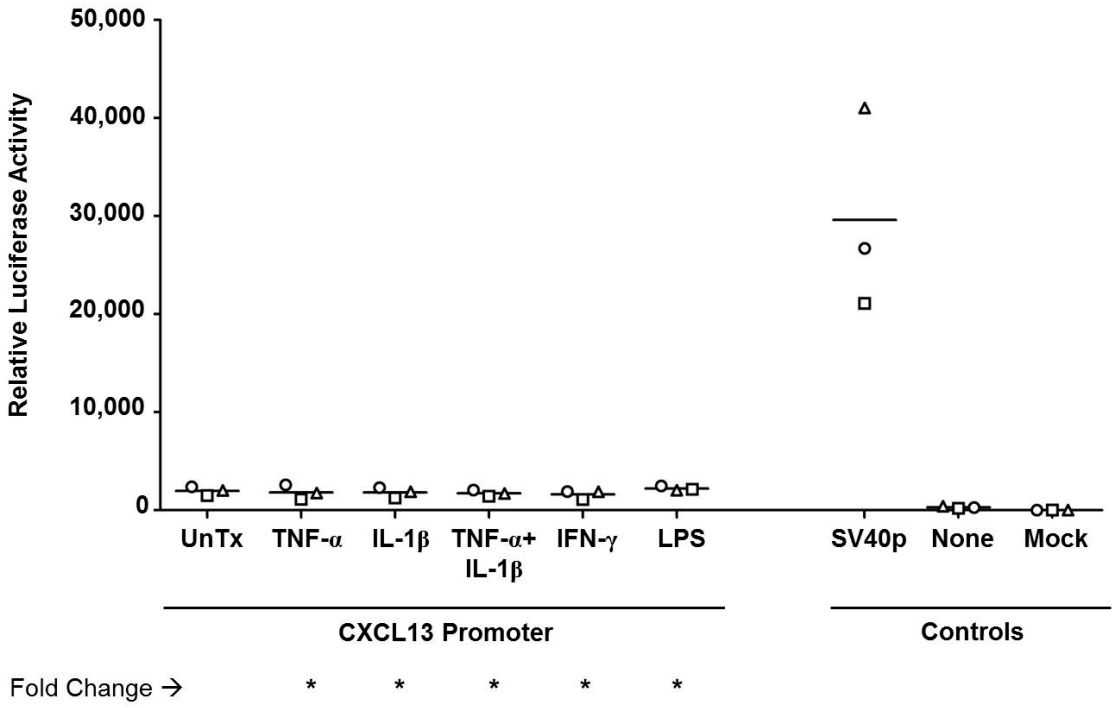

Figure 19. Cytokine stimulation of the cynomolgus CXCL13 promoter. 293T cells were transfected with the pGL2-Basic vector containing the cynomolgus CXCL13 promoter 20-24 hours after plating. Cells were stimulated with cytokines 18 hours post-transfection and lysates harvested 24 hours later. Luminescence was measured using the optimized DLR assay. Three independent experiments were performed, represented by different symbols. Each data point represents the average of two duplicate DLR readings of one experiment. Fold changes were calculated relative to an untreated control. * denotes fold change less than two.

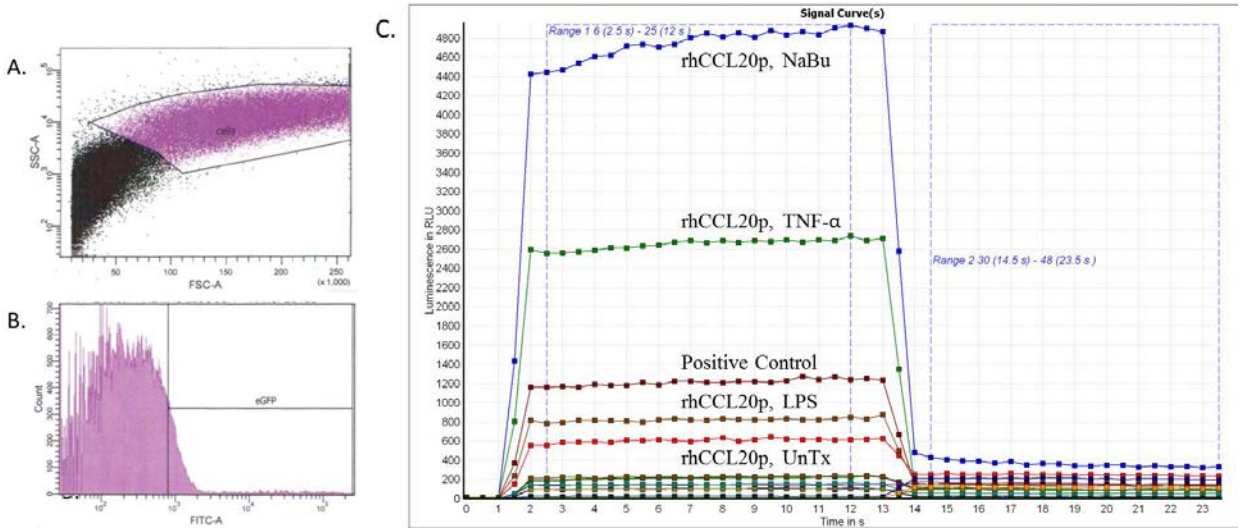

Figure 20. Transfection of and determination of transcription from chemokine promoters in LECs. (A,B) Flow cytometry on pEGFP-transfected LECs was used to determine transfection efficiency. Transfection efficiency was determined to be approximately 3%. (C) Signal curve shows low luminescence readings due to low transfection efficiency. LECs were transfected with pGL2-Basic vector containing CCL20, CCL21, and CXCL13 promoters inserted and stimulated with cytokines.

1) was also tried. Prox-1, an LEC marker, is a transcription factor imperative in the differentiation and development of LECs.[93, 94, 95] Prox-1 knockouts do not develop into LECs and do not express other LEC markers, including vascular endothelial growth factor receptor-3 (VEGFR-3), lymphatic endothelial receptor-1 (LYVE-1), podoplanin, and CCL21.[96, 97] Because CCL21 is not expressed without the Prox-1 transcription factor, I hypothesized adding Prox-1 to a cell line (293T) that does not normally express LEC markers may aid in stimulating transcription from the CCL21 promoter.

Results of these studies were difficult to interpret, as the addition of Prox-1 caused all luciferase readings, both firefly and *Renilla*, to decrease approximately 10-fold (data not shown). It is unsure what effect the Prox-1 plasmids were having on the cells and transcriptional regulation. Further experiments will need to be conducted.

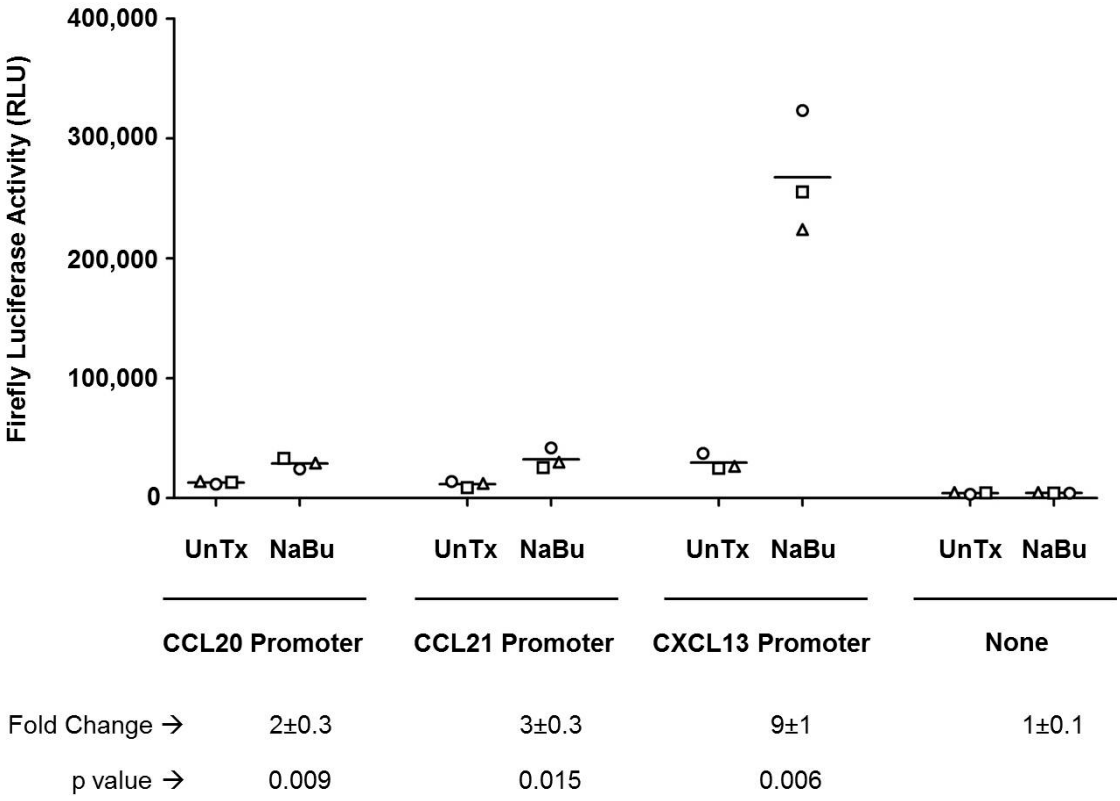

Figure 21. Sodium butyrate stimulation of rhesus macaque chemokine promoters. 293T cells were transfected with the pGL2-Basic vector containing rhesus chemokine promoters 20-24 hours after plating. Cells were stimulated with sodium butyrate 18 hours post-transfection and lysates were harvested 24 hours later. Luminescence was measured using the optimized DLR assay. Data represents unnormalized firefly luciferase activity because the compound affected the renilla luciferase readings by affecting the HSV-TK promoter of the pGL4.74 vector. Three independent experiments were performed, represented by different shapes. Each data point represents the averages of two duplicates of one experiment. Fold changes were calculated relative to untreated controls. Statistical significance was determined using a one-sided paired t-test.

4.7 SODIUM BUTYRATE STIMULATES THE MACAQUE CXCL13 PROMOTER

Apart from cytokine stimulation, stimulation of all three chemokine promoters was attempted with sodium butyrate. Sodium butyrate has been shown to stimulate the HSV-TK promoter by inhibiting histone deacetylases.[98] This is the promoter controlling *Renilla* luciferase expression in the pGL4.74 vector used as the normalization control. The results of these experiments proved complicated, as the treatment not only increased firefly luciferase

expression, but also increased the expression of *Renilla* luciferase. Because of this, normalization of firefly luciferase data was not possible. Comparison of unnormalized firefly luciferase data was done with confidence because the *Renilla* luciferase activities were consistently stimulated to similar levels in different co-transfection experiments, providing evidence for the likelihood of similar transfection efficiencies and cell numbers. For the

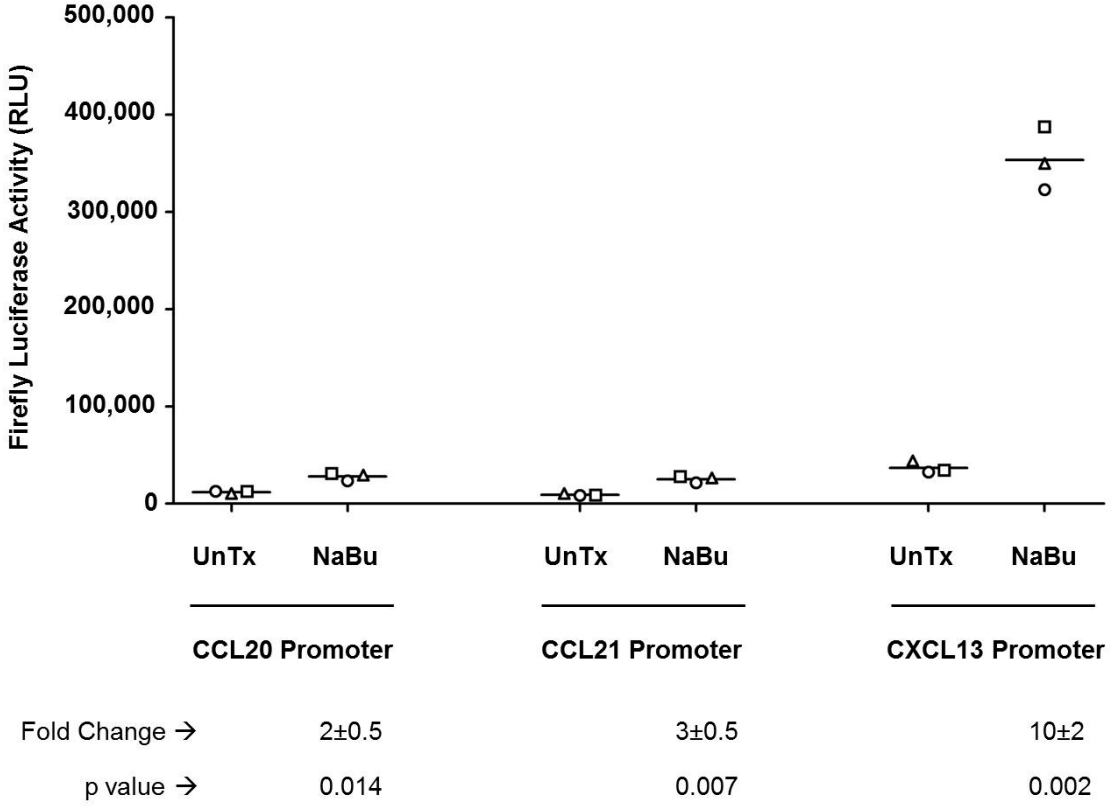

Figure 22. Sodium butyrate stimulation of cynomolgus macaque chemokine promoters. 293T cells were transfected with the pGL2-Basic vector containing cynomolgus chemokine promoters 20-24 hours after plating. Cells were stimulated with sodium butyrate 18 hours post-transfection and lysates were harvested 24 hours later. Luminescence was measured using the optimized DLR assay. Data represents unnormalized firefly luciferase activity because the compound affected the *Renilla* luciferase readings by affecting the HSV-TK promoter of the pGL4.74 vector. Three independent experiments were performed, represented by different shapes. Each data point represents the averages of two duplicates of one experiment. Fold changes were calculated relative to untreated controls. Statistical significance was determined using a one-sided paired t-test.

rhCCL20p and rhCCL21p constructs, only 2- and 3-fold increases, respectively, in luciferase activity, after treatment of cells with sodium butyrate, was seen. For the rhCXCL13p, however, a nearly 10-fold increase was observed (Figure 21). Similar results were obtained with the cynomolgus macaque chemokine promoters (Figure 22).

Sodium butyrate treated cells, after transfection with the empty pGL2-Basic vector, displayed no change in the level of firefly luciferase activity compared to untreated cells, indicating that the sodium butyrate was not acting broadly on all DNA sequences upstream of the luciferase ORF (Figure 21). In summary, it can be concluded sodium butyrate can be used to stimulate the CXCL13 promoter and that this stimulation is not a result of the sodium butyrate acting on the vector itself.

4.8 TRANSCRIPTION FROM THE RHESUS MACAQUE CCL20 PROMOTER IS AFFECTED BY POTENTIALLY ANTI-INFLAMMATORY AND/OR ANTI-VIRAL COMPOUNDS

After performing a dose-response experiment, it was concluded that GML, EGCG, and EG were relatively non-toxic to 293T cells, except at high concentrations (Figure 23). When treated with GML, some cytotoxicity was seen at a dose of 50 µg/mL, and more at 100 µg/mL. When treated with EGCG, slight decreases in cell number were seen as the dose increased from 1 µM to 50 µM to 100 µM, and a large drop was seen at 500 µM. Relatively no cells survived at a dose of 1,000 µM. However, at a macroscopic level, cells could be seen detaching from the plate at all concentrations as medium was removed before counting the cells. Treatment with 100 µM or greater of EG resulted in cytotoxicity to the cells.

I hypothesized, based on an article by Li *et al.*, adding GML to cells would inhibit transcription from macaque chemokine promoters.[81] In addition to this compound, cells were also treated with EGCG and EG. Similar to the results of the sodium butyrate experiments above, *Renilla* luciferase expression from the HSV-TK promoter of the pGL4.74 vector was affected by the addition of these potentially anti-inflammatory compounds. Therefore, the normalization control was once again lost. However, all transfected cells treated with GML saw approximately the same change in *Renilla* luciferase expression, as the RLU values were tight between the samples.

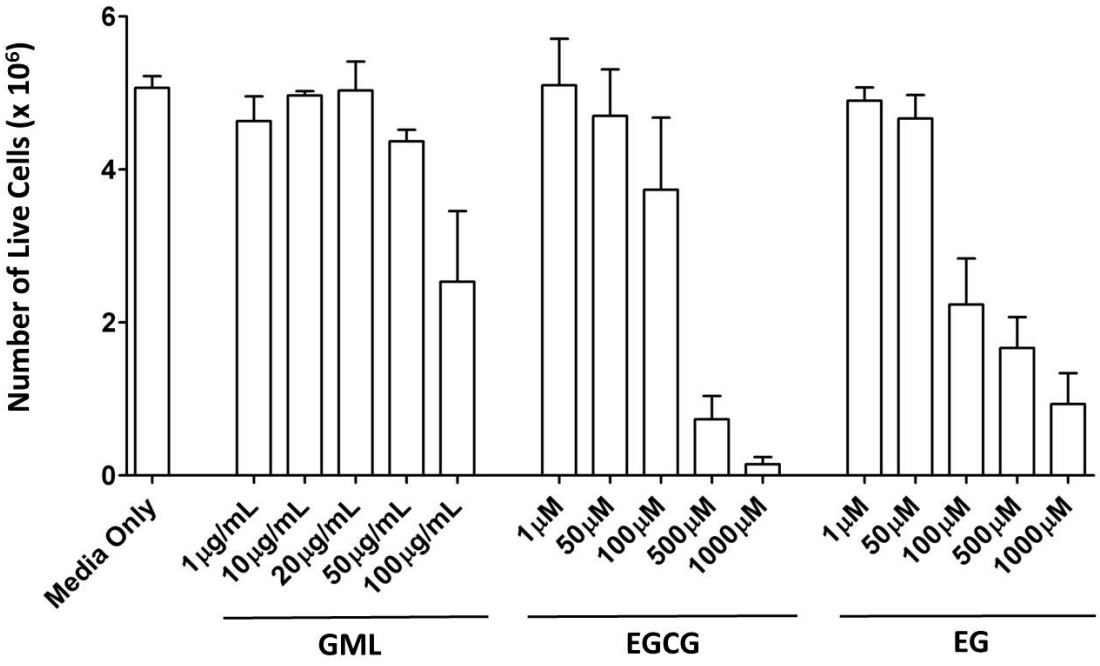

Figure 23. Cytotoxicity of GML, EGCG, and EG on 293T cells. 293T cells were plated on 6-well plates and medium changed 20-24 hours later to replicate transfection conditions. After a further 18 hours, cells were treated with varying dilutions of GML, EGCG, or EG. Cells were trypsinized 24 hours later and counted using trypan blue staining and a hemocytometer.

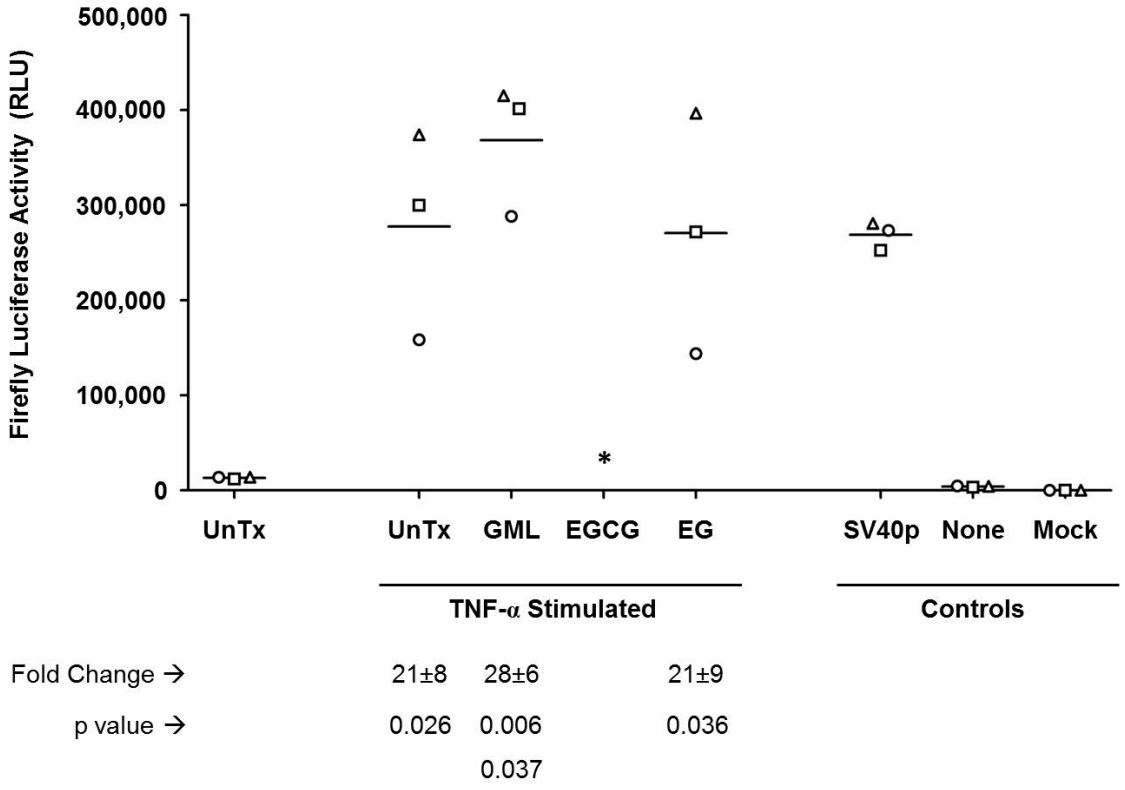

Figure 24. Treatment of TNF-α stimulated CCL20 promoter with potentially anti-inflammatory and/or anti-viral compounds. 293T cells were plated on 6-well plates and transfected with the CCL20 promoter plasmid and the pGL4.74 plasmid 20-24 hours later. After 18 hours, medium was removed and replaced with fresh medium supplemented with TNF-α and various potentially anti-inflammatory and/or anti-viral compounds. Luminescence was measured using the optimized DLR assay. Data represent unnormalized firefly luciferase activity because the compounds affected the *Renilla* luciferase readings by either stimulating or repressing the HSV-TK promoter of the pGL4.74 vector. Fold change was calculated relative to an unstimulated, untreated control. Three independent experiments were performed, represented by different shapes. Each data point represents the averages of two duplicates of one experiment. Statistical significance was performed using a one-sided paired t test. * denotes that EGCG values were unable to be obtained as the compounds caused cells to detach from the plate and, because the normalization control was lost, we cannot have certainty in these readings.

The same held true for EG. This provided confidence that using unnormalized values to evaluate these experiments gave an accurate depiction of how these compounds affected transcription.

Surprisingly, cells stimulated with TNF-α were further stimulated after treatment with GML. Untreated TNF-α stimulated cells boasted a 20-fold increase in firefly luciferase

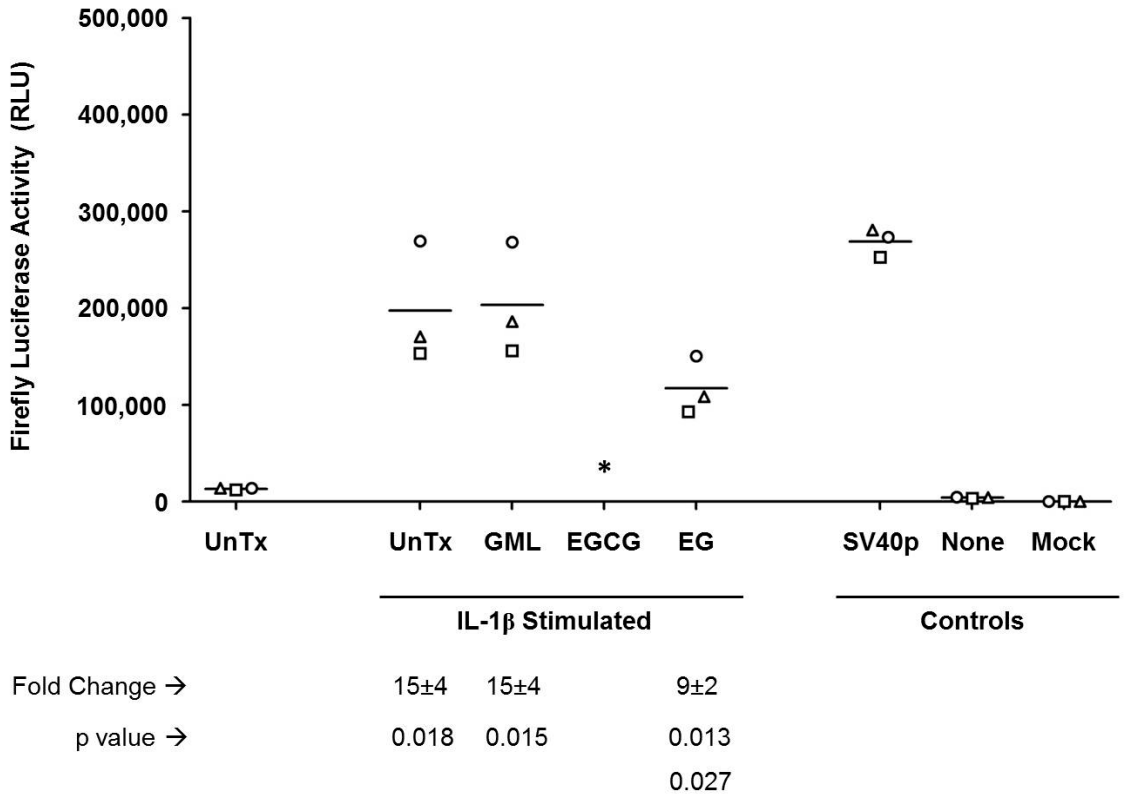

Figure 25. Treatment of IL-1β stimulated CCL20 promoter with potentially anti-inflammatory and/or anti-viral compounds. 293T cells were plated on 6-well plates and transfected with CCL20 promoter plasmid and pGL4.74 plasmid 20-24 hours later. After 18 hours, medium was removed and replaced with fresh medium supplemented with IL-1β and various potentially anti-inflammatory and/or anti-viral compounds. Luminescence was measured using the optimized DLR assay. Data represent unnormalized firefly luciferase activity because the compounds affected the *Renilla* luciferase readings by either stimulating or repressing the HSV-TK promoter of the pGL4.74 vector. Fold change was calculated relative to an unstimulated, untreated control. Three independent experiments were performed, represented by different shapes. Each data point represents the averages of two duplicates of one experiment. Statistical significance was performed using a one-sided paired t test. * denotes that EGCG values were unable to be obtained as the compounds caused cells to detach from the plate and, because the normalization control was lost, we cannot have certainty in these readings.

expression compared to an unstimulated control. When treated with GML, this increase became 28-fold (Figure 24). It was also interesting that, if the cells were instead stimulated with IL-1β, no change in transcriptional control was observed. It remained 15-fold, as compared to an unstimulated control, with or without GML treatment (Figure 25).

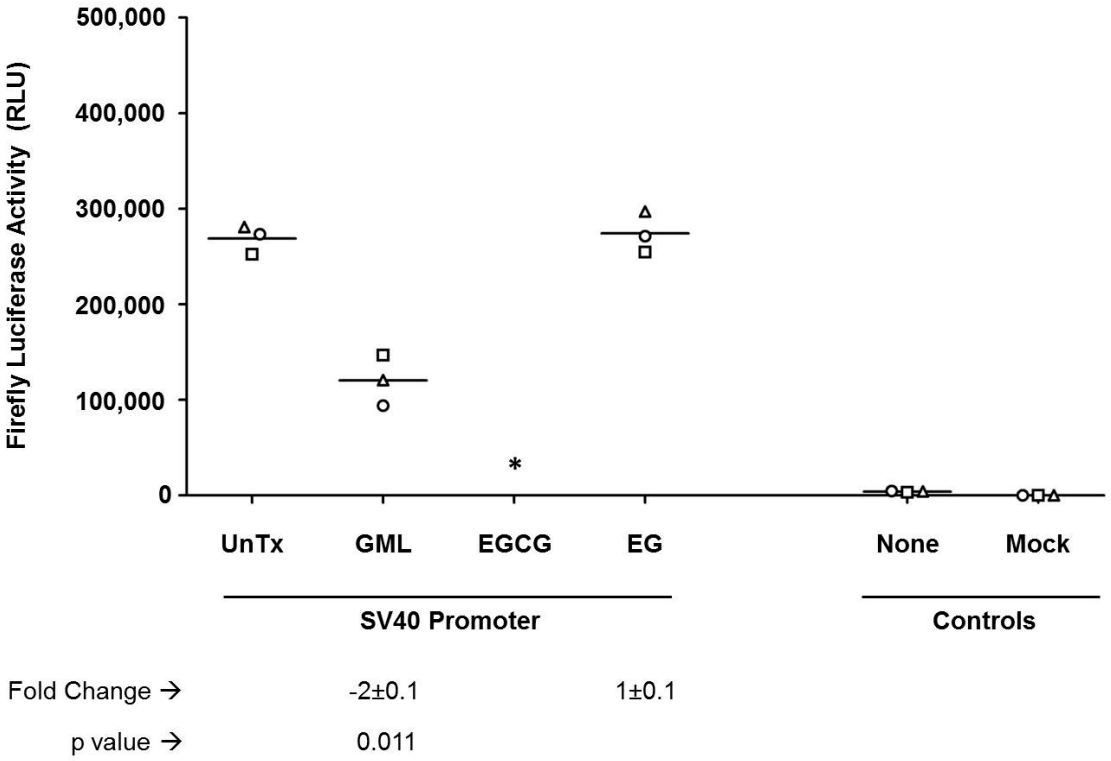

Figure 26. Treatment of SV-40 promoter with potentially anti-inflammatory and/or anti-viral compounds. 293T cells were plated on 6-well plates and transfected with the pGL2-Control plasmid and pGL4.74 plasmid 20-24 hours later. After 18 hours, medium was removed and replaced with fresh medium supplemented with TNF-α and various potentially anti-inflammatory and/or anti-viral compounds. Luminescence was measured using the optimized DLR assay. Data represent unnormalized firefly luciferase activity because the compounds affected the *Renilla* luciferase readings by either stimulating or repressing the HSV-TK promoter of the pGL4.74 vector. Fold change was calculated relative to an unstimulated, untreated control. Three independent experiments were performed, represented by different shapes. Each data point represents the averages of two duplicates of one experiment. Statistical significance was performed using a one-sided paired t test. * denotes that EGCG values were unable to be obtained as the compound caused cells to detach from the plate and, because the normalization control was lost, we cannot have certainty in these readings.

Inhibition of transcription from the rhCCL20p was also attempted using EG. This, unlike GML, did decrease transcription, but only when cells were stimulated with IL-1β. When compared to an unstimulated control, IL-1β increased transcription 15-fold. When EG was added to the cells, this increase in transcription decreased to nine-fold (Figure 25). No change in

transcription was observed on TNF-α stimulated cells, as it remained 15-fold for both treated and untreated samples (Figure 24).

Treatment of cells with EGCG proved difficult to interpret. Although EGCG did not appear to be harshly cytotoxic to 293T cells, the compound caused cells to detach from the plates. Therefore, EGCG data could not be taken with confidence since the normalization control to correct for differences in cell number was lost. It is uncertain why EGCG caused the cells to detach. It is possible it interacts with the poly l-lysine used to coat the plates in a way the other compounds do not.

In an attempt to further validate my results, cells transfected with the pGL2-Control vector were treated with the potentially anti-inflammatory and/or anti-viral compounds. This vector places luciferase expression under the control of the SV40 promoter. GML decreased transcription from this promoter two-fold and EG had no effect (Figure 26).

5.0 DISCUSSION

The objectives of this study were to obtain and analyze macaque chemokine promoter regions, to develop an assay for measuring transcription from these promoters, and to further utilize the developed assay to test the effects of various compounds that could possess anti-inflammatory and/or anti-viral properties. This study focused on three LN chemokines related to HIV-1/SIV infection and disease. The main focus of this project was on rhesus macaque chemokine promoters, but I was also able to analyze and compare these promoter sequences to the corresponding cynomolgus macaque and human sequences, as well as conduct additional functional analyses of the cynomolgus promoters.

To analyze the rhesus macaque chemokine promoters, multiple clones were sequenced. Alignments were performed to provide confidence that the correct sequences were obtained and to identify SNPs. Primer design was of utmost importance to ensure amplification of the correct region of gDNA. By locating the ORF and, more specifically, the ATG translation start site, of each chemokine gene on the appropriate chromosome, putative promoter regions could be identified and appropriate primers designed. Based on studies performed by previous groups looking at the huCCL20p, amplified stretches of DNA were approximately 1,200 nucleotides in length. The stretches of DNA consisted of approximately 1,000 nucleotides upstream and approximately 200 nucleotides downstream of the ATG translation start site. This same approach to primer design was used to predict the locations of the putative rhCCL21p and

rhCXCL13p regions. However, promoters likely vary in length and could possibly be thousands of nucleotides long. Therefore, it is possible that a length of gDNA shown to be sufficient for one promoter may be insufficient for other promoters and this could be true with those studied here.

Two PCR reactions were performed for each chemokine promoter with two different samples of rhesus gDNA, for a total of four PCR products. After cloning each of these four products into pGEMT, two clones from each were sequenced and analyzed. After examining a total of eight clones, it became apparent not all differences seen were likely SNPs, but that a number were likely the result of errors by the Taq polymerase as Taq polymerase has weaker fidelity. Using a higher fidelity polymerase, such as Pfu polymerase, would have allowed SNPs to be identified with greater certainty. For this study, any nucleotide difference observed in two or more clones was considered a SNP and any difference appearing in a single clone was considered likely to have resulted from Taq polymerase error. A weakness of this study is the use of Taq polymerase. However, the CCL20p promoter moved forward for functional studies harbored three of these likely Taq errors and yet showed strong functional activity. Determining the variability in the promoter regions was not the primary goal of these studies, and sequencing more clones would allow further confirmation of differences as SNPs or as Taq polymerase error.

Mapping of transcription factor binding sites showed these predicted sites were found in the different chemokine promoters and were generally, but not always, conserved between rhesus macaque, cynomolgus macaque, and human promoters. The results of these mapping analyses must be taken loosely. The TRANSFAC program used gave large numbers of potential matches. It is likely a number of these matches were false positives. It is also important to state this

software is only a first step binding site prediction tool. Further analyses of promoters must be conducted to confirm mapped sites were true transcription factor binding sites. Techniques such as EMSA, gel shift assays, and deletion constructs could be utilized.

Sequence analysis and mapping of putative transcription factor binding sites reaffirm the high genetic relatedness between the rhesus and cynomolgus macaque species. The human promoter sequence does not share as high a similarity to the rhesus macaque sequence as the cynomolgus macaque sequence does. However, the homology between the human and rhesus macaque sequences when all three chemokine promoters were compared across species was still greater than 90%.

As expected based on analysis of the huCCL20p, the rhCCL20p was stimulated by the cytokines TNF-α and IL-1β.[89] This confirmed that the gDNA fragment subcloned contained the rhCCL20p and provided the opportunity to attempt to inhibit transcription via the use of potentially anti-inflammatory and/or anti-viral compounds. GML was previously shown to possess inhibitory activity against CCL20 production, although the mechanism has not been determined.[81] Therefore, it was hypothesized that treating cells with GML would decrease transcription from the rhCCL20p. However, this treatment resulted in the opposite outcome. Whereas GML exhibited no effect on luciferase activity driven from the rhCCL20p in IL-1β-stimulated cells, those cells stimulated with TNF-α showed increased luciferase activity upon GML treatment. This increase in transcription from the rhCCL20p was unexpected and is not easily explained. Whereas previous studies looked at CCL20 mRNA levels after GML treatment, this study focused on the effects of GML on transcriptional control from the rhCCL20p. Studying the native gene could be different, as additional sequences in the 5'-UTR,

3'-UTR, or coding sequence could affect CCL20 production in ways that were not seen when the rhCCL20p was used to drive luciferase expression.

The unanticipated effects of GML on the rhCCL20p may have been due to the timing of the addition of the stimulants and potential inhibitors. The experimental design of these studies had all potential stimulants and/or inhibitors added to fresh media simultaneously. Following supplementation, the media was added to the cells. Perhaps adding the predicted inhibitor first and later treating the cells with stimulatory cytokines would result in an inhibitory effect from GML treatment. A previous experiment demonstrating inhibitory properties of GML against CCL20 production used HVECs in vivo, whereas my experiments utilized 293T cells in vitro.[81] These differences could also contribute to varying outcomes. Furthermore, GML decreased cytokine and chemokine production after exposure to staphylococcal toxins and inhibited production of CCL20 upon exposure to HIV-1.[75, 81, 99] In contrast to these studies, I did not challenge the transfected cells. The difference in response to GML based on the cytokine used for stimulation of the cells is interesting, suggesting GML might be targeting specific signaling pathways or transcription factors, such as the TRADD pathway in the TNF-α stimulated cells and/or the MyD88 pathway in the IL-1β stimulated cells.

The antioxidant EG, which has shown antimicrobial and anti-inflammatory properties, was also used in an effort to inhibit cytokine-driven stimulation of transcription from the rhCCL20p.[71, 78] In contrast to GML, EG decreased the extent of stimulation of transcription. However, this decrease was only observed when the cells were stimulated with IL-1β. Cells stimulated with TNF-α showed no change in luciferase activities. The mechanism of inhibition is not clear and will require further analysis.

The effect of EGCG on transcription from the rhCCL20p could not be measured. Treatment of 293T cells with EGCG resulted in the detachment of the cells from the culture plates, a new observation skewing the number of cells available for lysis and measurement of luminescence. Because *Renilla* luciferase expression appeared to be affected by EGCG treatment, the normalization to *Renilla* luciferase could not be used as an internal control. The reason for cell detachment, even at low concentrations of 50 μM, was not clear. It is possible EGCG interacted with the poly L-lysine used to coat the plates or with the 293T cells themselves. Further experiments are needed to find a method to study the potential inhibitory effects of EGCG on chemokine transcriptional regulation.

Achieving stimulation of the rhCCL21p and rhCXCL13p proved more difficult than achieving stimulation of the rhCCL20p. Surprisingly, neither TNF-α nor IL-1β stimulated either promoter. There are a number of possible explanations for why this occurred. It is possible I failed to actually subclone the promoter regions of these genes. A BLAST search with the fragments amplified from gDNA as the query showed the 3' ends were identical to the respective chemokine ORF. Further, a TATA box can be identified just upstream of the ATG translation start site. Therefore, although ultimately some transcriptional activity will be required to demonstrate that these are indeed promoters, structurally they are approximately 1 kbp of sequence upstream of the chemokine ORF.

With confidence that the correct region of gDNA was obtained, it remains possible that the 5' end of the putative promoter region is not far enough upstream of the TATA box and, therefore, does not contain a fully functional minimal promoter. The promoter regions of these two chemokine genes could be larger than the estimated 1,000 bp. In addition, upstream enhancer regions might be necessary for transcriptional activity. This could be examined by

amplifying and cloning a larger stretch of gDNA and looking for increased transcriptional levels through the DLR assay.

A potential explanation for the lack of activity from the CCL21 promoter was the pool of transcription factors available in the 293T cells. CCL21 is typically expressed by LECs in the periphery and by stromal cells in the LN paracortices. Because CCL21 is expressed by LECs, the transfection experiments were repeated in this cell type. Although the transfection efficiencies with these primary cells were low, it did not appear that transcription from the rhCCL21p was enhanced by the use of this other cell population.

Another strategy I used in an attempt to improve the transcription factor pool to increase the activity of the rhCCL21p was to co-transfect 293T cells with plasmid expressing either human or rhesus Prox-1, a transcription factor that drives the differentiation of endothelial cells into LECs. However, co-expression of the Prox-1 transcription factor did not increase basal or stimulated luciferase activity from the rhCCL21p and, instead, somewhat decreased both firefly and *Renilla* luciferase expression. It is possible Prox-1 co-transfection could work in stimulating the rhCCL21p, but further experiments are needed to determine the mechanism by which the Prox-1 plasmids are affecting the expression of both the firefly and *Renilla* luciferases.

In a further attempt to stimulate these promoters, cells were treated with sodium butyrate, a short chain fatty acid. This chemical has been used by our lab and others to treat cells expressing chemokine receptors prior to chemotaxis assays to increase transcription. Sodium butyrate works as an inhibitor of histone deacetylase, the inhibition of which is necessary for transcription to occur.[100, 101] All three rhesus macaque chemokine promoters examined here were stimulated, at varying levels, by sodium butyrate. The rhCCL20p and rhCCL21p, as well as the cyCCL20p and cyCCL21p, yielded two- and three-fold increases respectively, whereas the

rhCXCL13p and cyCXCL13p yielded a 10-fold increase. The mechanism for the greater increase in transcription from the CXCL13 promoter compared with the CCL20 and CCL21 promoters is not clear, but nevertheless interesting.

Our lab has shown CXCL13 is abundantly expressed in Paneth cells of the small intestine (C. Lucero, unpublished observation). This is interesting, as Paneth cells are a type of epithelial cell involved in the production of antimicrobial peptides in intestinal crypts. This finding suggests that CXCL13 not only plays a role as a lymphoid homeostatic chemokine in LNs, but also as an antimicrobial peptide in the intestine. This further suggests multiple transcriptional regulators of the gene. Along these lines, sodium butyrate stimulates the production of antimicrobial peptides and is a fermentation product of intestinal bacteria.[102, 103, 104, 105] The increased stimulation of the CXCL13 promoter by sodium butyrate might, therefore, be consistent with CXCL13's properties as an antimicrobial peptide, rather than as a homeostatic chemokine.

Scaffold attachment regions (SARs) may also address why the different promoters saw different levels of transcriptional stimulation after sodium butyrate treatment. These SARs, rich in AT nucleotides, promote the attachment of chromatin loops to the nuclear scaffold and can increase transcription without the presence of an enhancer.[106] Genes in close proximity to a SAR show increased sensitivity to transcription when stimulated by sodium butyrate.[107] It is possible the CXCL13 promoter possesses one of these regions, whereas the CCL20 and CCL21 promoters do not.

Additionally, changes in transcription due to sodium butyrate treatment may be minimal, but may be increased when a pro-inflammatory agent is added, indicating that sodium butyrate exerts a greater effect in the presence of inflammation.[105] Adding a pro-inflammatory agent in

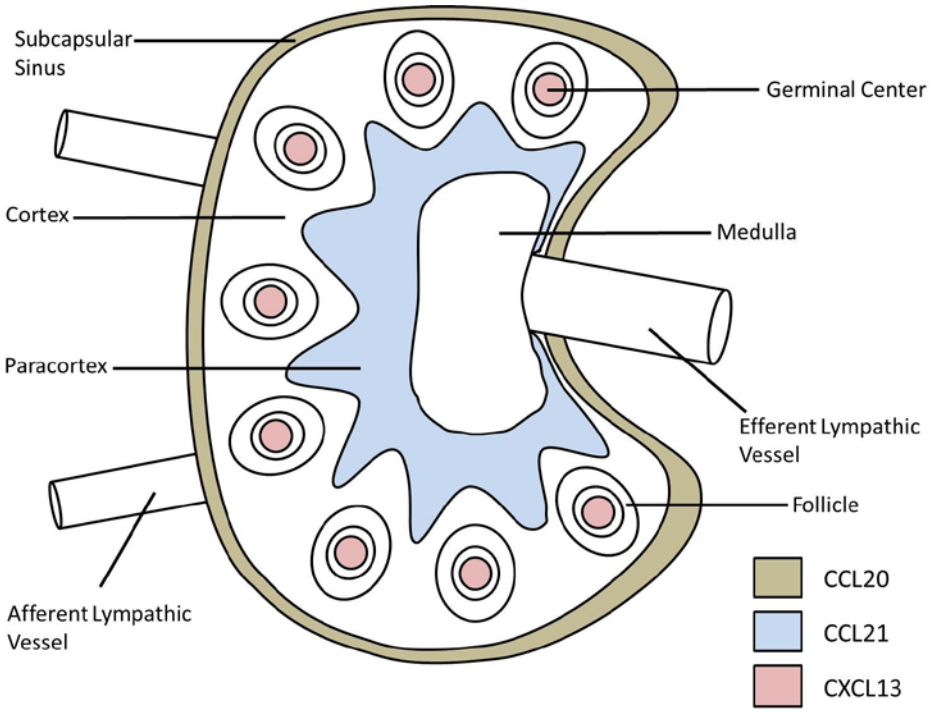

Figure 27. Chemokines are expressed in various compartments of the lymph node. Lymph node chemokines are each expressed in specialized lymph node compartments. CCL20 is found in the subcapsular sinus, CCL21 in the paracortex, and CXCL13 in the germinal centers within the follicles. This compartmentalization of lymph node chemokines may correspond to the levels of transcriptional regulation observed from the promoters of these chemokines.

addition to the sodium butyrate could stimulate the chemokine promoters further than sodium butyrate or cytokine treatment alone.

The lack of literature published on the CCL21 and CXCL13 promoters may be a consequence of the tight regulation of these regulatory sequences. It is possible other researchers have encountered similar problems in studying these promoters. In sum, it is not clear why the CCL21 and CXCL13 promoters are not readily upregulated by the inflammatory cytokines examined and further analysis is needed.

Repeating all experiments using putative cynomolgus chemokine promoter regions gave highly similar results compared to the results obtained with the putative rhesus promoters. This

was expected due to the close genetic relationship between the two species. As demonstrated by sequence alignments, each promoter was approximately 99% identical between the species. Additional information gained from repeating the experiments is useful as both species are models for HIV-1 infection and disease by using SIV. In addition, cynomolgus macaques are frequently used for pharmacology studies.

In summary, chemokine transcriptional promoters can be studied via a DLR assay. The CCL20 promoter was highly responsive to treatment of cells with the inflammatory cytokines TNF-α and IL-1β, whereas the CCL21 and CXCL13 promoters were not. The compartmentalization of these chemokines in the LN could be associated with the levels of transcriptional regulation (Figure 27). CCL20 is located more externally, in the subcapsular sinus, whereas CCL21 and CXCL13 are expressed in the paracortex and germinal centers respectively. The location of CCL20 in the subcapsular sinus of the LN may be to bring $CCR6^+$ cells into the LNs via high endothelial venules (HEVs). In addition, CCL20 has been shown to possess antimicrobial activity, and this may be one example, as CCL20 could be acting as a barrier to microbes trying to enter the LN. The tighter regulation of the CCL21 and CXCL13 promoters may be because of their roles in the homeostatic events of B and T cell development and lymphoneogenesis. If these promoters were less tightly controlled, this might lead to the development of new secondary lymphoid tissue given the roles of CCL21 and CXCL13 in this process, and although this might be helpful to the individual at times, development of secondary lymphoid tissues could also contribute to different pathologies.

6.0 CONCLUSION

Chemokine transcriptional control is regulated by promoter regions that can be characterized and studied in depth. Putative promoter regions of the macaque chemokines CCL20, CCL21, and CXCL13 can be identified and PCR amplified from rhesus and cynomolgus gDNA, and further mapped for putative transcription factor binding sites. In addition, these regions show high similarity to the corresponding predicted human promoter regions, adding further support for the macaque as a good model system for the human. By placing luciferase expression under the control of putative chemokine promoters, we confirm these regions are, in fact, promoters, and have developed a method for measuring both basal and stimulated levels of transcription from these promoters. We can further use this assay to test the effects of various potentially anti-inflammatory and/or anti-viral compounds on the levels of transcription, as well as exploring other transcriptional factors and pathways that have positive and negative effects on expression of these genes.

6.1 FUTURE DIRECTIONS

Because I was only slightly successful in stimulating the CCL21 and CXCL13 promoters, I was unable to test the effects of the potentially anti-inflammatory and/or anti-viral compounds. One next step is to find a more effective way of stimulating these promoters, or perhaps subclone

a larger portion of DNA that could include necessary enhancers for transcription. Experiments could then be done in an attempt to further stimulate and/or inhibit transcription from these promoters utilizing natural compounds.

Work involving LECs could be improved by increasing the transfection efficiency. A protocol for hard-to-transfect cells could be tried next. One could then select for positively transfected cells via flow cytometry and further grow these cells in culture to obtain a homogenous population of transfected cells. These cells could then be subjected to stimulations and/or inhibitions and read using the DLR assay. By doing so, the luminescence readings will be higher and, therefore, more accurate and trustworthy.

Additional studies to stimulate the CCL21 promoter could continue with further experiments involving the co-transfection of Prox-1. Studies to determine the method by which the Prox-1 plasmid is affecting luciferase expression are necessary before further experiments can be performed.

Because of the problem I ran into with certain stimulants and inhibitors affecting the HSV-TK promoter of the pGL4.74 vector and thereby affecting the *Renilla* luciferase normalization values, different methods of normalization could be utilized in the future to account for the uncertainty accompanying exclusion of the *Renilla* readings. Instead of cotransfecting cells with a *Renilla* luciferase vector, one could cotransfect with an eGFP construct. It would be beneficial to find a vector using a promoter not affected by the experimental stimuli (i.e. sodium butyrate). The amount of fluorescence can be measured via flow cytometry, allowing for a normalization of transfection efficiency between transfected samples.

To determine the mechanism by which sodium butyrate is working on the CXCL13 promoter, one could design deletion constructs, shortening the promoter region from the 5' and 3' ends. This could result in finding the portion of the promoter controlling sodium butyrate stimulation, allowing for further understanding of why sodium butyrate stimulates the CXCL13 promoter more strongly than it does the CCL20 and CCL21 promoters.

It would also be interesting to attempt stimulating promoters with both sodium butyrate and pro-inflammatory cytokines simultaneously. It has been shown sodium butyrate increases transcription in the presence of inflammation.[105] Therefore, the addition of pro-inflammatory cytokines would mock inflammation and perhaps increase transcription to levels greater than either treatment on its own.

When considering the generated TRANSFAC data, it would be appropriate to conduct further studies with which to solidify transcription factor binding sites. For this, mutagenesis studies would be appropriate, where the predicted binding sites are mutated or obliterated in order to determine if that particular site was necessary for transcription via a certain promoter.

6.2 PUBLIC HEALTH RELEVANCE

HIV/AIDS has a tremendous impact on worldwide public health, taking over 25 million lives throughout the past 30 years.[31] Currently, no cure exists for HIV, although there are antiretroviral therapies that slow viral replication. By developing an assay for studying chemokine transcriptional regulation, we can further examine factors that may upregulate or downregulate the expression of chemokines involved in HIV-1/SIV infection. Findings of such investigations could pave the way for additional approaches to modulating chemokine expression

as a method of combating the inflammation that is associated with HIV-1-driven disease, as well as for the development of possible vaccination and/or treatment strategies for HIV/AIDS research.

BIBLIOGRAPHY

1. Takeuchi, H., Fujimoto, A., Tanaka, M., Yamano, T., Hsueh, E. & Hoon, D. S. (2004). CCL21 chemokine regulates chemokine receptor CCR7 bearing malignant melanoma cells. *Clin Cancer Res* **10**, 2351-8.

2. Schutyser, E., Struyf, S. & Van Damme, J. (2003). The CC chemokine CCL20 and its receptor CCR6. *Cytokine Growth Factor Rev* **14**, 409-26.

3. Balkwill, F. R. (2012). The chemokine system and cancer. *J Pathol* **226**, 148-57.

4. Zlotnik, A. & Yoshie, O. (2000). Chemokines: a new classification system and their role in immunity. *Immunity* **12**, 121-7.

5. Rossi, D. & Zlotnik, A. (2000). The biology of chemokines and their receptors. *Annu Rev Immunol* **18**, 217-42.

6. Princen, K. & Schols, D. (2005). HIV chemokine receptor inhibitors as novel anti-HIV drugs. *Cytokine Growth Factor Rev* **16**, 659-77.

7. Kalinkovich, A., Weisman, Z. & Bentwich, Z. (1999). Chemokines and chemokine receptors: role in HIV infection. *Immunol Lett* **68**, 281-7.

8. Wu, Y. (2010). Chemokine control of HIV-1 infection: beyond a binding competition. *Retrovirology* **7**, 86.

9. Holst, P. J. & Rosenkilde, M. M. (2003). Microbiological exploitation of the chemokine system. *Microbes Infect* **5**, 179-87.

10. De Paepe, B., Creus, K. K. & De Bleecker, J. L. (2009). Role of cytokines and chemokines in idiopathic inflammatory myopathies. *Curr Opin Rheumatol* **21**, 610-6.

11. Reinhart, T. A., Fallert, B. A., Pfeifer, M. E., Sanghavi, S., Capuano, S., 3rd, Rajakumar, P., Murphey-Corb, M., Day, R., Fuller, C. L. & Schaefer, T. M. (2002). Increased expression of the inflammatory chemokine CXC chemokine ligand 9/monokine induced by interferon-gamma in lymphoid tissues of rhesus macaques during simian immunodeficiency virus infection and acquired immunodeficiency syndrome. *Blood* **99**, 3119-28.

12. Fallert, B. A., Poveda, S., Schaefer, T. M., Pfeifer, M. E., Sanghavi, S. K., Watkins, S. C., Murphey-Corb, M. A., Tarwater, P. M., Kirschner, D. E. & Reinhart, T. A. (2008). Virologic and immunologic events in hilar lymph nodes during simian immunodeficiency virus infection: development of polarized inflammation. *J Acquir Immune Defic Syndr* **47**, 16-26.

13. Giustizieri, M. L., Mascia, F., Frezzolini, A., De Pita, O., Chinni, L. M., Giannetti, A., Girolomoni, G. & Pastore, S. (2001). Keratinocytes from patients with atopic dermatitis and psoriasis show a distinct chemokine production profile in response to T cell-derived cytokines. *J Allergy Clin Immunol* **107**, 871-7.

14. Kelley, J. F., Kaufusi, P. H., Volper, E. M. & Nerurkar, V. R. (2011). Maturation of dengue virus nonstructural protein 4B in monocytes enhances production of dengue hemorrhagic fever-associated chemokines and cytokines. *Virology* **418**, 27-39.

15. Guabiraba, R., Marques, R. E., Besnard, A. G., Fagundes, C. T., Souza, D. G., Ryffel, B. & Teixeira, M. M. (2010). Role of the chemokine receptors CCR1, CCR2 and CCR4 in the pathogenesis of experimental dengue infection in mice. *PLoS One* **5**, e15680.

16. Lam, W. Y., Yeung, A. C., Chu, I. M. & Chan, P. K. (2010). Profiles of cytokine and chemokine gene expression in human pulmonary epithelial cells induced by human and avian influenza viruses. *Virol J* **7**, 344.

17. Kaufmann, A., Salentin, R., Meyer, R. G., Bussfeld, D., Pauligk, C., Fesq, H., Hofmann, P., Nain, M., Gemsa, D. & Sprenger, H. (2001). Defense against influenza A virus infection: essential role of the chemokine system. *Immunobiology* **204**, 603-13.

18. Marro, B. S., Hosking, M. P. & Lane, T. E. (2012). CXCR2 signaling and host defense following coronavirus-induced encephalomyelitis. *Future Virol* **7**, 349-359.

19. Carlson, T., Kroenke, M., Rao, P., Lane, T. E. & Segal, B. (2008). The Th17-ELR+ CXC chemokine pathway is essential for the development of central nervous system autoimmune disease. *J Exp Med* **205**, 811-23.

20. Glabinski, A. R., Tani, M., Strieter, R. M., Tuohy, V. K. & Ransohoff, R. M. (1997). Synchronous synthesis of alpha- and beta-chemokines by cells of diverse lineage in the central nervous system of mice with relapses of chronic experimental autoimmune encephalomyelitis. *Am J Pathol* **150**, 617-30.

21. von Andrian, U. H. & Mempel, T. R. (2003). Homing and cellular traffic in lymph nodes. *Nat Rev Immunol* **3**, 867-78.

22. Harant, H., Eldershaw, S. A. & Lindley, I. J. (2001). Human macrophage inflammatory protein-3alpha/CCL20/LARC/Exodus/SCYA20 is transcriptionally upregulated by tumor necrosis factor-alpha via a non-standard NF-kappaB site. *FEBS Lett* **509**, 439-45.

23. Battaglia, F., Delfino, S., Merello, E., Puppo, M., Piva, R., Varesio, L. & Bosco, M. C. (2008). Hypoxia transcriptionally induces macrophage-inflammatory protein-3alpha/CCL-20 in primary human mononuclear phagocytes through nuclear factor (NF)-kappaB. *J Leukoc Biol* **83**, 648-62.

24. Yang, D., Chen, Q., Hoover, D. M., Staley, P., Tucker, K. D., Lubkowski, J. & Oppenheim, J. J. (2003). Many chemokines including CCL20/MIP-3alpha display antimicrobial activity. *J Leukoc Biol* **74**, 448-55.

25. Starner, T. D., Barker, C. K., Jia, H. P., Kang, Y. & McCray, P. B., Jr. (2003). CCL20 is an inducible product of human airway epithelia with innate immune properties. *Am J Respir Cell Mol Biol* **29**, 627-33.

26. Imaizumi, Y., Sugita, S., Yamamoto, K., Imanishi, D., Kohno, T., Tomonaga, M. & Matsuyama, T. (2002). Human T cell leukemia virus type-I Tax activates human macrophage inflammatory protein-3 alpha/CCL20 gene transcription via the NF-kappa B pathway. *Int Immunol* **14**, 147-55.

27. Lalor, S. J. & Segal, B. M. (2010). Lymphoid chemokines in the CNS. *J Neuroimmunol* **224**, 56-61.

28. Sugaya, M., Fang, L., Cardones, A. R., Kakinuma, T., Jaber, S. H., Blauvelt, A. & Hwang, S. T. (2006). Oncostatin M enhances CCL21 expression by microvascular endothelial cells and increases the efficiency of dendritic cell trafficking to lymph nodes. *J Immunol* **177**, 7665-72.

29. Forster, R., Davalos-Misslitz, A. C. & Rot, A. (2008). CCR7 and its ligands: balancing immunity and tolerance. *Nat Rev Immunol* **8**, 362-71.

30. Ohl, L., Mohaupt, M., Czeloth, N., Hintzen, G., Kiafard, Z., Zwirner, J., Blankenstein, T., Henning, G. & Forster, R. (2004). CCR7 governs skin dendritic cell migration under inflammatory and steady-state conditions. *Immunity* **21**, 279-88.

31. Schiffer, L., Kielstein, J. T., Haubitz, M., Luhrs, H., Witte, T., Haller, H., Kumpers, P. & Schiffer, M. (2011). Elevation of serum CXCL13 in SLE as well as in sepsis. *Lupus* **20**, 507-11.

32. Ezzat, M., El-Gammasy, T., Shaheen, K. & Shokr, E. (2011). Elevated production of serum B-cell-attracting chemokine-1 (BCA-1/CXCL13) is correlated with childhood-onset lupus disease activity, severity, and renal involvement. *Lupus* **20**, 845-54.

33. Pranzatelli, M. R., Tate, E. D., Travelstead, A. L. & Verhulst, S. J. (2011). Chemokine/cytokine profiling after rituximab: reciprocal expression of BCA-1/CXCL13 and BAFF in childhood OMS. *Cytokine* **53**, 384-9.

34. Saez de Guinoa, J., Barrio, L., Mellado, M. & Carrasco, Y. R. (2011). CXCL13/CXCR5 signaling enhances BCR-triggered B-cell activation by shaping cell dynamics. *Blood* **118**, 1560-9.

35. Tsai, C. J. & Nussinov, R. (2011). Gene-specific transcription activation via long-range allosteric shape-shifting. *Biochem J* **439**, 15-25.

36. Ma, J. (2011). Transcriptional activators and activation mechanisms. *Protein Cell* **2**, 879-88.

37. Nechaev, S. & Adelman, K. (2011). Pol II waiting in the starting gates: Regulating the transition from transcription initiation into productive elongation. *Biochim Biophys Acta* **1809**, 34-45.

38. Juven-Gershon, T. & Kadonaga, J. T. (2010). Regulation of gene expression via the core promoter and the basal transcriptional machinery. *Dev Biol* **339**, 225-9.

39. Roy, A. L., Sen, R. & Roeder, R. G. (2011). Enhancer-promoter communication and transcriptional regulation of Igh. *Trends Immunol* **32**, 532-9.

40. Hayden, M. S. & Ghosh, S. (2012). NF-kappaB, the first quarter-century: remarkable progress and outstanding questions. *Genes Dev* **26**, 203-34.

41. Jacob, J., Cabarcas, S., Veras, I., Zaveri, N. & Schramm, L. (2007). The green tea component EGCG inhibits RNA polymerase III transcription. *Biochem Biophys Res Commun* **360**, 778-83.

42. Schreck, R., Rieber, P. & Baeuerle, P. A. (1991). Reactive oxygen intermediates as apparently widely used messengers in the activation of the NF-kappa B transcription factor and HIV-1. *EMBO J* **10**, 2247-58.

43. Singh, B. N., Shankar, S. & Srivastava, R. K. (2011). Green tea catechin, epigallocatechin-3-gallate (EGCG): mechanisms, perspectives and clinical applications. *Biochem Pharmacol* **82**, 1807-21.

44. Del Prete, A., Allavena, P., Santoro, G., Fumarulo, R., Corsi, M. M. & Mantovani, A. (2011). Molecular pathways in cancer-related inflammation. *Biochem Med (Zagreb)* **21**, 264-75.

45. Huang, C. J., Nazarian, R., Lee, J., Zhao, P. M., Espinosa-Jeffrey, A. & de Vellis, J. (2002). Tumor necrosis factor modulates transcription of myelin basic protein gene through nuclear factor kappa B in a human oligodendroglioma cell line. *Int J Dev Neurosci* **20**, 289-96.

46. Sugita, S., Kohno, T., Yamamoto, K., Imaizumi, Y., Nakajima, H., Ishimaru, T. & Matsuyama, T. (2002). Induction of macrophage-inflammatory protein-3alpha gene expression by TNF-dependent NF-kappaB activation. *J Immunol* **168**, 5621-8.

47. Bonello, G. B., Pham, M. H., Begum, K., Sigala, J., Sataranatarajan, K. & Mummidi, S. (2011). An evolutionarily conserved TNF-alpha-responsive enhancer in the far upstream region of human CCL2 locus influences its gene expression. *J Immunol* **186**, 7025-38.

48. Liddiard, K., Welch, J. S., Lozach, J., Heinz, S., Glass, C. K. & Greaves, D. R. (2006). Interleukin-4 induction of the CC chemokine TARC (CCL17) in murine macrophages is mediated by multiple STAT6 sites in the TARC gene promoter. *BMC Mol Biol* **7**, 45.

49. Hiscott, J., Kwon, H. & Genin, P. (2001). Hostile takeovers: viral appropriation of the NF-kappaB pathway. *J Clin Invest* **107**, 143-51.

50. Yamaguchi, K., Honda, M., Ikigai, H., Hara, Y. & Shimamura, T. (2002). Inhibitory effects of (-)-epigallocatechin gallate on the life cycle of human immunodeficiency virus type 1 (HIV-1). *Antiviral Res* **53**, 19-34.

51. Karamouzis, M. V., Konstantinopoulos, P. A. & Papavassiliou, A. G. (2007). The activator protein-1 transcription factor in respiratory epithelium carcinogenesis. *Mol Cancer Res* **5**, 109-20.

52. Mburu, Y. K., Egloff, A. M., Walker, W. H., Wang, L., Seethala, R. R., van Waes, C. & Ferris, R. L. (2012). Chemokine receptor 7 (CCR7) gene expression is regulated by NF-kappaB and activator protein 1 (AP1) in metastatic squamous cell carcinoma of head and neck (SCCHN). *J Biol Chem* **287**, 3581-90.

53. Aranburu, A., Carlsson, R., Persson, C. & Leanderson, T. (2001). Transcription factor AP-4 is a ligand for immunoglobulin-kappa promoter E-box elements. *Biochem J* **354**, 431-8.

54. Hu, Y. F., Luscher, B., Admon, A., Mermod, N. & Tjian, R. (1990). Transcription factor AP-4 contains multiple dimerization domains that regulate dimer specificity. *Genes Dev* **4**, 1741-52.

55. Poetsch, A. R. & Plass, C. (2011). Transcriptional regulation by DNA methylation. *Cancer Treat Rev* **37 Suppl 1**, S8-12.

56. Ayanbule, F., Belaguli, N. S. & Berger, D. H. (2011). GATA factors in gastrointestinal malignancy. *World J Surg* **35**, 1757-65.

57. Corre, S. & Galibert, M. D. (2005). Upstream stimulating factors: highly versatile stress-responsive transcription factors. *Pigment Cell Res* **18**, 337-48.

58. Sadowski, I. & Mitchell, D. A. (2005). TFII-I and USF (RBF-2) regulate Ras/MAPK-responsive HIV-1 transcription in T cells. *Eur J Cancer* **41**, 2528-36.

59. Weiss, R. A. (2003). HIV and AIDS in relation to other pandemics. Among the viruses plaguing humans, HIV is a recent acquisition. Its outstanding success as an infection poses immense scientific challenges to human health and raises the question "What comes nest?". *EMBO Rep* **4 Spec No**, S10-4.

60. Bergmeier, L. A., Wang, Y. & Lehner, T. (2002). The role of immunity in protection from mucosal SIV infection in macaques. *Oral Dis* **8 Suppl 2**, 63-8.

61. Zhang, W., Tong, Q., Conrad, K., Wozney, J., Cheung, J. Y. & Miller, B. A. (2007). Regulation of TRP channel TRPM2 by the tyrosine phosphatase PTPL1. *Am J Physiol Cell Physiol* **292**, C1746-58.

62. Hoxie, J. A., LaBranche, C. C., Endres, M. J., Turner, J. D., Berson, J. F., Doms, R. W. & Matthews, T. J. (1998). CD4-independent utilization of the CXCR4 chemokine receptor by HIV-1 and HIV-2. *J Reprod Immunol* **41**, 197-211.

63. Rizzuto, C. D., Wyatt, R., Hernandez-Ramos, N., Sun, Y., Kwong, P. D., Hendrickson, W. A. & Sodroski, J. (1998). A conserved HIV gp120 glycoprotein structure involved in chemokine receptor binding. *Science* **280**, 1949-53.

64. Wu, L., Gerard, N. P., Wyatt, R., Choe, H., Parolin, C., Ruffing, N., Borsetti, A., Cardoso, A. A., Desjardin, E., Newman, W., Gerard, C. & Sodroski, J. (1996). CD4-induced interaction of primary HIV-1 gp120 glycoproteins with the chemokine receptor CCR-5. *Nature* **384**, 179-83.

65. Trkola, A., Dragic, T., Arthos, J., Binley, J. M., Olson, W. C., Allaway, G. P., Cheng-Mayer, C., Robinson, J., Maddon, P. J. & Moore, J. P. (1996). CD4-dependent, antibody-sensitive interactions between HIV-1 and its co-receptor CCR-5. *Nature* **384**, 184-7.

66. Hesselgesser, J., Halks-Miller, M., DelVecchio, V., Peiper, S. C., Hoxie, J., Kolson, D. L., Taub, D. & Horuk, R. (1997). CD4-independent association between HIV-1 gp120 and CXCR4: functional chemokine receptors are expressed in human neurons. *Curr Biol* **7**, 112-21.

67. Ahmed, R. K., Biberfeld, G. & Thorstensson, R. (2005). Innate immunity in experimental SIV infection and vaccination. *Mol Immunol* **42**, 251-8.

68. Bosinger, S. E., Sodora, D. L. & Silvestri, G. (2011). Generalized immune activation and innate immune responses in simian immunodeficiency virus infection. *Curr Opin HIV AIDS* **6**, 411-8.

69. Chackerian, B., Long, E. M., Luciw, P. A. & Overbaugh, J. (1997). Human immunodeficiency virus type 1 coreceptors participate in postentry stages in the virus replication cycle and function in simian immunodeficiency virus infection. *J Virol* **71**, 3932-9.

70. Caufour, P., Le Grand, R., Cheret, A., Neildez, O., Theodoro, F., Boson, B., Vaslin, B. & Dormont, D. (1999). Secretion of beta-chemokines by bronchoalveolar lavage cells during primary infection of macaques inoculated with attenuated nef-deleted or pathogenic simian immunodeficiency virus strain mac251. *J Gen Virol* **80 (Pt 3)**, 767-76.

71. Shibata, H., Kondo, K., Katsuyama, R., Kawazoe, K., Sato, Y., Murakami, K., Takaishi, Y., Arakaki, N. & Higuti, T. (2005). Alkyl gallates, intensifiers of beta-lactam susceptibility in methicillin-resistant Staphylococcus aureus. *Antimicrob Agents Chemother* **49**, 549-55.

72. Reinhart, T. A., Qin, S. & Sui, Y. (2009). Multiple roles for chemokines in the pathogenesis of SIV infection. *Curr HIV Res* **7**, 73-82.

73. Ghosh, M., Shen, Z., Schaefer, T. M., Fahey, J. V., Gupta, P. & Wira, C. R. (2009). CCL20/MIP3alpha is a novel anti-HIV-1 molecule of the human female reproductive tract. *Am J Reprod Immunol* **62**, 60-71.

74. Lin, Y. C., Schlievert, P. M., Anderson, M. J., Fair, C. L., Schaefers, M. M., Muthyala, R. & Peterson, M. L. (2009). Glycerol monolaurate and dodecylglycerol effects on Staphylococcus aureus and toxic shock syndrome toxin-1 in vitro and in vivo. *PLoS One* **4**, e7499.

75. Peterson, M. L. & Schlievert, P. M. (2006). Glycerol monolaurate inhibits the effects of Gram-positive select agents on eukaryotic cells. *Biochemistry* **45**, 2387-97.

76. Strandberg, K. L., Peterson, M. L., Lin, Y. C., Pack, M. C., Chase, D. J. & Schlievert, P. M. (2010). Glycerol monolaurate inhibits Candida and Gardnerella vaginalis in vitro and in vivo but not Lactobacillus. *Antimicrob Agents Chemother* **54**, 597-601.

77. Haase, A. T. (2011). Early events in sexual transmission of HIV and SIV and opportunities for interventions. *Annu Rev Med* **62**, 127-39.

78. Park, P. H., Hur, J., Kim, Y. C., An, R. B. & Sohn, D. H. (2011). Involvement of heme oxygenase-1 induction in inhibitory effect of ethyl gallate isolated from Galla Rhois on nitric oxide production in RAW 264.7 macrophages. *Arch Pharm Res* **34**, 1545-52.

79. Calderon, A. I., Romero, L. I., Ortega-Barria, E., Solis, P. N., Zacchino, S., Gimenez, A., Pinzon, R., Caceres, A., Tamayo, G., Guerra, C., Espinosa, A., Correa, M. & Gupta, M. P. (2010). Screening of Latin American plants for antiparasitic activities against malaria, Chagas disease, and leishmaniasis. *Pharm Biol* **48**, 545-53.

80. Sawai, Y., Moon, J. H., Sakata, K. & Watanabe, N. (2005). Effects of structure on radical-scavenging abilities and antioxidative activities of tea polyphenols: NMR analytical approach using 1,1-diphenyl-2-picrylhydrazyl radicals. *J Agric Food Chem* **53**, 3598-604.

81. Li, Q., Estes, J. D., Schlievert, P. M., Duan, L., Brosnahan, A. J., Southern, P. J., Reilly, C. S., Peterson, M. L., Schultz-Darken, N., Brunner, K. G., Nephew, K. R., Pambuccian, S., Lifson, J. D., Carlis, J. V. & Haase, A. T. (2009). Glycerol monolaurate prevents mucosal SIV transmission. *Nature* **458**, 1034-8.

82. Moon, P. D., Choi, I. H. & Kim, H. M. (2012). Epigallocatechin-3-O-gallate inhibits the production of thymic stromal lymphopoietin by the blockade of caspase-1/NF-kappaB pathway in mast cells. *Amino Acids* **42**, 2513-9.

83. Gotes, J., Kasian, K., Jacobs, H., Cheng, Z. Q. & Mink, S. N. (2012). Benefits of ethyl gallate versus norepinephrine in the treatment of cardiovascular collapse in Pseudomonas aeruginosa septic shock in dogs. *Crit Care Med* **40**, 560-72.

84. Kalaivani, T., Rajasekaran, C. & Mathew, L. (2011). Free radical scavenging, cytotoxic, and hemolytic activities of an active antioxidant compound ethyl gallate from leaves of Acacia nilotica (L.) Wild. Ex. Delile subsp. indica (Benth.) Brenan. *J Food Sci* **76**, T144-9.

85. Saleem, A., Husheem, M., Harkonen, P. & Pihlaja, K. (2002). Inhibition of cancer cell growth by crude extract and the phenolics of Terminalia chebula retz. fruit. *J Ethnopharmacol* **81**, 327-36.

86. Mehla, K., Balwani, S., Kulshreshtha, A., Nandi, D., Jaisankar, P. & Ghosh, B. (2011). Ethyl gallate isolated from Pistacia integerrima Linn. inhibits cell adhesion molecules by blocking AP-1 transcription factor. *J Ethnopharmacol* **137**, 1345-52.

87. Varesio, L., Battaglia, F., Raggi, F., Ledda, B. & Bosco, M. C. (2010). Macrophage-inflammatory protein-3alpha/CCL-20 is transcriptionally induced by the iron chelator desferrioxamine in human mononuclear phagocytes through nuclear factor (NF)-kappaB. *Mol Immunol* **47**, 685-93.

88. Porath, D., Riegger, C., Drewe, J. & Schwager, J. (2005). Epigallocatechin-3-gallate impairs chemokine production in human colon epithelial cell lines. *J Pharmacol Exp Ther* **315**, 1172-80.

89. Fujiie, S., Hieshima, K., Izawa, D., Nakayama, T., Fujisawa, R., Ohyanagi, H. & Yoshie, O. (2001). Proinflammatory cytokines induce liver and activation-regulated chemokine/macrophage inflammatory protein-3alpha/CCL20 in mucosal epithelial cells through NF-kappaB [correction of NK-kappaB]. *Int Immunol* **13**, 1255-63.

90. Pegu, A., Qin, S., Fallert Junecko, B. A., Nisato, R. E., Pepper, M. S. & Reinhart, T. A. (2008). Human lymphatic endothelial cells express multiple functional TLRs. *J Immunol* **180**, 3399-405.

91. Randolph, G. J., Angeli, V. & Swartz, M. A. (2005). Dendritic-cell trafficking to lymph nodes through lymphatic vessels. *Nat Rev Immunol* **5**, 617-28.

92. Garrafa, E., Imberti, L., Tiberio, G., Prandini, A., Giulini, S. M. & Caimi, L. (2011). Heterogeneous expression of toll-like receptors in lymphatic endothelial cells derived from different tissues. *Immunol Cell Biol* **89**, 475-81.

93. Francois, M., Harvey, N. L. & Hogan, B. M. (2011). The transcriptional control of lymphatic vascular development. *Physiology (Bethesda)* **26**, 146-55.

94. Kato, S., Shimoda, H., Ji, R. C. & Miura, M. (2006). Lymphangiogenesis and expression of specific molecules as lymphatic endothelial cell markers. *Anat Sci Int* **81**, 71-83.

95. Makinen, T., Norrmen, C. & Petrova, T. V. (2007). Molecular mechanisms of lymphatic vascular development. *Cell Mol Life Sci* **64**, 1915-29.

96. Hong, Y. K. & Detmar, M. (2003). Prox1, master regulator of the lymphatic vasculature phenotype. *Cell Tissue Res* **314**, 85-92.

97. Kiefer, F. & Adams, R. H. (2008). Lymphatic endothelial differentiation: start out with Sox--carry on with Prox. *Genome Biol* **9**, 243.

98. Lawinger, P., Rastelli, L., Zhao, Z. & Majumder, S. (1999). Lack of enhancer function in mammals is unique to oocytes and fertilized eggs. *J Biol Chem* **274**, 8002-11.

99. Schlievert, P. M., Deringer, J. R., Kim, M. H., Projan, S. J. & Novick, R. P. (1992). Effect of glycerol monolaurate on bacterial growth and toxin production. *Antimicrob Agents Chemother* **36**, 626-31.

100. Li, H., Gao, Z., Zhang, J., Ye, X., Xu, A., Ye, J. & Jia, W. (2012). Sodium butyrate stimulates expression of fibroblast growth factor 21 in liver by inhibition of histone deacetylase 3. *Diabetes* **61**, 797-806.

101. Gao, Z., Yin, J., Zhang, J., Ward, R. E., Martin, R. J., Lefevre, M., Cefalu, W. T. & Ye, J. (2009). Butyrate improves insulin sensitivity and increases energy expenditure in mice. *Diabetes* **58**, 1509-17.

102. Ochoa-Zarzosa, A., Villarreal-Fernandez, E., Cano-Camacho, H. & Lopez-Meza, J. E. (2009). Sodium butyrate inhibits Staphylococcus aureus internalization in bovine mammary epithelial cells and induces the expression of antimicrobial peptide genes. *Microb Pathog* **47**, 1-7.

103. Schauber, J., Svanholm, C., Termen, S., Iffland, K., Menzel, T., Scheppach, W., Melcher, R., Agerberth, B., Luhrs, H. & Gudmundsson, G. H. (2003). Expression of the cathelicidin LL-37 is modulated by short chain fatty acids in colonocytes: relevance of signalling pathways. *Gut* **52**, 735-41.

104. Schauber, J., Iffland, K., Frisch, S., Kudlich, T., Schmausser, B., Eck, M., Menzel, T., Gostner, A., Luhrs, H. & Scheppach, W. (2004). Histone-deacetylase inhibitors induce the cathelicidin LL-37 in gastrointestinal cells. *Mol Immunol* **41**, 847-54.

105. Fusunyan, R. D., Quinn, J. J., Fujimoto, M., MacDermott, R. P. & Sanderson, I. R. (1999). Butyrate switches the pattern of chemokine secretion by intestinal epithelial cells through histone acetylation. *Mol Med* **5**, 631-40.

106. Bode, J., Winkelmann, S., Gotze, S., Spiker, S., Tsutsui, K., Bi, C., A, K. P. & Benham, C. (2006). Correlations between scaffold/matrix attachment region (S/MAR) binding activity and DNA duplex destabilization energy. *J Mol Biol* **358**, 597-613.

107. Klehr, D., Schlake, T., Maass, K. & Bode, J. (1992). Scaffold-attached regions (SAR elements) mediate transcriptional effects due to butyrate. *Biochemistry* **31**, 3222-9.

108. World Health Organization-HIV/AIDS Data and Statistics. http://www.who.int/hiv/data/en/

109. "Glycerol monolaurate." *Wikipedia, The Free Encyclopedia*.Wikimedia Foundation, Inc.. 16 Jul 2012. Web. 2 Apr 2012. <http://en.wikipedia.org/wiki/Glycerol_monolaurate>

110. "Epigallocatechin gallate." *Wikipedia, The Free Encyclopedia*.Wikimedia Foundation, Inc.. 28 Jun 2012. Web. 2 Apr 2012. <http://en.wikipedia.org/wiki/Epigallocatechin_gallate>

111. "Ethyl gallate." *Wikipedia, The Free Encyclopedia*.Wikimedia Foundation, Inc.. 14 May 2012. Web. 2 Apr 2012. <http://en.wikipedia.org/wiki/Ethyl_gallate>